RADMEP 2023 Workshop at CERN

Accelerator Radiation Environments

Rubén García Alía

SY department, R2E activity coordinator

4th December 2023
https://indico.cern.ch/event/1350062/

Outline

- Introduction to this course and the Radiation Hardness Assurance discipline
- Basics of radiation-matter interactions and the FLUKA Monte Carlo code
- Radiation environment in the LHC
  - Setting the scene
  - Radiation sources and environment description
  - Tools for radiation monitoring and calculation
  - Radiation levels in the LHC areas relevant to electronics operation
- SPS radiation levels
- FCC-ee radiation levels
- Extra slides

Outline

- **Introduction to this course and the Radiation Hardness Assurance discipline**
- Basics of radiation-matter interactions and the FLUKA Monte Carlo code
- Radiation environment in the LHC
  - Setting the scene
  - Radiation sources and environment description
  - Tools for radiation monitoring and calculation
  - Radiation levels in the LHC areas relevant to electronics operation
- SPS radiation levels
- FCC-ee radiation levels
- Extra slides

Topic of the course: basic intro to radiation effects on electronics, with a focus on CERN applications

Impact of beam losses on accelerator operation

PHYSICAL REVIEW ACCELERATORS AND BEAMS **22,** 071003 (2019)

Editors' Suggestion

Validation of energy deposition simulations for proton and heavy ion losses in the CERN Large Hadron Collider

A. Lechner,* B. Auchmann,† T. Baer,‡ C. Bahamonde Castro, R. Bruce, F. Cerutti, L. S. Esposito, A. Ferrari, J. M. Jowett, A. Mereghetti, F. Pietropaolo, S. Redaelli, B. Salvachua, M. Sapinski,§ M. Schaumann, N. V. Shetty, and V. Vlachoudis

European Organization for Nuclear Research (CERN), Esplanade des Particules 1, 1211 Geneva, Switzerland

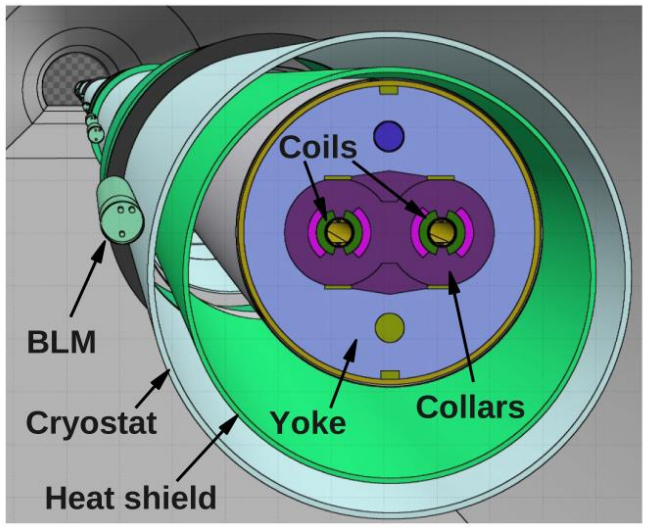

FIG. 1. Geometry model of a main arc dipole embedded in the LHC tunnel, with a BLM mounted on the outside of the magnet cryostat. A more detailed picture of the BLM model is shown in Fig. 2.

Beam losses and the resulting showers adversely affect collider operation, experiments, equipment, and personnel in several ways. For example, they can lead to magnet quenches, i.e., the sudden loss of superconductivity [21]; they contribute to the heat load to the cryogenic system [22,23]; they cause long-term radiation damage and aging of equipment components [22–25]; they lead to the production of radioactive isotopes and are therefore a concern for radiation protection [26]; they give rise to background in experiments [27]; and they can induce single-event effects in equipment electronics [28]. In the worst case, if the beam is lost in an uncontrolled way, it can induce destructive damage because of the thermal shock or because of phase transitions if the temperatures are high enough. In order to assess the consequences of beam losses …

Radiation Hardness Assurance, as defined for space applications

2. Radiation Hardness Assurance – A Definition

The Radiation Hardness Assurance (RHA) process consists in deploying all activities needed to insure that all the potentially radiation sensitive units of a space system, including the space system itself, will meet their design specifications up to the end of the targeted mission. A top level description of its content is presented in Figure 1.

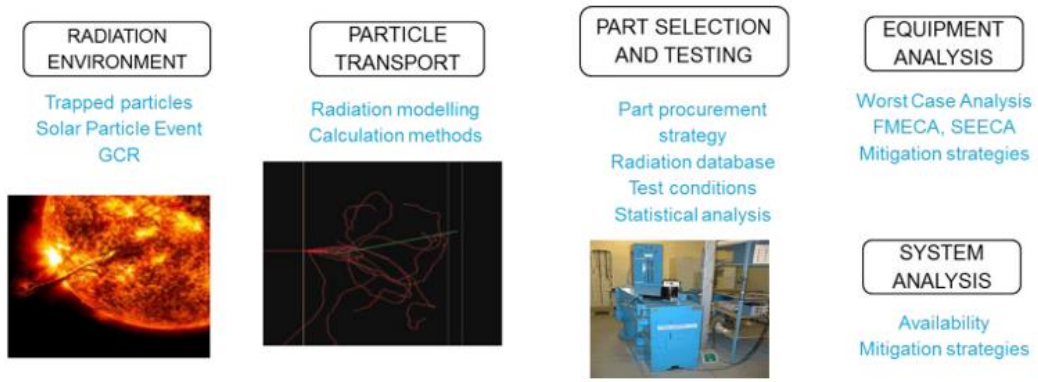

Figure 1: top level description of the Radiation Hardness Assurance coverage

This process is iterative. It starts first with top-level estimations of the radiation environment (provided in the mission radiation environment specification), then the radiation levels are transported at sensitive element levels and the electronic designs analyzed in order to validate the most sensitive parts:

- The mission radiation environment specification provides the radiation inputs outside the spacecraft: the particle spectra (heavy ion Linear Energy Transfer (LET) spectra, proton and electron energy spectra and dose-depth curves). This will be used later on for the definition of the radiation levels within spacecraft and/or the radiation specification levels.
- Assessment on parts radiation sensitivity: The radiation hardness of the parts is estimated on the basis of part selection, radiation databases relevant radiation tests, Radiation Design Margin, etc...
- Radiation aspects in Worst Case Analysis (WCA, Failure Mode, Effects and Criticality Analysis FMECA) of circuit, equipment and system design. The overall equipment and spacecraft worst case performance over the mission length, taking into account radiation effects, aging and other causes of degradation is estimated.
- System or equipment level countermeasure: Countermeasures can be implemented to either increase the acceptable sensitivity level of the part or reduce the radiation environment level: additional shielding at component level (spot shielding) or at box level (additional thickness of box cover), switching of redundant component or function, error correction system, specific memory organization, latch-up protection circuitry, etc.

Radiation effects at CERN

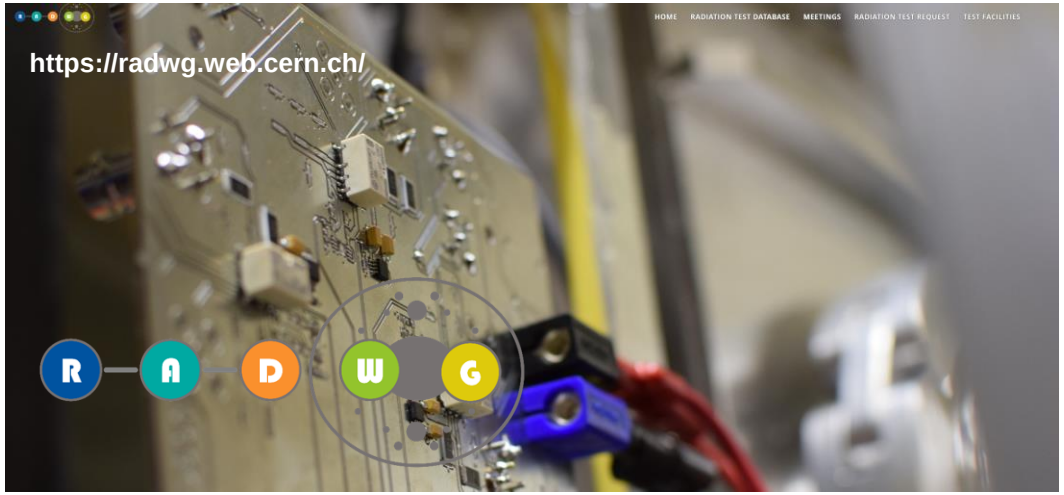

CHARM

CELESTA, the first CERN-driven satellite, will enter orbit during the maiden flight of Europe's Vega-C launch vehicle. It will be launched by the European Space Agency from the French Guiana Space Centre (CSG) in July 2022 (see 14/07/2022 News article below). (Image: CERN)

The “Radiation to Electronics” (R2E) challenge in high-energy accelerators

- High-energy accelerators are subject to **beam losses** and hence generate prompt radiation in their vicinity
- Part of the accelerator equipment needs to be installed near the machine itself, and is therefore subject to a complex and challenging **radiation environment**
- Such equipment is critical for the successful operation of the accelerator, and uses microelectronic components which are **sensitive to radiation**

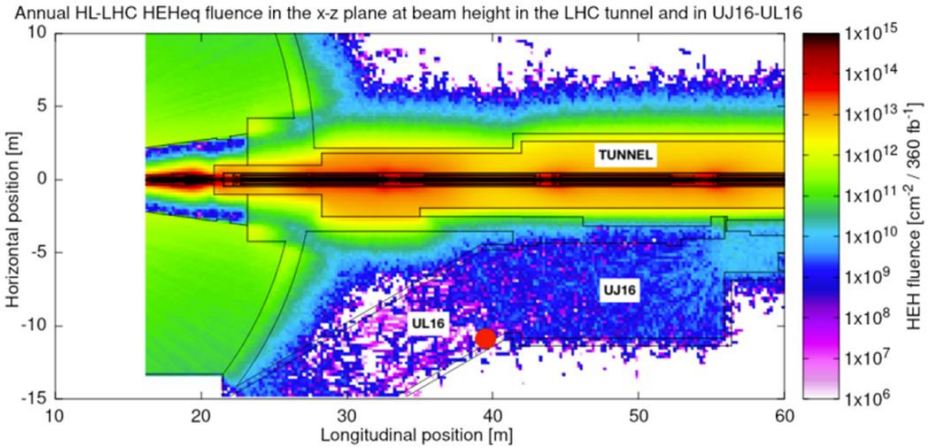

Expected HL-LHC radiation levels around the ATLAS interaction point (IP1), as simulated in FLUKA

FLUKA

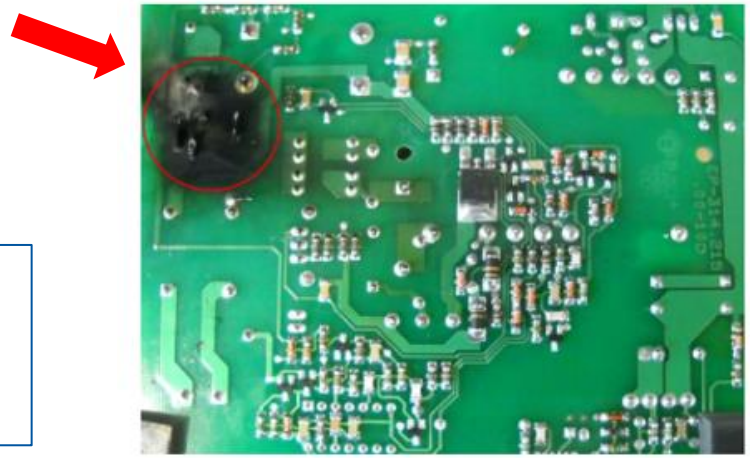

Tens of thousands of electronic boards in the LHC (and millions of individual components), all capable of negatively affecting its operation through radiation effects

R2E mandate: to ensure the successful operation of CERN accelerators in view of radiation effects on electronics

Radiation Hardness Assurance at CERN

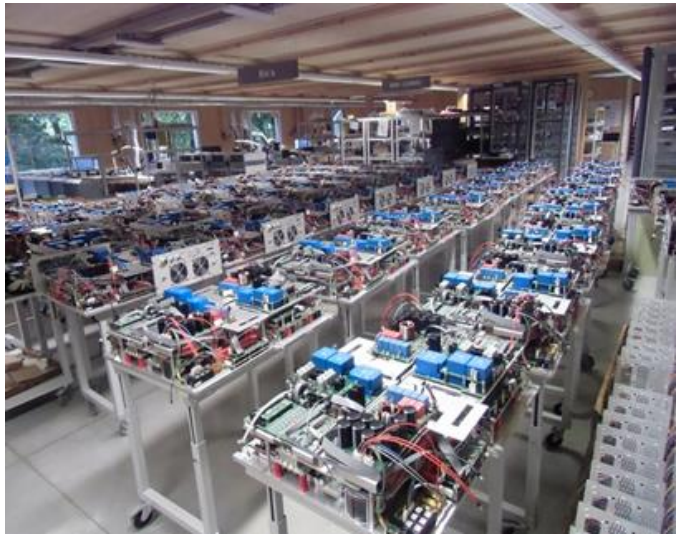

Radiation tolerant design and production (standards, guidelines, quality assurance, reviews…)

Radiation effects facilities and tests

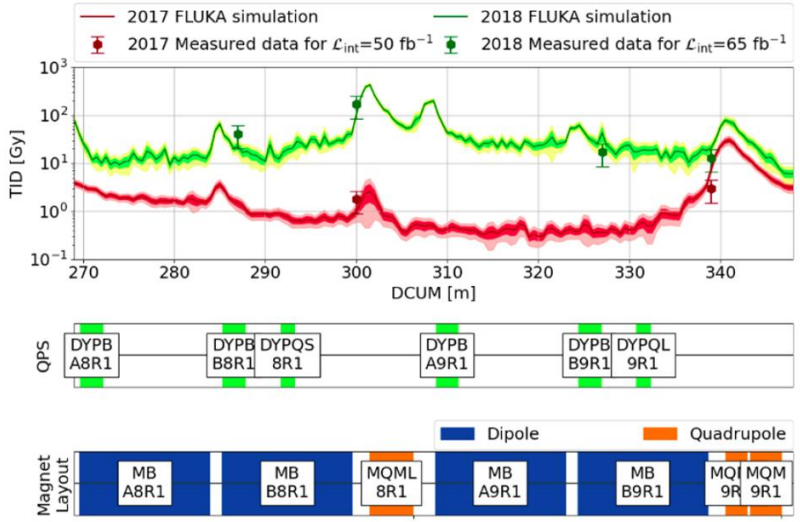

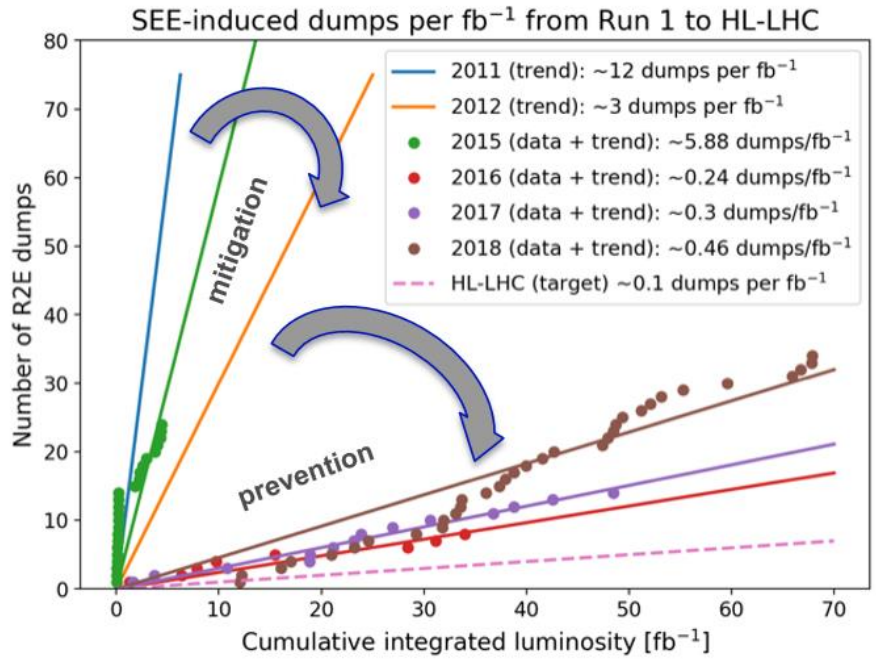

Follow-up and mitigation of radiation effects impact on operation; mission-critical also for HL-LHC objectives

Radiation environment simulation and monitoring

Multidisciplinary and transversal activity

"From atoms to systems" (through semiconductors, circuits, etc.)

New radiation environments, new technologies, new effects… → "Never-ending learning story"

Accelerator technology

Nuclear and high-energy physics

Microelectronic engineering

Radiation-Matter interaction; Detector physics

Reliability engineering

Radiation Hardness Assurance at CERN

Semiconductor physics

Systems engineering

Physical modelling and computational simulations (e.g. Monte Carlo)

Outline

- Introduction to this course and the Radiation Hardness Assurance discipline
- **Basics of radiation-matter interactions and FLUKA Monte Carlo code**
- Radiation environment in the LHC
  - Setting the scene
  - Radiation sources and environment description
  - Tools for radiation monitoring and calculation
  - Radiation levels in the LHC areas relevant to electronics operation
- SPS radiation levels
- FCC-ee radiation levels
- Extra slides

Radiation-matter interaction and FLUKA

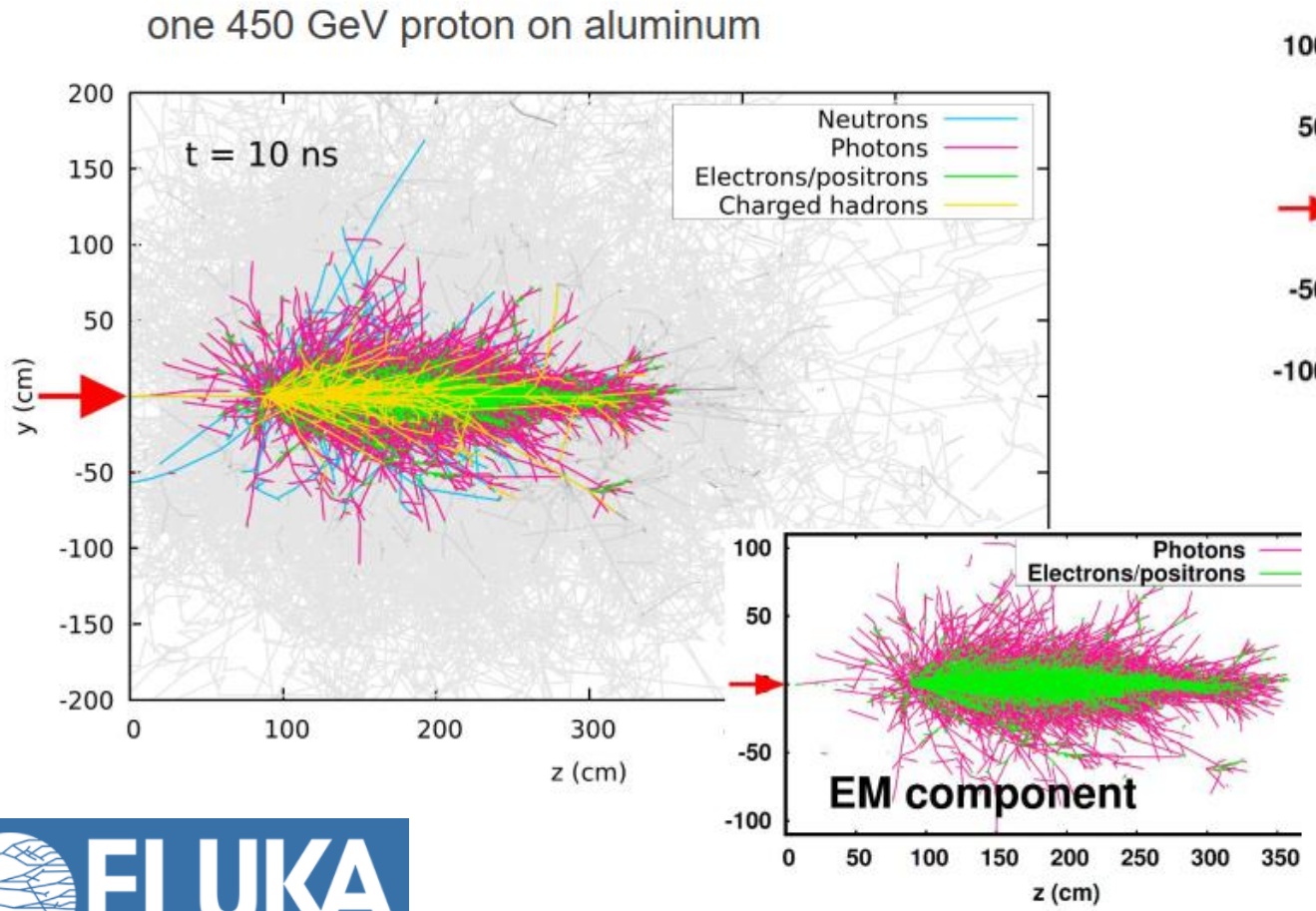

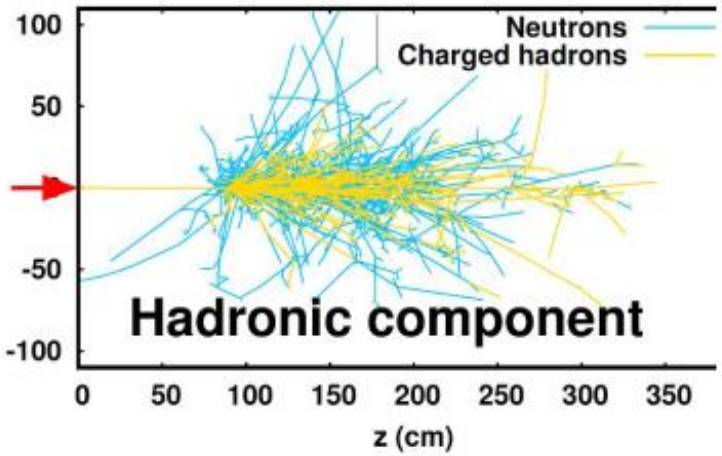

Radiation-matter interaction and FLUKA

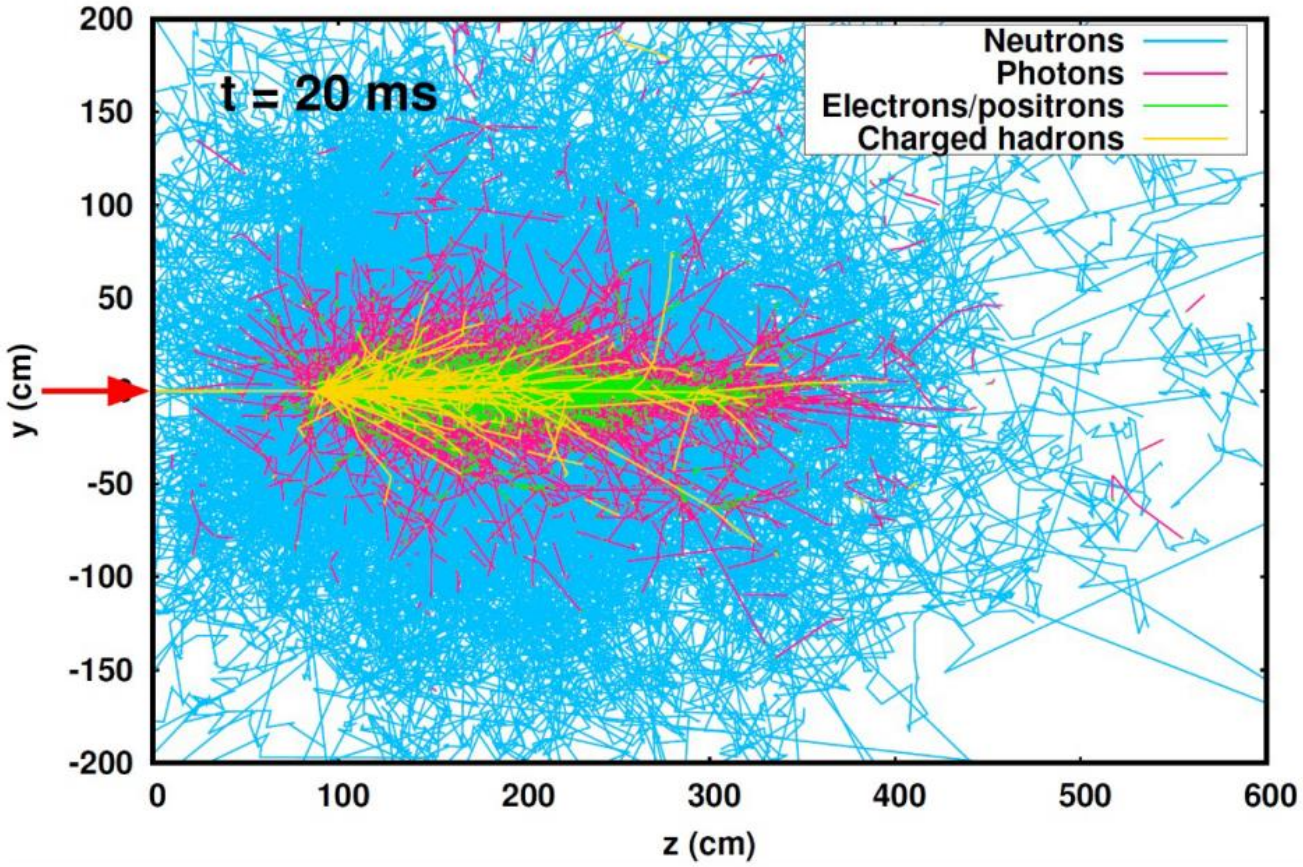

Radiation shower set up by a single 450 GeV/c proton in Al

Physical quantities: fluence vs current

Surface crossing estimation

- Imagine a surface having an infinitesimal thickness dt A particle incident with an angle θ with respect to the normal of the surface S will travel a segment $dt/cos\theta$.

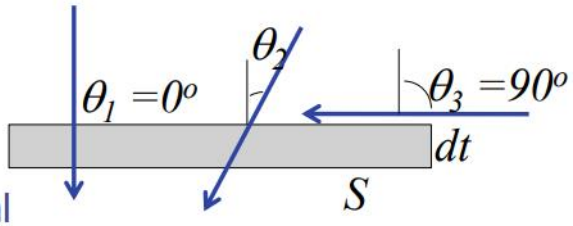

- Therefore, we can calculate an average surface fluence by adding $dt/cos\,\theta$ for each particle crossing the surface, and dividing by the volume $S\,dt$

$$\Phi = \lim_{dt \to 0} \frac{\sum_i \frac{dt}{\cos\theta_i}}{S\,dt}$$

- While the current J counts the number of particles crossing the surface divided by the surface:

$$J = dN/dS$$

The fluence is independent of the orientation of the surface S, while the current is NOT!

In an *isotropic field* it can be easily seen that for a flat surface $J = \Phi/2$

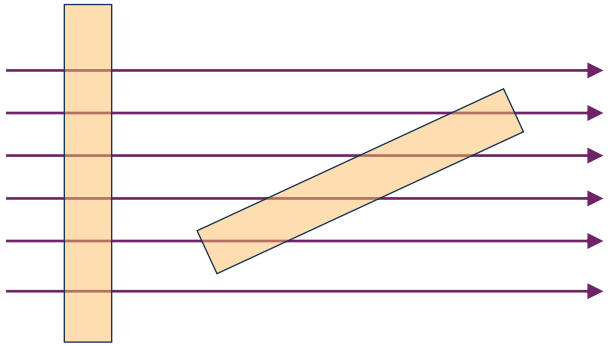

- Fluence is measured in particles per cm^2 but in reality it describes the **density of particle tracks**

Physical quantities and units: fluence, LET, dose

(Differential) fluence: particles per unit surface per unit energy (e.g. $MeV^{-1}cm^{-2}$)

Dose: absorbed energy per unit mass (e.g. MeV/g, or, more typically, J/kg = Gy)

Flux = Fluence / time

Linear Energy Transfer: deposited energy per unit length, typically normalized to density (e.g. $MeV \cdot cm^{-1}/(g \cdot cm^3) = MeVcm^2/g$)

Dose Rate = Dose / time

Stochastic, Single Event Effects

Cumulative, deterministic, lifetime related

For a given energy and (charged) particle:

Dose (MeV/g) = Fluence (cm^{-2}) x LET ($MeVcm^2/g$)

Cumulative radiation effects on electronics

TOTAL IONISING DOSE (TID)

- Major source of lifetime degradation for LHC electronics and equipment (e.g. magnets). Measured in Gray (Gy).
- Generally dominated by the **EM component** of radiation showers, but also **charged hadrons** can contribute.

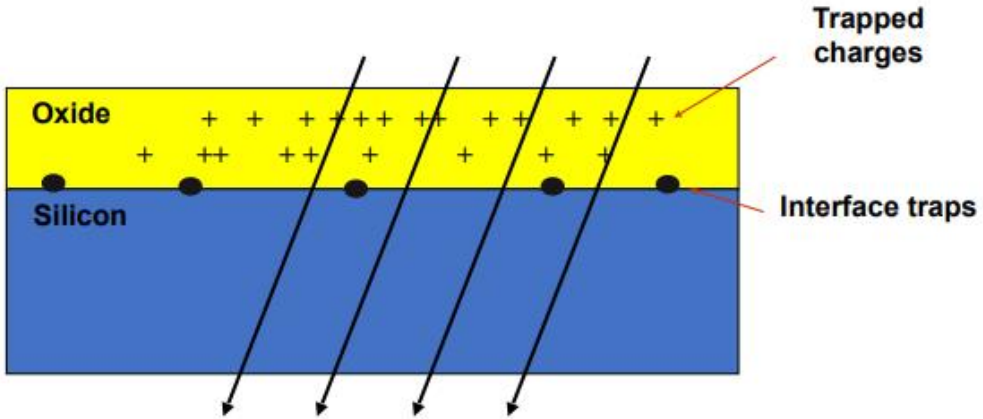

Charge accumulation in oxide

DISPLACEMENT DAMAGE (DD)

- Non Ionising Energy Loss (NIEL) causing defects in materials.
- Parametrised by the equivalent fluence (in cm^{-2}) of 1-MeV **neutrons** in Silicon.
- Often not the most critical effect at the LHC, with exceptions (e.g. optocouplers).

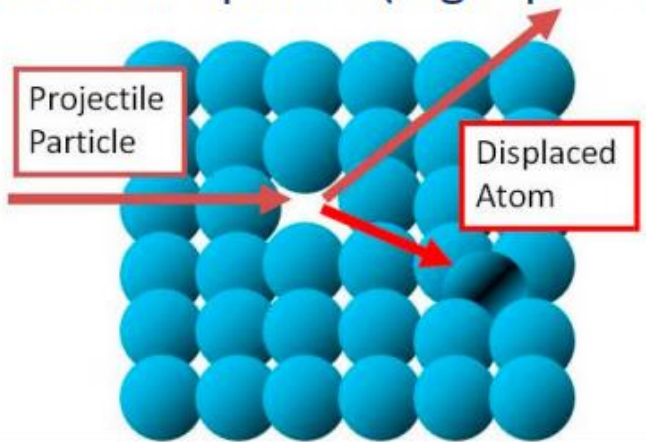

Silicon structure alteration

Single Event Effects: direct and indirect ionisation

Stochastic events caused by energy deposited in a sensitive volume (e.g. memory cell)

DIRECT IONISATION

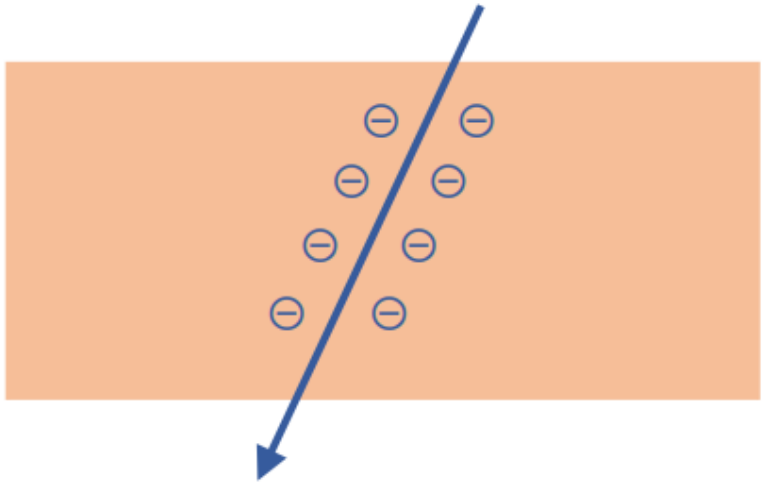

- Caused by particles with high Linear Energy Transfer (LET), e.g. **heavy ions**
- **Not relevant at the LHC** (negligible amount of ions reaching electronic equipment)

INDIRECT IONISATION

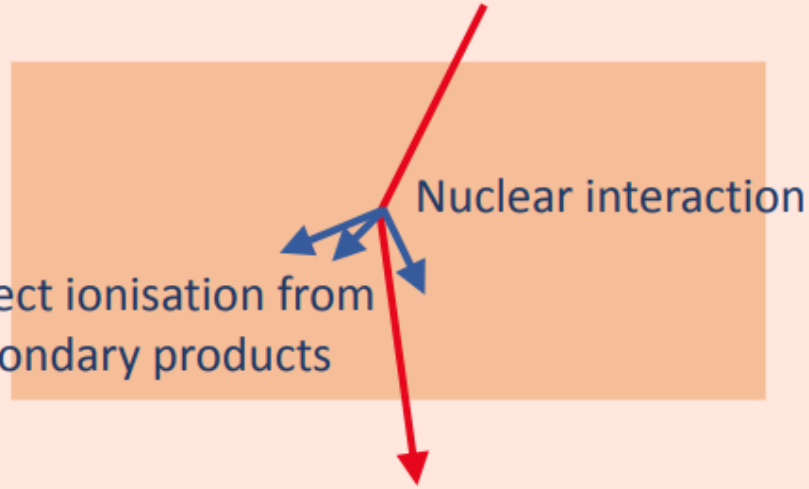

- Caused by neutral or low-LET particles, e.g. **protons**, **neutrons**, **pions**, etc.
- **Dominant source of SEEs at the LHC.**

R2E order of magnitude levels and effects (very approximative!)

High-energy hadron fluence (cm^{-2} $year^{-1}$)	Total Ionizing Dose for 10 years (Gy)	Effects on Electronics
10^5	<<1	Possible SEE impact for commercial systems with MANY units and VERY demanding availability and reliability requirements
10^7	<1	SEE impact for systems with multiple units and demanding availability and reliability requirements
10^9	10	SEE mitigation (e.g. redundancy) at system level; cumulative effects can start to play a role
10^{11}	1000	SEE mitigation (e.g. redundancy) at system level, very challenging TID level for COTS
10^{15}	10 MGy	Rad-hard by design ASICs

Approximation (mainly for high-energy accelerator environment): 10^9 HEH/cm^2 ~ 1 Gy

The FLUKA particle-transport code

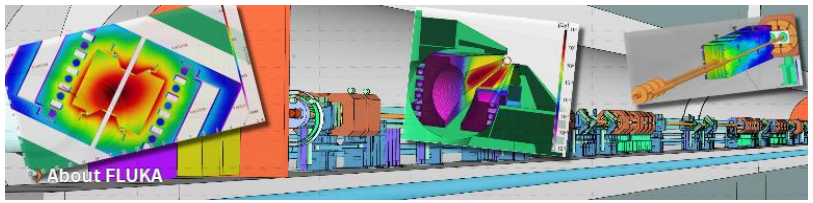

https://fluka.cern/

- **General-purpose** code for the **Monte-Carlo** simulation of radiation transport
- Maintained by the FLUKA.CERN Collaboration
- Worldwide community of **~2000 active users**
- Mature simulation code: development started in the 1960s
- **Coupled hadronic/electromagnetic** particle shower simulation
- Over **60 particle species tracked**, including γ, $e^{\pm}$, $\mu^{\pm}$, $\tau^{\pm}$, ν, hadrons, ions
- Energy range:
  - up to 10 PeV
  - down to 100 eV for γ, 1 keV for $e^{\pm}$/p, 10^{-14} GeV for n
- **Not** a simulation toolkit: most reasonable physics models adopted on behalf of our users
- **Very few simulation parameters**: transport/production thresholds, toggling exotic/time-consuming processes, etc
- **Combinatorial geometry** package for arbitrarily complex geometries
- Tracking in **magnetic fields** (and **electric** fields in vacuum)
- **Built-in variance reduction / biasing** techniques
- **Built-in scoring** capabilities for a broad variety of radiometric quantities

FLUKA's graphical user interface: Flair

- Assists users in all simulation stages:
  - Input setup
  - Geometry definition, visualization & debugging
  - Running (distributed)
  - Processing output
  - Visualizing results
- https://flair.cern
- Able to import GDML and convert to FLUKA geometry
- Broad range of applications of FLUKA/Flair!

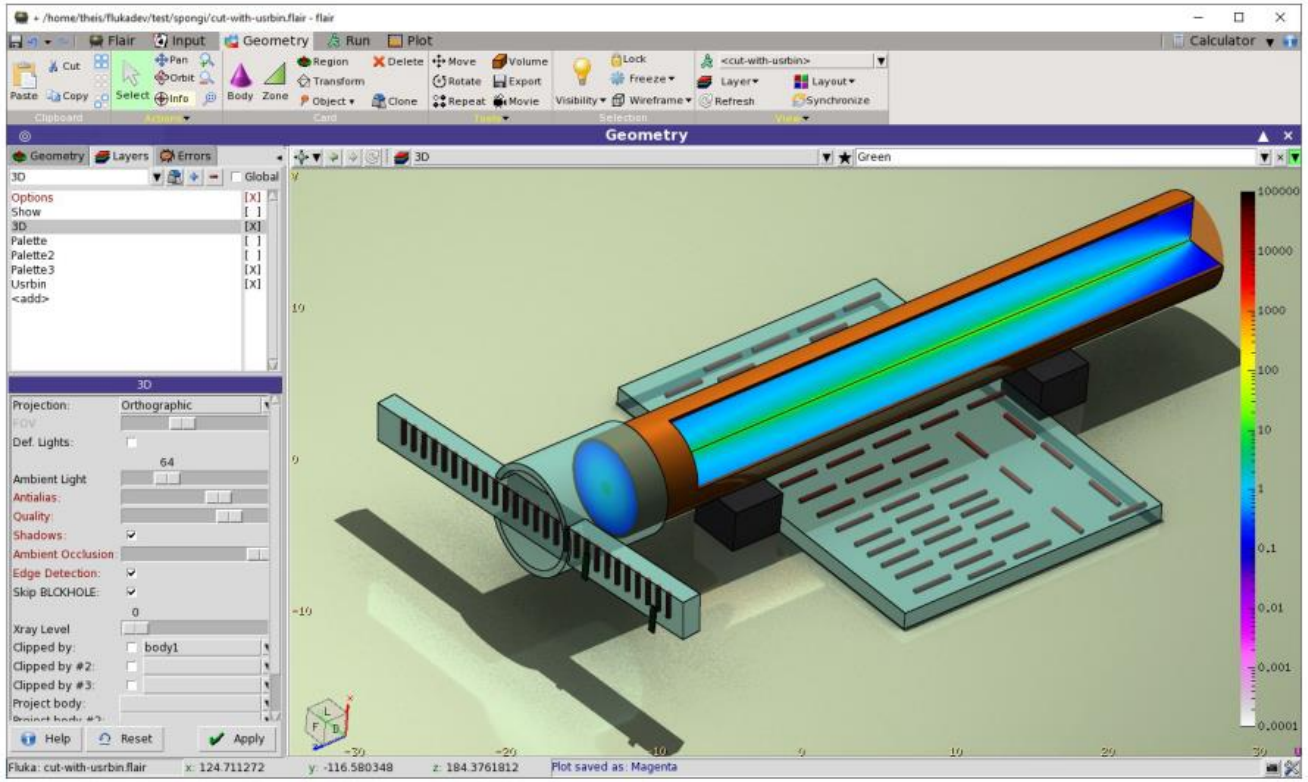

E.g. energy deposition (GeV/cm^3 in a test target at CERN's H4IRRAD, subject to 280 GeV/c mixed hadron beam)

FLUKA geometry

- FLUKA relies on a combinatorial geometry package to build arbitrarily complex geometries
- Building blocks:
  - Geometrical primitive shapes: plane, sphere, cylinder, etc
  - Boolean operations
  - Transformations: shifts, rotations, lattices (replicas)
- E.g.: LHC collimation insertion region

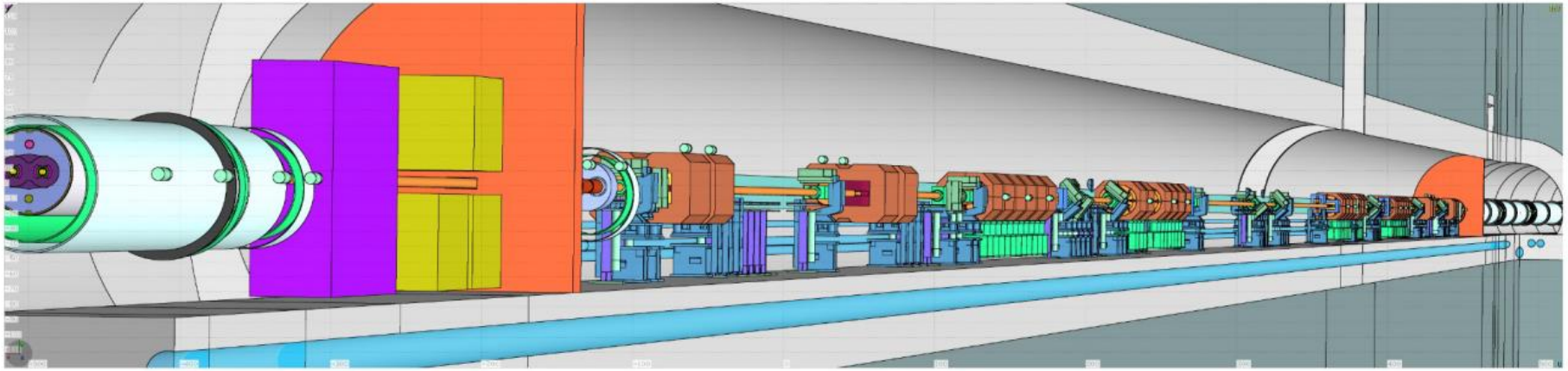

Ionization loss benchmark example

SEEs are typically caused by "stopping" charged particles, present in the environment (direct ionization) or generated locally (micrometric level) near the sensitive volume (indirect ionization)

- Depth-dose profile of 54.19 MeV protons in water
- Ref: Battistoni G. *et al., Front. Oncol.* **6** 116 (2016)
- Additionally: depth-dose profile for ions (He, C, O), with fragmentation tail behind the Bragg peak

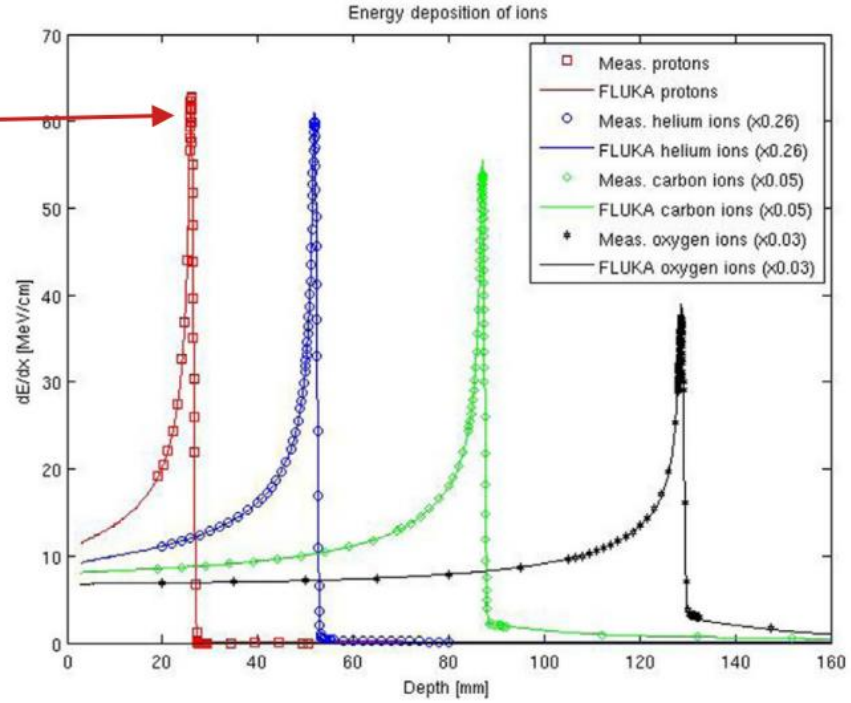

FIGURE 4 | FLUKA simulations of depth–dose profiles of protons, helium, carbon, and oxygen ions with therapeutic ranges in comparison with measured data at HIT. The nominal energies before the beamline are 54.19, 79.78, 200.28, and 300.13 MeV/u, for protons, helium, carbon, and oxygen ions, respectively.

Ionization loss benchmark example

- Broad spectrum for e-
- Sharp Bragg peak for p and α
- Fragmentation tails

- Clear implications for radiotherapy

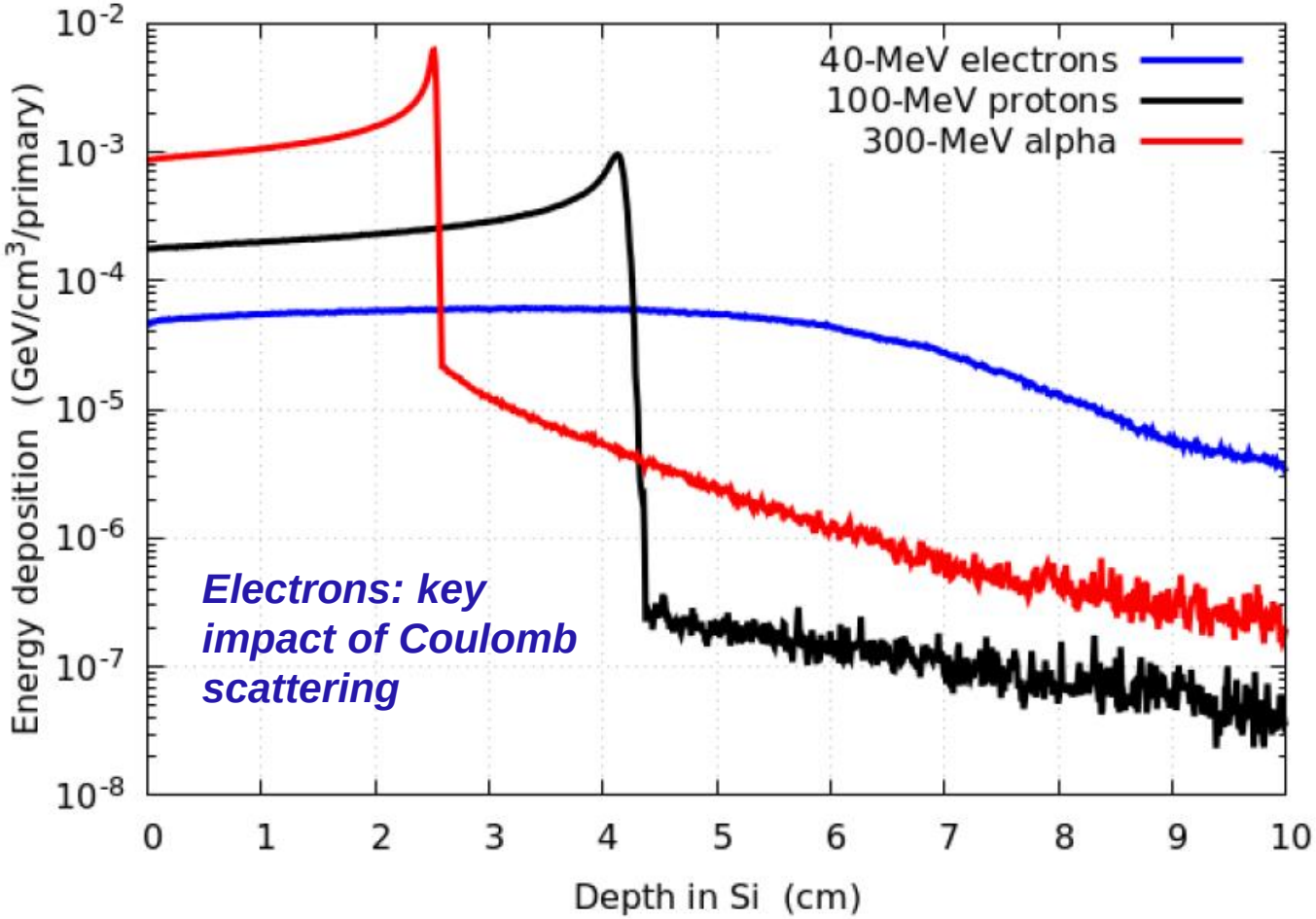

Hadron-nucleus interactions: 90Zr(p,xn)

- Neutron emission from ^{90}Zr under bombardment with 80.5 MeV protons
- Energy-differential cross section (integrated over all emission angles)
- Solid lines: FLUKA
- Dots: experimental data from *Trabandt M. et al., Phys Rev C* ***39*** *452 (1989)*

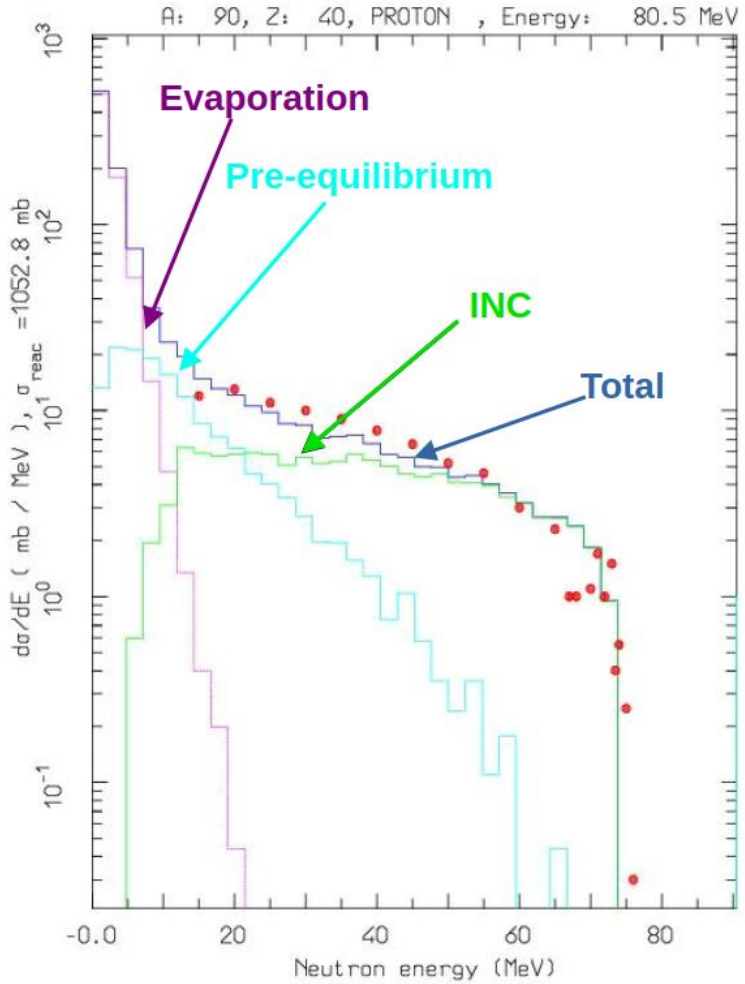

Energy deposition through neutron-silicon interactions

IEEE TRANSACTIONS ON NUCLEAR SCIENCE, VOL. 69, NO. 3, MARCH 2022 273

G4SEE: A Geant4-Based Single Event Effect Simulation Toolkit and Its Validation Through Monoenergetic Neutron Measurements

Dávid Lucsányi, Rubén García Alía, *Member, IEEE*, Kacper Biłko, Matteo Cecchetto, Salvatore Fiore, *Member, IEEE*, and Elisa Pirovano

Short-ranged, high LET recoil → capable of inducing SEEs

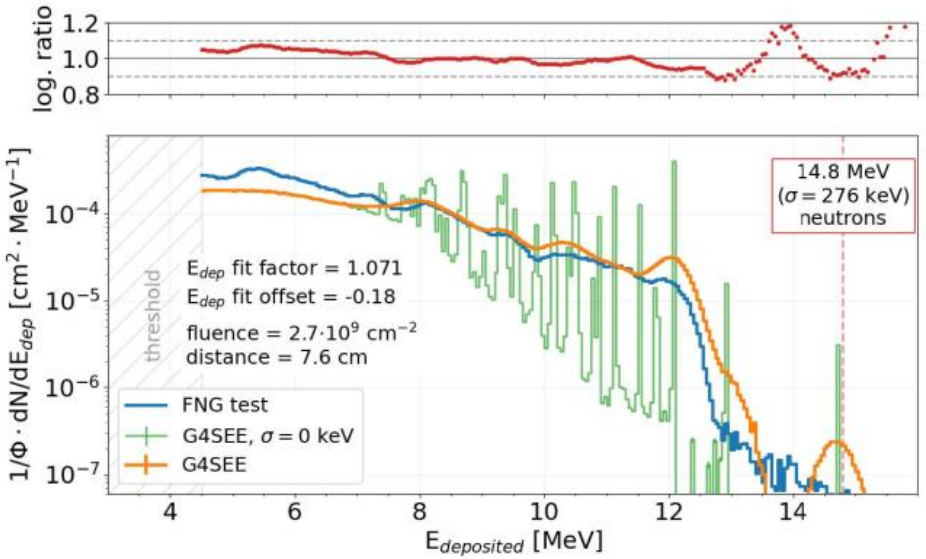

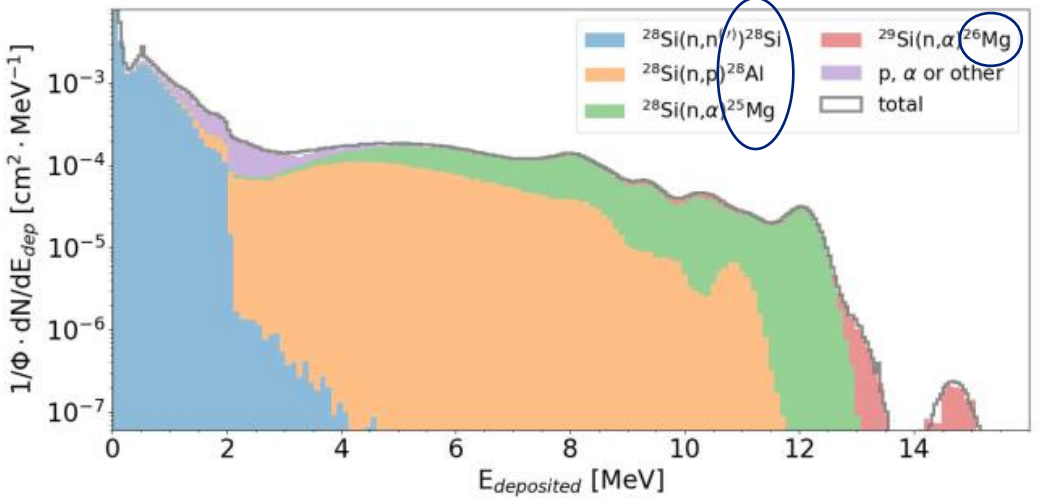

Bremsstrahlung and photo-neutrons

Important for electron accelerators, including medical linacs

IEEE TRANSACTIONS ON NUCLEAR SCIENCE, VOL. 69, NO. 7, JULY 2022 1541

Analysis of the Photoneutron Field Near the THz Dump of the CLEAR Accelerator at CERN With SEU Measurements and Simulations

Giuseppe Lerner, Andrea Coronetti, *Associate Member, IEEE*, Jean Maël Kempf, Rubén García Alía, *Member, IEEE*, Francesco Cerutti, Daniel Prelipcean, Matteo Cecchetto, Antonio Gilardi, *Member, IEEE*, Wilfrid Farabolini, and Roberto Corsini

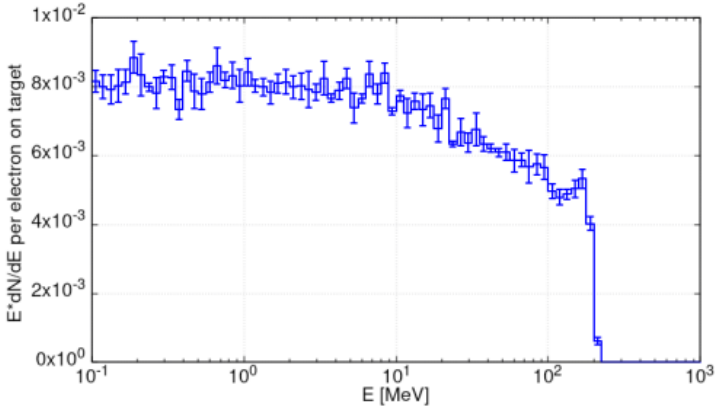

Fig. 2. Simulated distribution per unit lethargy of bremsstrahlung photons produced by a 205-MeV electron beam in a thin (0.1 mm) target made of Fe.

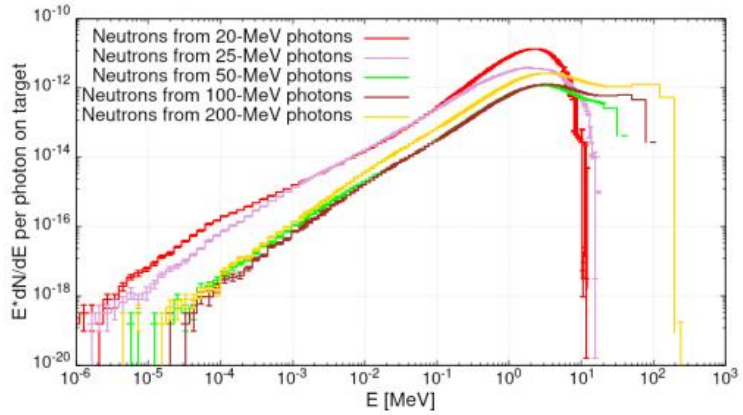

Fig. 4. Photoneutron distribution per unit lethargy simulated with FLUKA for photons of different energies impacting on a target made of Fe.

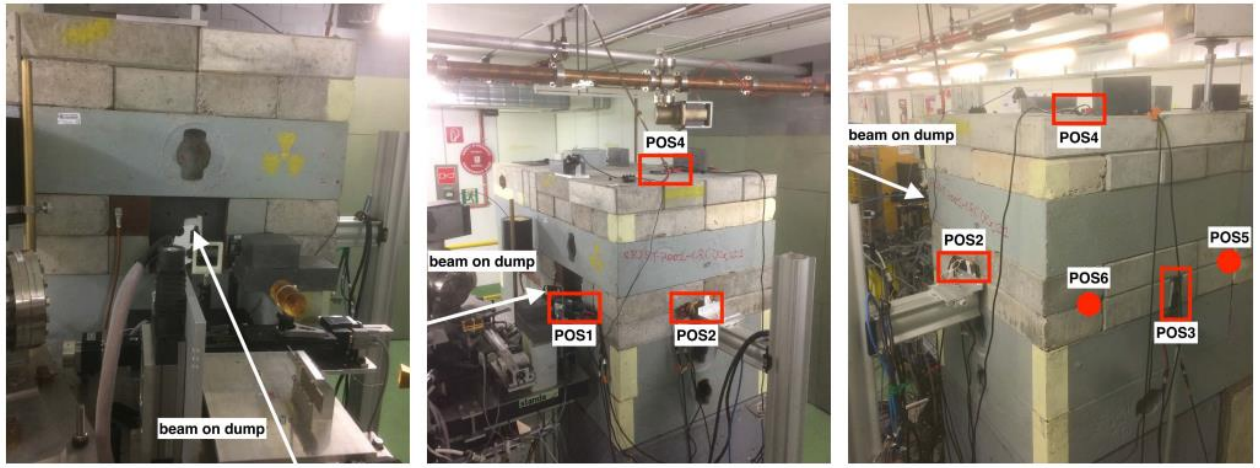

(a) (b) (c)

Fig. 1. (a) Front, (b) side, and (c) back views of the CLEAR THz test station and beam dump, showing the beam axis and the reference test positions where SEU measurements have been taken.

Summary of radiation-matter interactions relevant for (stochastic) radiation effects in accelerators

- **High energy protons** generate (spallation) neutrons, through nuclear reactions
- These **neutrons** travel long distances, scattering off nuclei, and penetrating through thick shielding materials
- When reaching the electronics, these neutrons can create nuclear reactions near the sensitive nodes, which produce heavy, short-ranged, **highly ionizing recoils** and fragments with a large enough LETs to cause SEEs
- (a similar process can be triggered with **high energy electrons** as a source, via synchrotron and bremsstrahlung photons first, and photon-neutrons later)

Outline

- Introduction to this course and the Radiation Hardness Assurance discipline
- Basics of radiation-matter interactions and the FLUKA Monte Carlo code
- **Radiation environment in the LHC**
  - **Setting the scene**
  - Radiation sources and environment description
  - Tools for radiation monitoring and calculation
  - Radiation levels in the LHC areas relevant to electronics operation
- SPS radiation levels
- FCC-ee radiation levels
- Extra slides

The LHC accelerator complex

- Long sequence of accelerators and transfer lines to reach the LHC, for proton and ion operation.
- Energy increase by a factor ≈30 at each step.
- Four LHC Interaction Points (ATLAS, CMS, ALICE and LHCb detectors).
- Many experiments and facilities (e.g. CHARM test facility, discussed later).

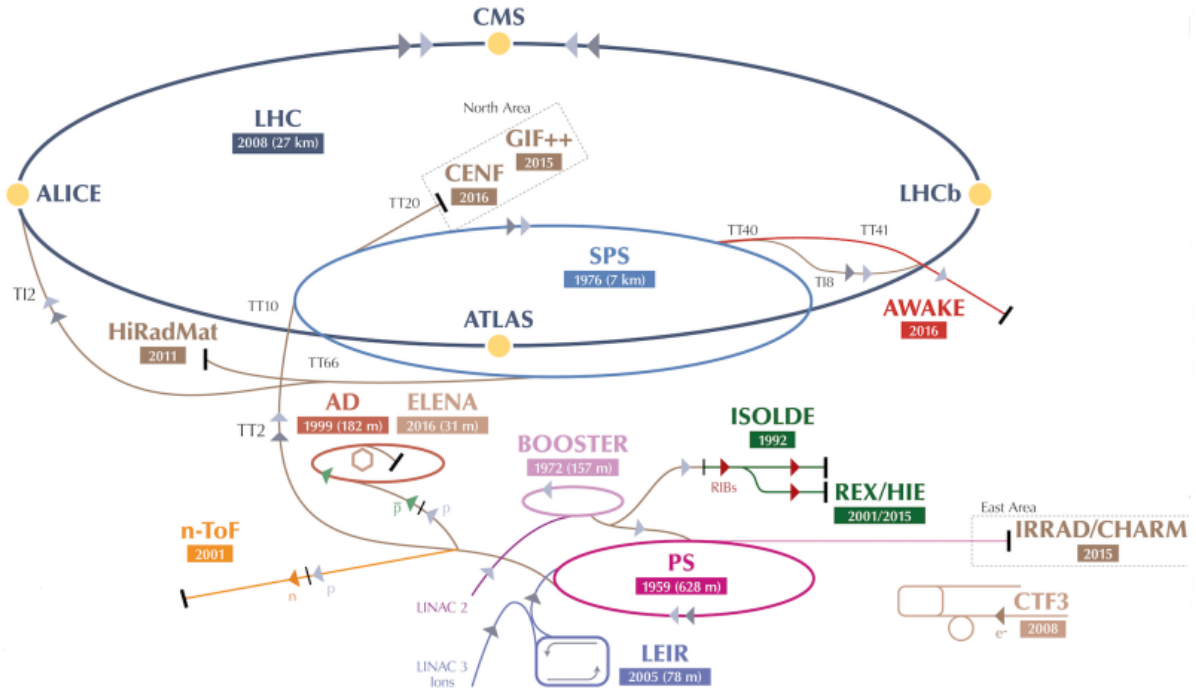

What are the relevant systems, and where are they located?

Electronic systems at the LHC can contain up to thousands of COTS-based units. Some examples:

- **Power converters:** carrying the necessary currents from the external supplies into the magnets.
- **Quench Protection System (QPS):** protecting the superconducting equipment from incidents (quenches) caused by excessive heat.
- Many others (**vacuum, beam instrumentation, cryogenics, RF,** etc.).

The racks can be in the tunnel, to reduce cabling distance from the equipment, or in nearby shielded areas with lower radiation levels.

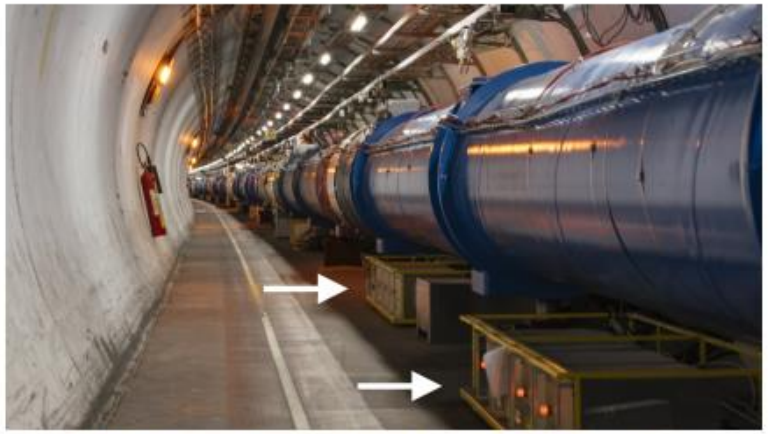

LHC tunnel racks below the beam line

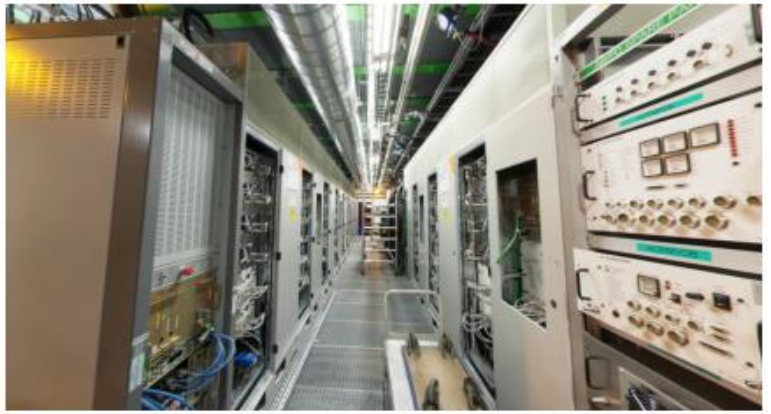

LHC racks in a shielded area

Focusing on the LHC: a typical cycle

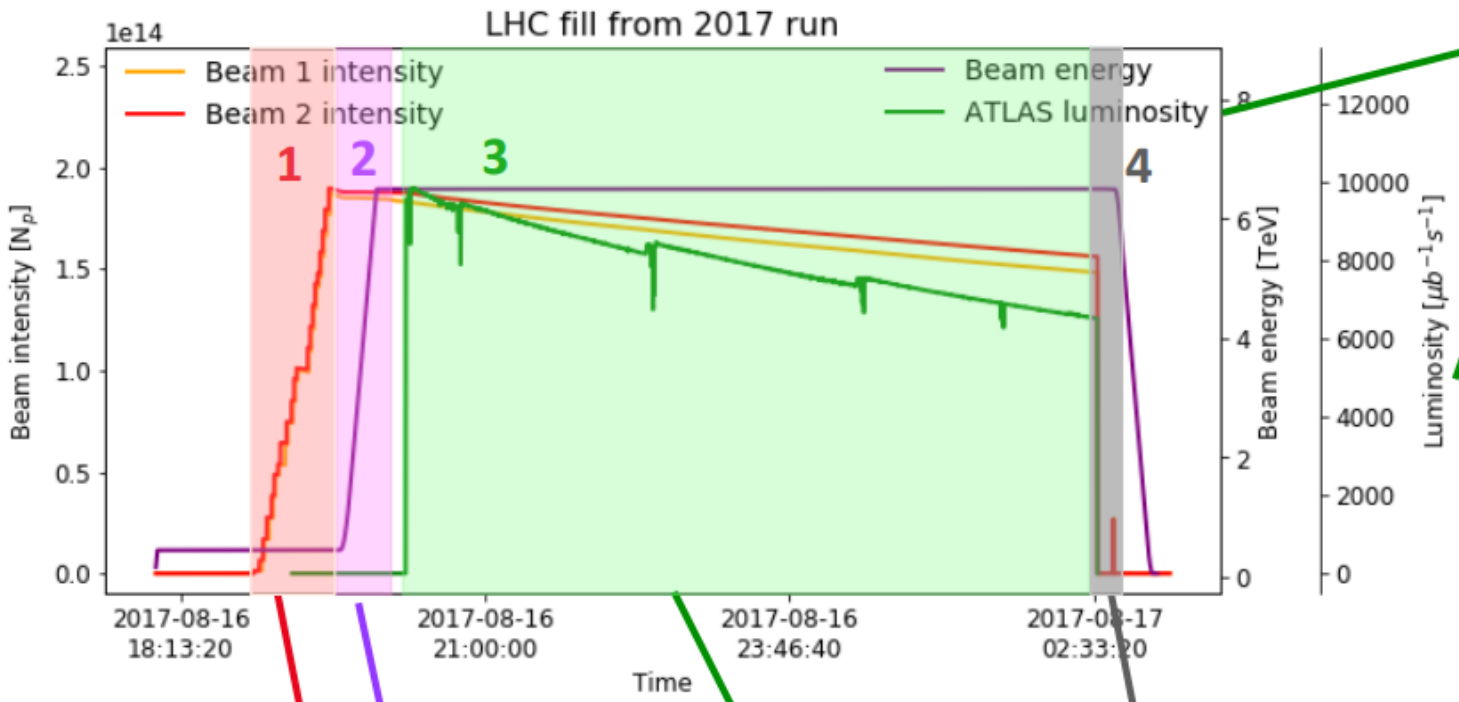

Instantaneous luminosity, proportional to the rate of proton collisions in the IPs.

Beam injection at low energy (450 GeV)

Energy ramp from 450 GeV to 6.5 TeV

Stable beams in collision mode for many hours.

Beam dump, either scheduled or accidental.

LHC fill: simplified sequence

LHC cycles are designed to deliver collisions to the experiments for many hours

→ **goal: maximize time-integrated luminosity.**

R2E failures in critical systems can lead to **premature beam dumps**.

R2E issues at the LHC

Cumulative effects:

- Total Ionising Dose (TID) and Displacement Damage (DD) affecting the equipment lifetime (electronics, magnets, cryogenics…).

Stochastic effects:

- Single Event Effects (SEEs) on electronics, limiting the availability of the LHC by inducing premature beam dumps.

SEE-induced dumps per unit integrated luminosity decreased in the last years of operation thanks to **mitigation** measures. **More improvements are needed for HL-LHC**.

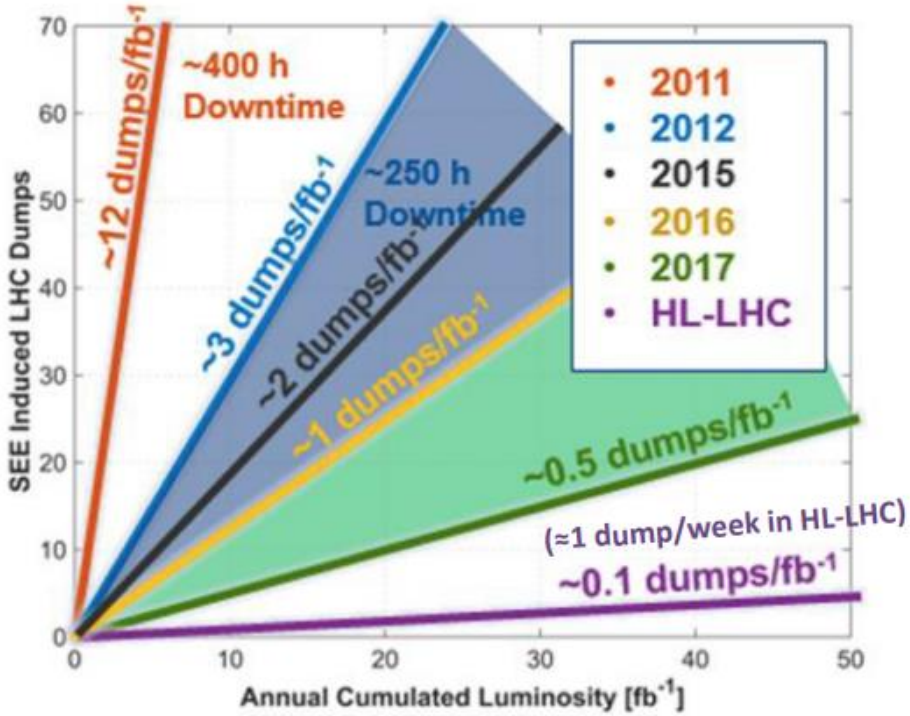

SEE-induced dumps per unit integrated luminosity (in fb^{-1}) from 2011 to HL-LHC. 1 fb^{-1} (with 1b = 10^{24} cm^{-2}) corresponds to ≈10^{14} proton collisions at the TeV scale.

Layout of the LHC

The LHC radiation levels **depend on the location**. The **layout** consists of **eight octants** with left/right sides of 34 **cells**.

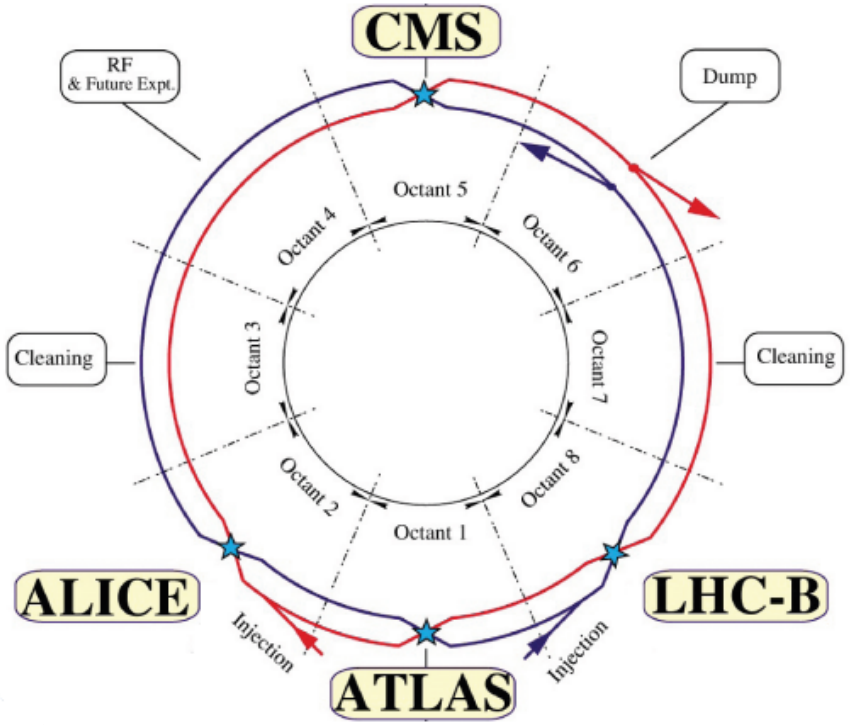

STRUCTURE OF EACH OCTANT

- **Long Straight Section (LSS)**, cells 1-7: key LHC elements (Interaction Points, collimators..).
- **Arc**, cells 14-34: curved section with sequence of dipole and quadrupole magnets.
- **Dispersion Suppressor (DS)**, cells 8-13: curved section connecting LSS and arc.

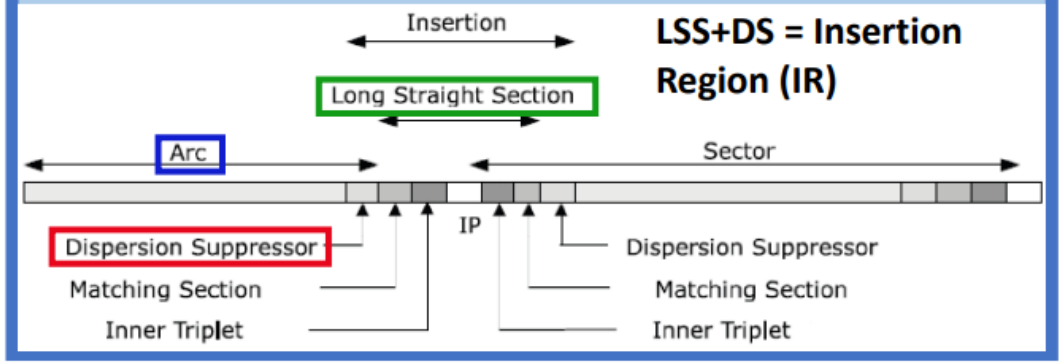

Outline

- Introduction to this course and the Radiation Hardness Assurance discipline
- Basics of radiation-matter interactions and FLUKA Monte Carlo code
- **Radiation environment in the LHC**
  - Setting the scene
  - **Radiation sources and environment description (*)**
  - Tools for radiation monitoring and calculation
  - Radiation levels in the LHC areas relevant to electronics operation
- SPS radiation levels
- FCC-ee radiation levels
- Extra slides

(*) here we only consider prompt radiation sources, but radioactive nuclei are also a very important radiation source, e.g. for radiation protection, but also in some specific cases, for radiation effects on electronics (uranium decay chain contaminants in chip packages; as sources for radiation effects testing, etc.)

Sources of radiation: LHC collisions

Inelastic scattering collisions in the IPs:

$$N_{coll-inel} = \sigma_{inel} \cdot \mathcal{L}_{int}$$

Cross section:
≈ 80 mb for 13-14 TeV collisions

Integrated luminosity in the main IPs (ATLAS and CMS):
≈ 50 fb^{-1}/y in Run 2 (2015-18)
≈ 250 fb^{-1}/y in HL-LHC

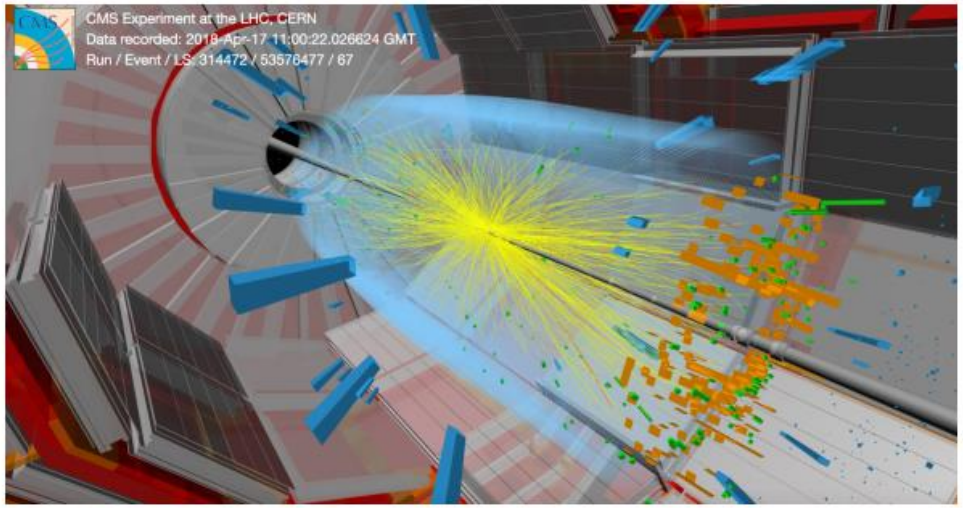

→ ≈ 4·10^{15} inelastic collisions per year in ATLAS/CMS in Run 2, ≈ 2·10^{16} per year in HL-LHC.

The collisions produce particles in all directions, but a major fraction of high-energy products are scattered at **low angles** → they **propagate in the tunnel around the IPs (LSS and DS)** causing **luminosity-driven radiation showers**.

Sources of radiation: beam-machine and beam-gas interactions

Beam-machine interactions

- Before reaching the tunnel, LHC particles typically interact with machine elements, e.g. collimators, absorbers, magnets.
- This is true both for collision products (e.g. IR1-IR5) and in IRs where no collisions are produced, where beam-machine interactions can be seen as the primary source of radiation.

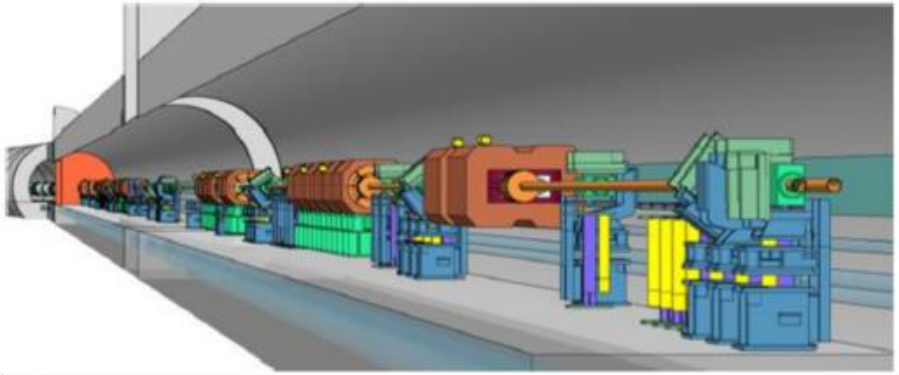

Beam-gas interactions

- Despite the vacuum system, the beam pipes are not empty → the beams can interact with residual gas molecules.
- Sub-dominant effect compared to other sources. Relevant in the arcs, where it can cause R2E issues in distributed systems with many units.

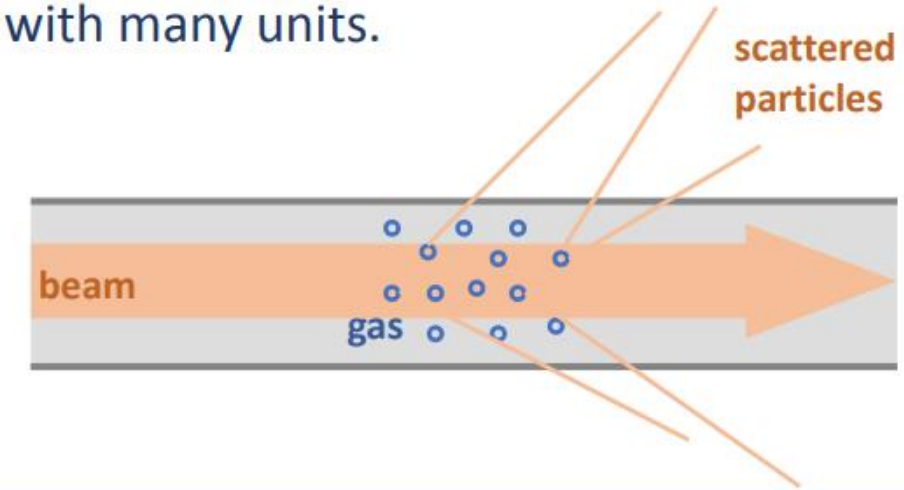

LHC radiation showers

1) **Primary nuclear interaction** (e.g. proton on machine element) producing a cascade of hadrons (p, n, K, π).
2) The shower develops into an **EM component** (from fast $\pi^0 \rightarrow \gamma\gamma$ decay) and a **hadronic component**.
3) **Muons** (and neutrinos) appear from the decay of charged K and π.

Radiation **composition** and **energy spectra** depend on the **energy of the primary interaction**, the **distance travelled** and the **amount of shielding material**.

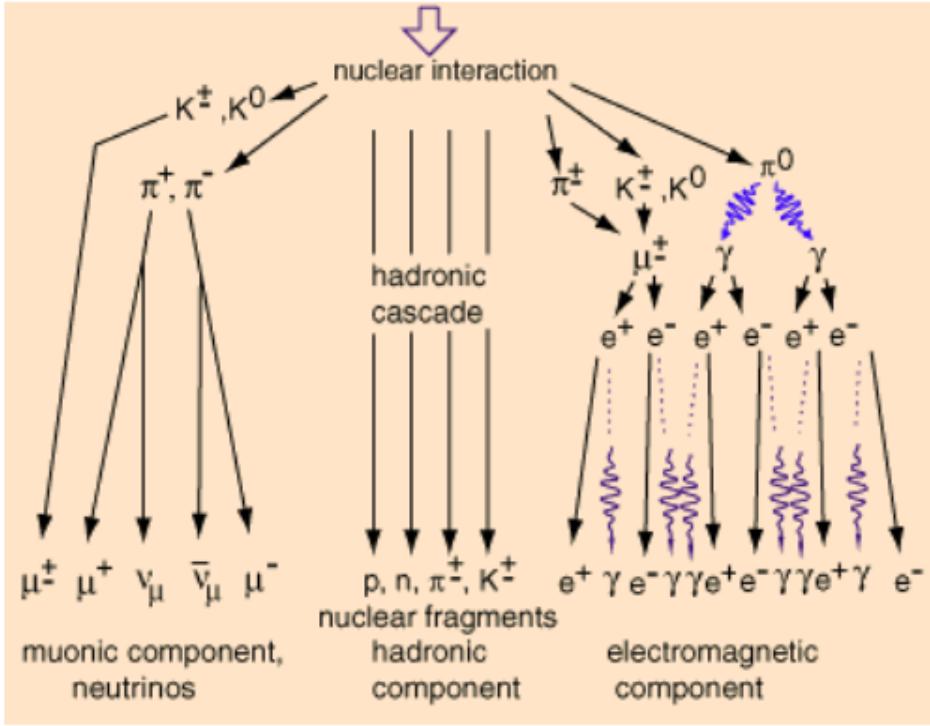

((Atmospheric radiation environment))

- The interactions of galactic cosmic radiation and solar energetic particles with the atmosphere lead to the generation of a cascade of secondary particles which affect the lower reaches of the atmosphere
- These affect microelectronics systems at aircraft altitudes and on the ground through single event effects and enhance the natural background radiation exposure to humans which would normally come from primordial radiation (radioisotopes from the uranium, thorium decay-chains and potassium-40 decays).
- In the European Union, the awareness of the risk to aircrew and passengers resulted in the requirement to monitor and limit aircrew exposure enacted into law as a result of an EU (Euratom) Directive issued in 1996.
- *"Soft errors from radiation are the primary limit on digital electronic reliability. This phenomenon is more important than all other causes of computing reliability put together. As we enter the era of ubiquitous computing, with interlaced intelligence controlling our machines and information, system crashes without hardware defects are black clouds threatening these complex networks."* - Cypress Semiconductor
- In this context traditional cumulative damage effects on microelectronics are not of concern for the natural GCR- and SEP-induced atmospheric environment. However, radiobiological dose and SEEs are potential issues, the latter subject to the microelectronics technology and application.

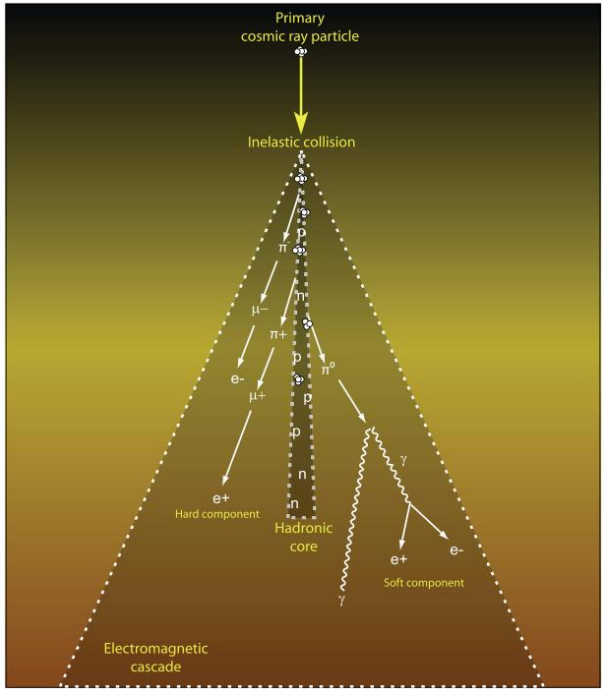

Illustration of an atmospheric secondary particle (air shower) cascade initiated by a primary cosmic ray particle colliding with an atmospheric neutral. The air shower consists of a central hadronic core, surrounded by a spreading cone of muons (the "hard component") and electrons, positrons and photons (the "soft component").

Nordheim, T. A., et al. "Ionization of the Venusian atmosphere from solar and galactic cosmic rays." Icarus 245 (2015): 80-86.

High Energy Hadrons and thermal neutrons

(highlighting the importance of particle energy spectra when describing radiation environment)

Two categories of indirectly ionising radiation responsible for SEEs:

High Energy Hadrons (HEH): p, n, π with E ≳ 20 MeV

- Responsible for both soft and destructive SEEs.
- High energy → local shielding not effective.
- More abundant in the LHC tunnel.

Thermal neutrons: E ≈ 0.25 eV

- Responsible for soft SEEs only, e.g. through the ^{10}B (n,α) reaction.
- Typically more abundant in shielded alcoves.

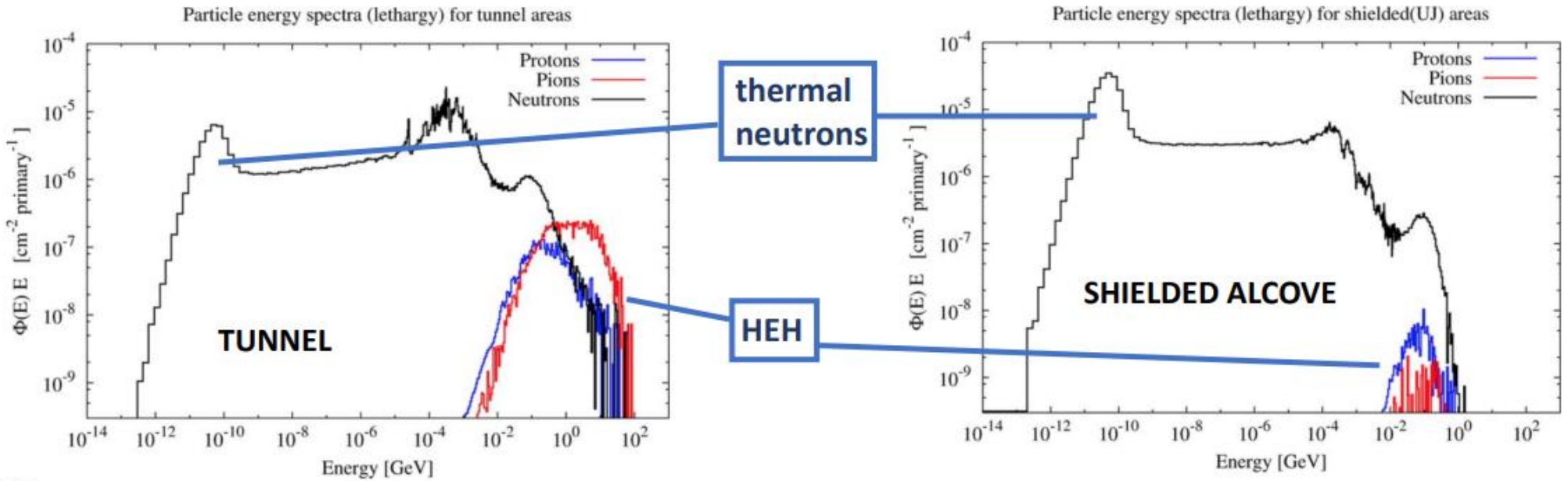

The High Energy Hadron (HEH) approach

- The SEE rate is the product of **fluence (ϕ, in units of cm^{-2})** and **cross section (σ, in cm^2)**:

$$N_{SEE} = \Phi_{th}\sigma_{th} + \Phi_{HEH_{eq}}\sigma_{HEH} \qquad R \equiv \Phi_{th}/\Phi_{HEH_{eq}}$$

Thermal neutron term | **HEH term** | **R-factor: ratio of thermal and HEH fluence**

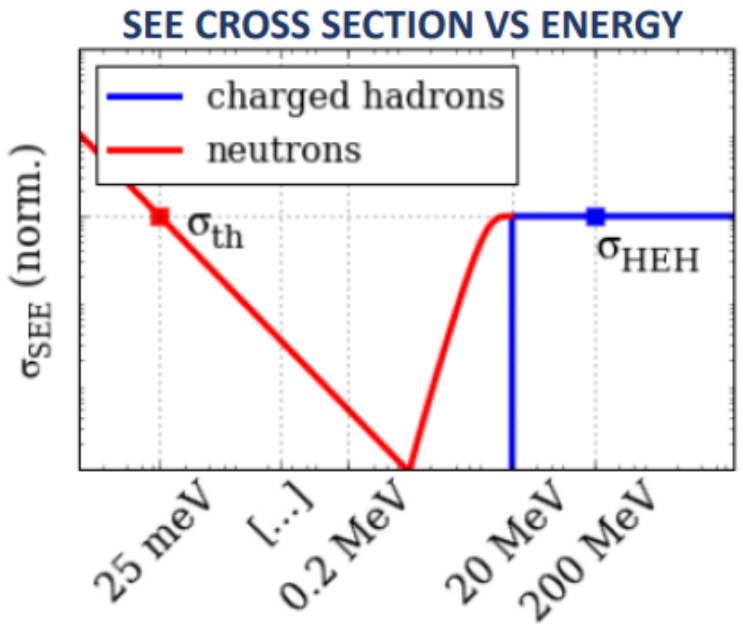

- The **cross sections** σ_{th} and σ_{HEH} are measured in radiation test campaigns in specific conditions (energy, particle type).
- We then define energy-integrated **fluences**, weighted to absorb the **energy dependence of the cross sections**:
  - $\phi_{HEH\text{-}eq}$: constant weight above 20 MeV for all hadrons, weighted (Weibull) contribution of 0.2-20 MeV neutrons.
  - ϕ_{th}: thermal-energy neutrons weighted with the inverse of velocity ($E^{-1/2}$)

Outline

- Introduction to this course and the Radiation Hardness Assurance discipline
- Basics of radiation-matter interactions and FLUKA Monte Carlo code
- **Radiation environment in the LHC**
  - Setting the scene
  - Radiation sources and environment description
  - **Tools for radiation monitoring and calculation**
  - Radiation levels in the LHC areas relevant to electronics operation
- SPS radiation levels
- FCC-ee radiation levels
- Extra slides

Monitoring and calculation tools

Main tools for the measurement and prediction of radiation levels at the LHC, often used in combination:

≈4000 **Beam Loss Monitors (BLMs)** in the tunnel.

Gas-filled ionisation chambers used for machine protection, also providing **online TID** measurements → used within the R2E team to perform radiation level analyses.

≈400 **RadMons** in tunnel and shielded areas

Each measures **TID** and **HEH**, **thermal neutron** and **1MeV neutron equivalent** fluences with COTS-based detectors.

FLUKA: Monte Carlo code that simulates radiation showers and is able to calculate R2E-relevant quantities (TID, fluences).

Monitoring and calculation tools

Distributed Optical Fibre Radiation Sensors

DOFRS is based on:
- **Radiation Induced Attenuation** (RIA) in suitable specialty OFs (*not any optical fibre*)
- **Optical Time Domain Reflectometry**

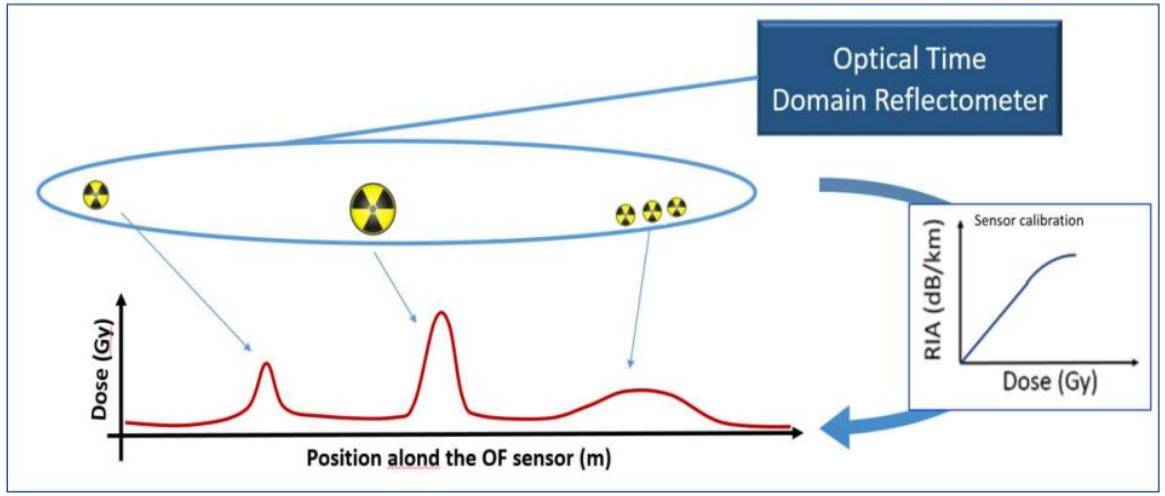

First implementation reported by *H. Henschel et al., Nucl. Instr. & Meth. in Phys. Res. A, vol. 526, no. 3, pp. 537–550, 2004*

"Optical Fibre Dosimetry", D. Di Francesca, R2E Annual Meeting 2022

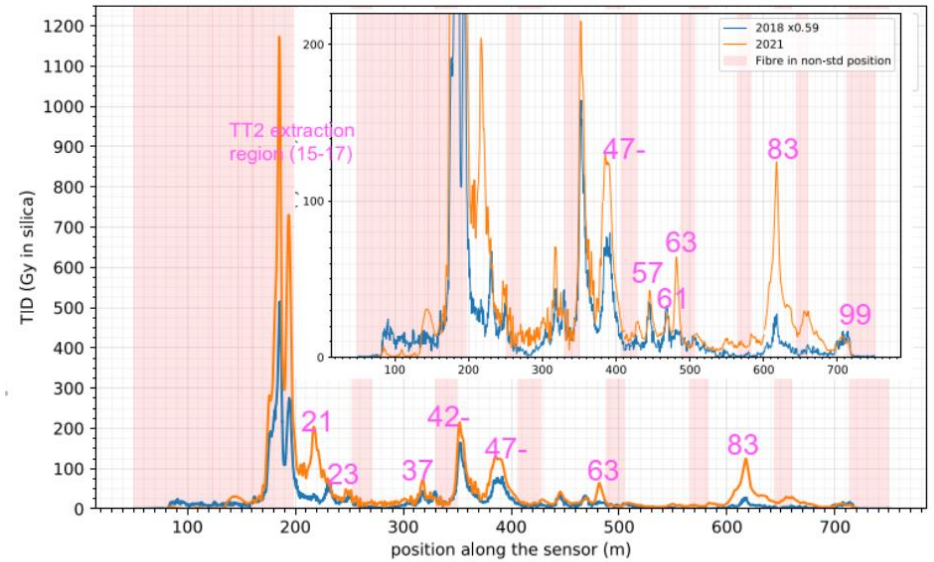

PS

"Overview of 2021 prompt radiation levels in the injector chain" , K. Bilko, IPP meeting 13th January 2022

Monitoring and calculation tools

Solid state detector with fast readout electronics

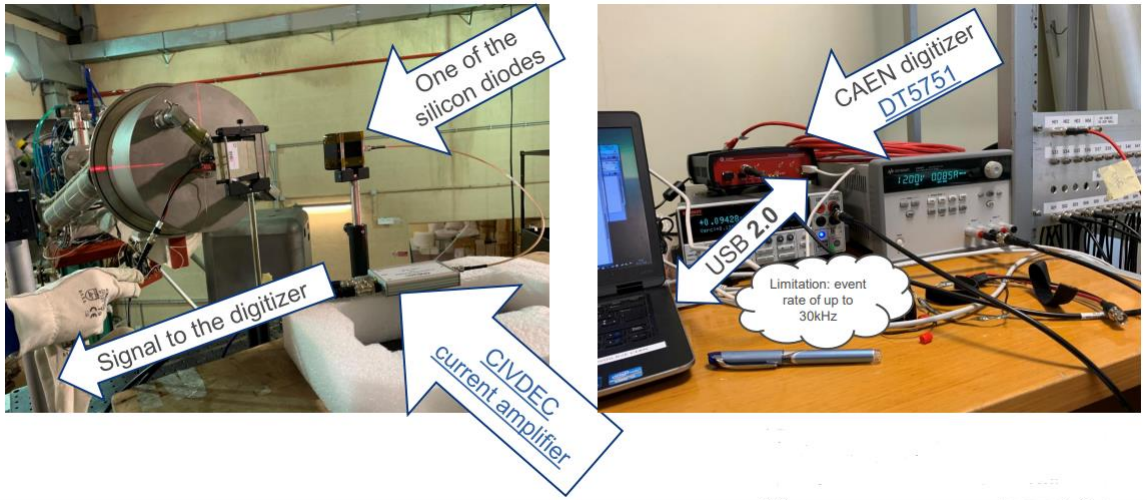

"Silicon Diode as R2E detector", K. Bilko, R2E Annual Meeting 2021

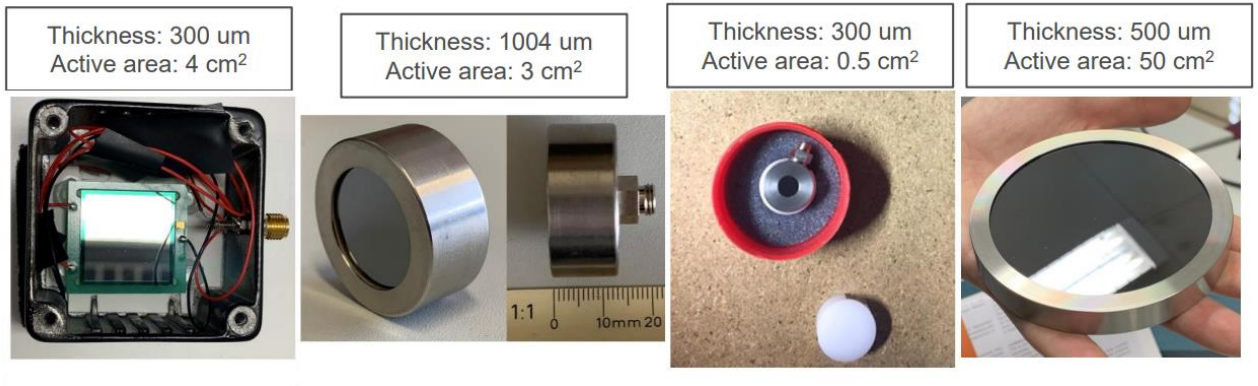

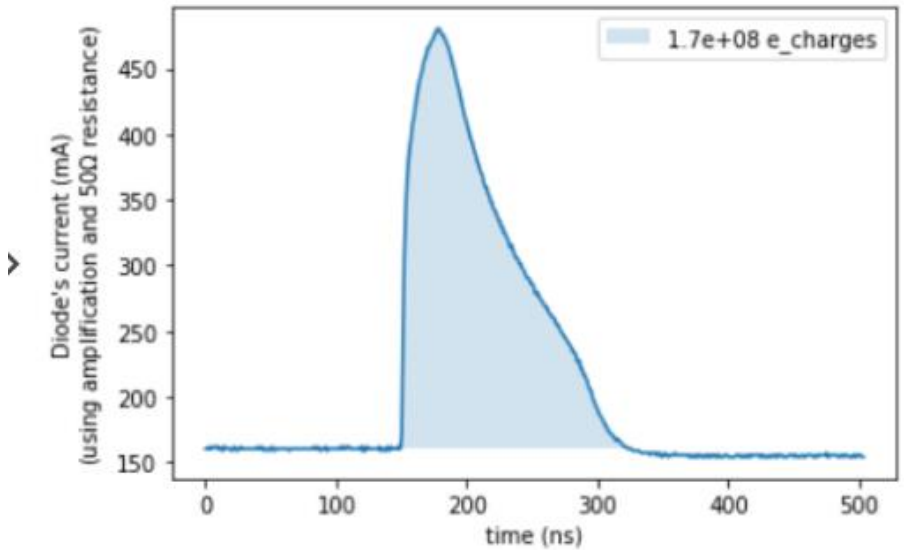

Monitoring and calculation tools

High level dosimetry

Radio-Photo-Luminescence Dosimeter (RPL)

- Cylinder: **Ag-activated metaphosphate glass** (length: 8.5mm, diameter: 1.5mm)
- Irradiation creates Radio-Photo-Luminescence (RPL) and colour centres
- Readout measurement based on an in-house setup
  - **Dose range: 1 Gy - MGy**

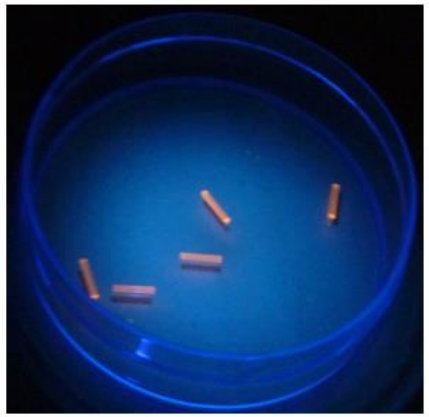

Irradiated RPL dosimeters when being illuminated with UV light

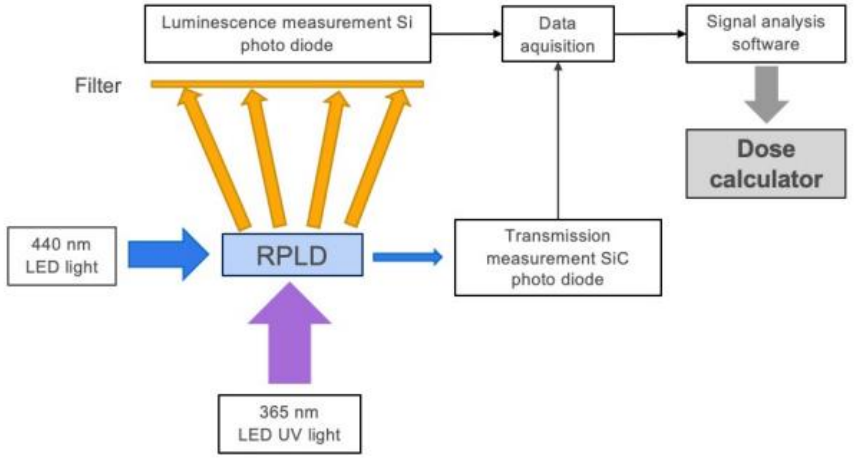

"High Level Dosimetry", Y. Aguiar, R2E Annual Meeting 2022

Outline

- Introduction to this course and the Radiation Hardness Assurance discipline
- Basics of radiation-matter interactions and FLUKA Monte Carlo code
- **Radiation environment in the LHC**
  - Setting the scene
  - Radiation sources and environment description
  - Tools for radiation monitoring and calculation
  - **Radiation levels in the LHC areas relevant to electronics operation**
- SPS radiation levels
- FCC-ee radiation levels
- Extra slides

The ATLAS Insertion Region (IR1)

Highest radiation levels in the Insertion Regions hosting the interaction points. Below I show **IR1** (ATLAS) but **IR5** (CMS) has a similar geometry (with few layout differences).

The ATLAS cavern, the LHC tunnel (LSS of IR1, ± ≈250m from ATLAS) and several shielded areas (e.g. UJ16, see next slides) are shown in the layout below:

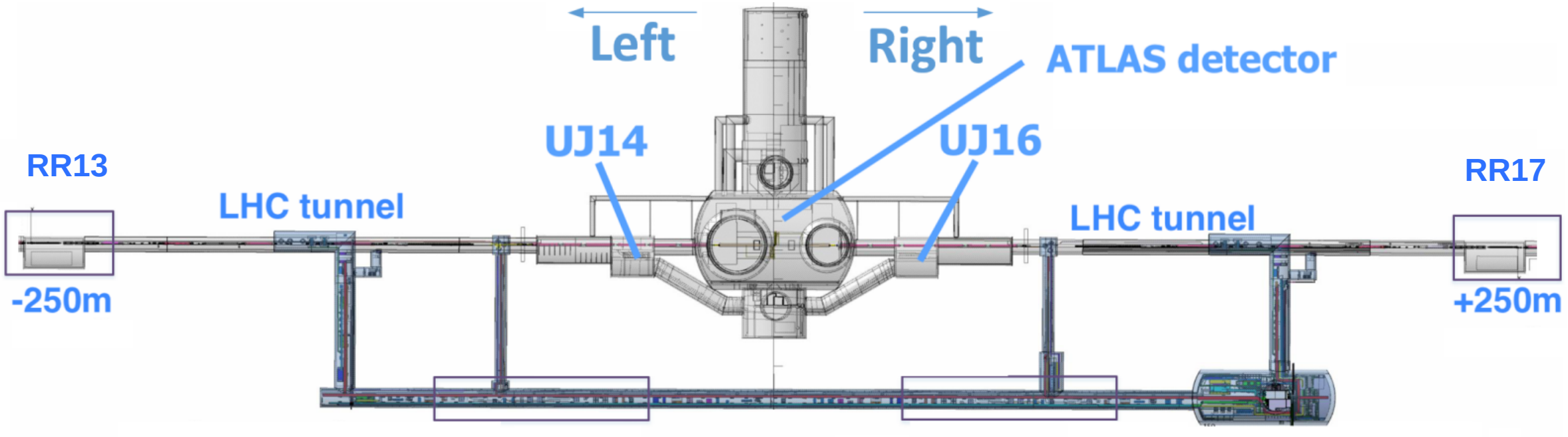

Radiation levels in the ATLAS detector

Cylindrical shape around the Interaction Point where the collisions take place → highest radiation levels in the inner layers (silicon detectors for particle tracking).

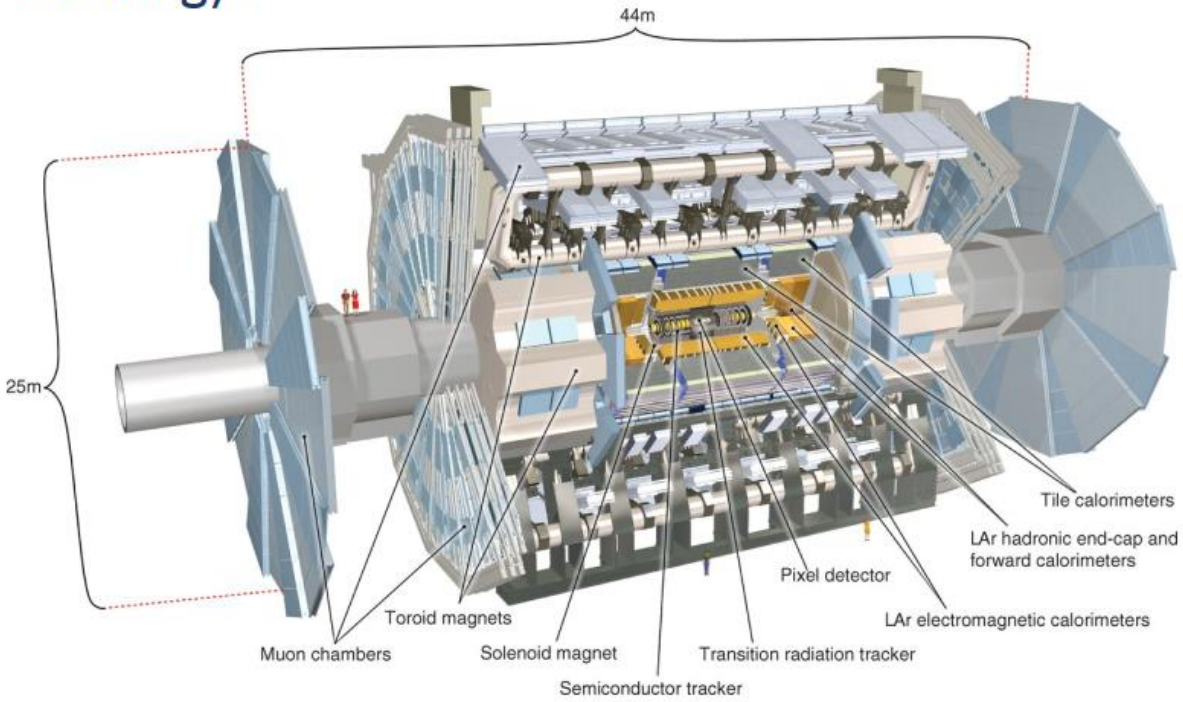

Up to **10 MGy** and **10^{16} $n_{1MeV-eq}/cm^2$** for HL-LHC (4000 fb^{-1} in 12 years).

Requires rad-hard electronics.

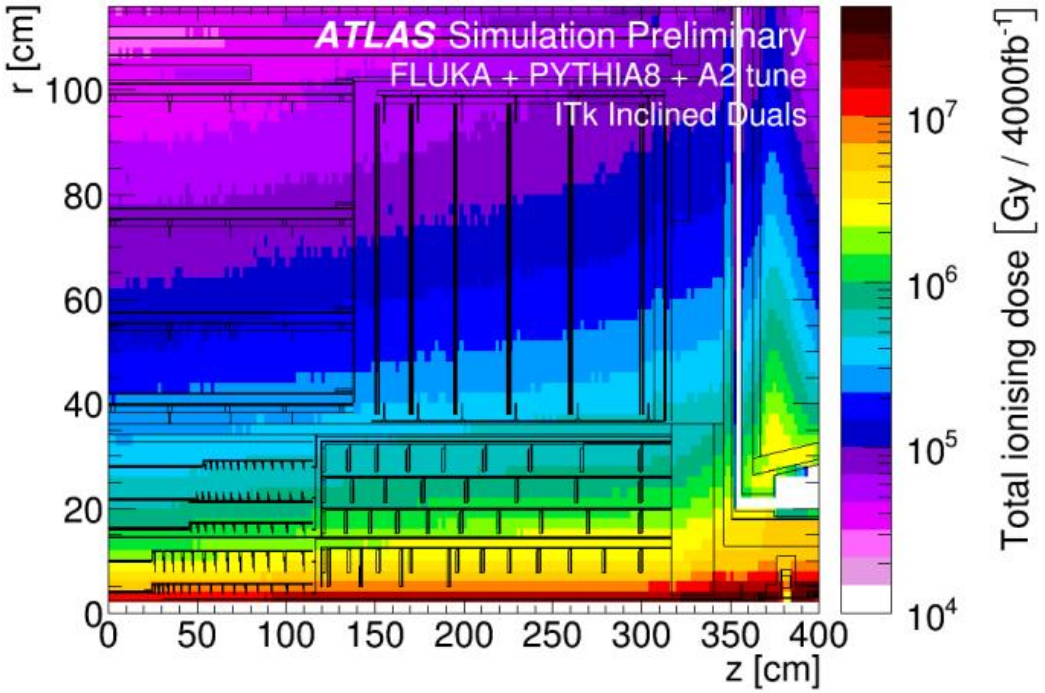

Radiation level specification document for HL-LHC

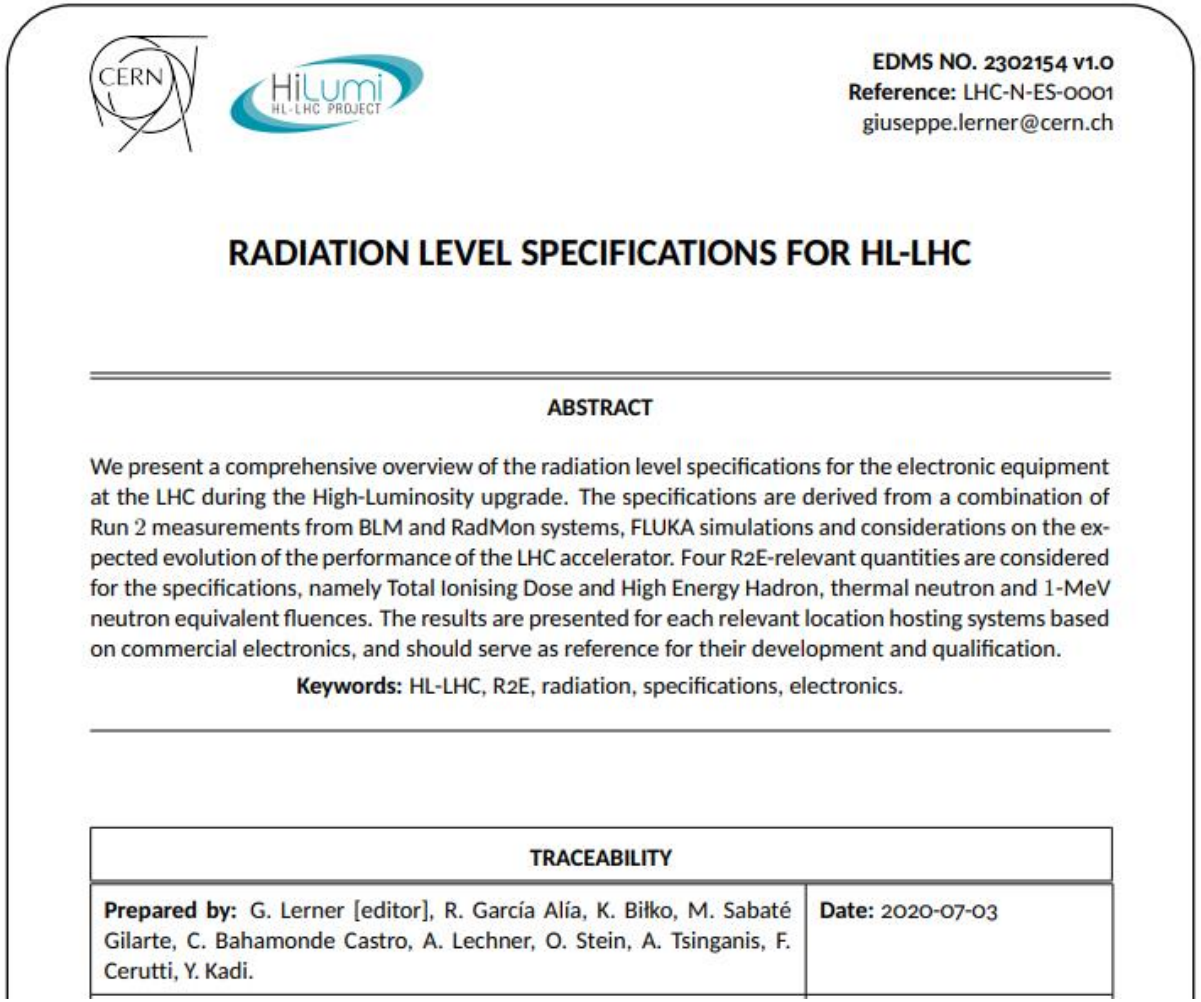

CERN HiLumi HL-LHC PROJECT

EDMS NO. 2302154 v1.0
Reference: LHC-N-ES-0001
giuseppe.lerner@cern.ch

RADIATION LEVEL SPECIFICATIONS FOR HL-LHC

ABSTRACT

We present a comprehensive overview of the radiation level specifications for the electronic equipment at the LHC during the High-Luminosity upgrade. The specifications are derived from a combination of Run 2 measurements from BLM and RadMon systems, FLUKA simulations and considerations on the expected evolution of the performance of the LHC accelerator. Four R2E-relevant quantities are considered for the specifications, namely Total Ionising Dose and High Energy Hadron, thermal neutron and 1-MeV neutron equivalent fluences. The results are presented for each relevant location hosting systems based on commercial electronics, and should serve as reference for their development and qualification.

Keywords: HL-LHC, R2E, radiation, specifications, electronics.

TRACEABILITY	
Prepared by: G. Lerner [editor], R. García Alía, K. Biłko, M. Sabaté Gilarte, C. Bahamonde Castro, A. Lechner, O. Stein, A. Tsinganis, F. Cerutti, Y. Kadi.	**Date:** 2020-07-03

IR1 (ATLAS) and IR5 (CMS) Long Straight Sections (LSS)

Collision products leak from the interaction region at the centre of the experiments into the LSS (and DS). The levels vary with the **distance from the IP** due to the interactions with different beamline elements.

Main message: the levels in the LSS are too high for COTS electronics.

For 4000 fb^{-1}:

- **TID: 1 kGy-1MGy.**
- **$n_{1MeV-eq}$ fluence: 10^{12}-10^{16} cm^{-2}.**
- **HEH fluence: 10^{12}-10^{15} cm^{-2}.**

Total HL-LHC dose 80cm below the beam in the LSS of IP1 and IP5

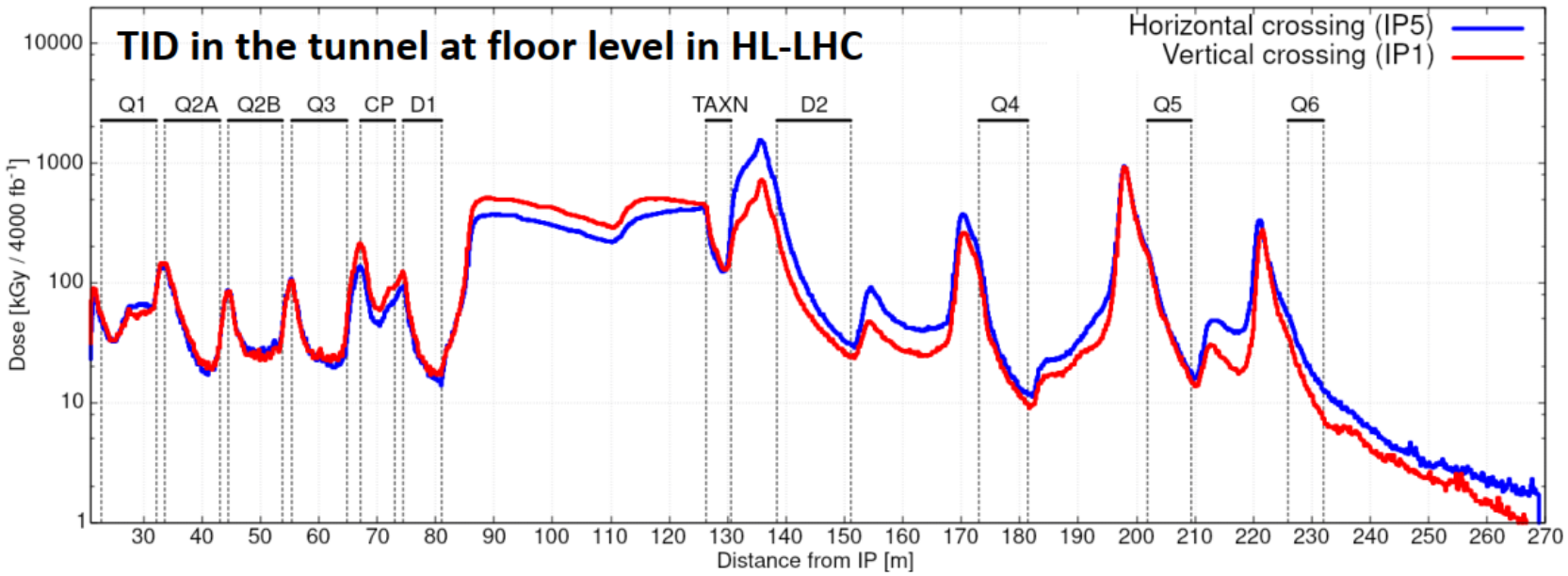

Radiation levels in the UJ

A lot of electronics relocated away from the UJs (and e.g. into the ULs) during Run 1 and LS1

UJ16: heavily shielded area (2m of concrete and cast iron, maze-shaped entrance) close to ATLAS (IR1). It hosts **active electronics** → we focus on **HEH fluence for SEE risks.**

Heavy shielding → HEH fluence from ≈10^{13} cm^{-2}/y in the tunnel to ≈10^{9} cm^{-2}/y in the UJ.

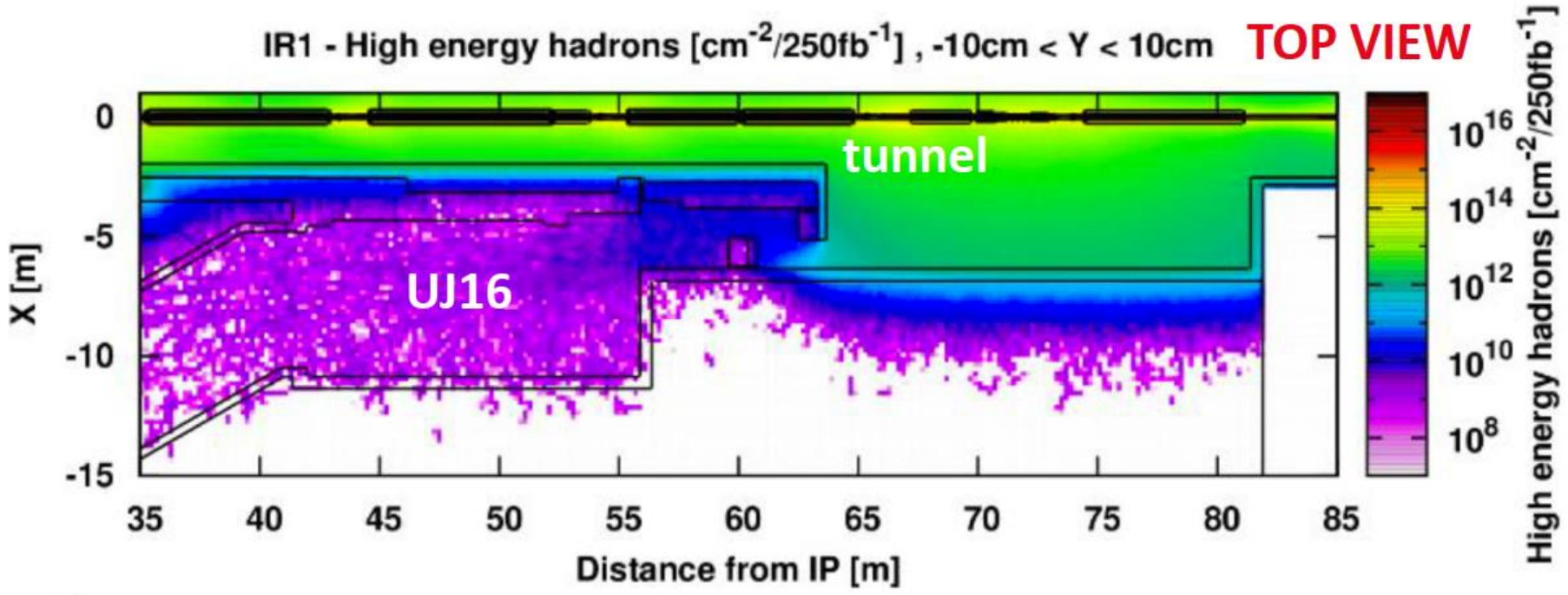

Other quantities:

- **TID ≈1 Gy/y**
- **thermal neutrons >10^{10} cm^{-2}/y, R-factor ≈ 50**

Radiation levels in the RR

RR vs UJ: farther from the IP (≈250 m), less shielding (40 cm cast iron).
Main radiation source: scattered protons from the IP hitting the **TCL6 collimator**.

Below: FLUKA top view of **annual (250 fb^{-1}) HL-LHC HEH fluence** in the LHC tunnel and in RR57 (IR5).

Annual RR levels (for 250 fb^{-1}):

- **HEH fluence ≈3·10^{9} cm^{-2}/y**
- **TID ≈5 Gy/y**
- **thermal neutron fluence ≈3·10^{10} cm^{-2}/y, R-factor ≈ 10** (less shielding → harder energy spectrum with respect to the UJ)

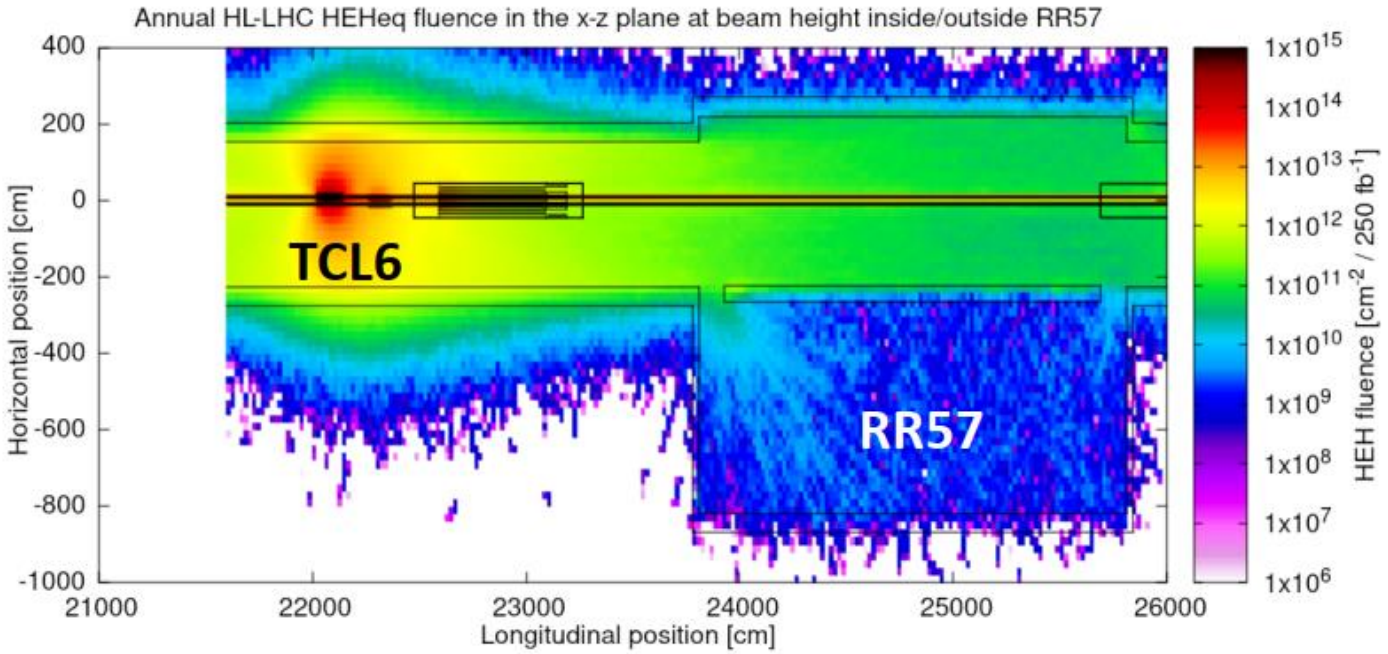

IR1 and IR5 Dispersion Suppressor (DS): TID

Scattered protons from the IPs can reach the **DS**.

HL-LHC FLUKA TID below the beamline for **proton operation (4000 fb^{-1})** and **ion operation (10 nb^{-1})**:

- TID in the **10Gy - 10kGy** range (peaks in cells 9-11): less than in the LSS but still significant.
- ion TID peak caused by the **Bound Free Pair Production (BFPP)** process: high radiation levels cumulated locally (cell 11) in short runs.
- Typical qualification limit for electronic racks: **200 Gy**. Dedicated strategies where these levels are exceeded.

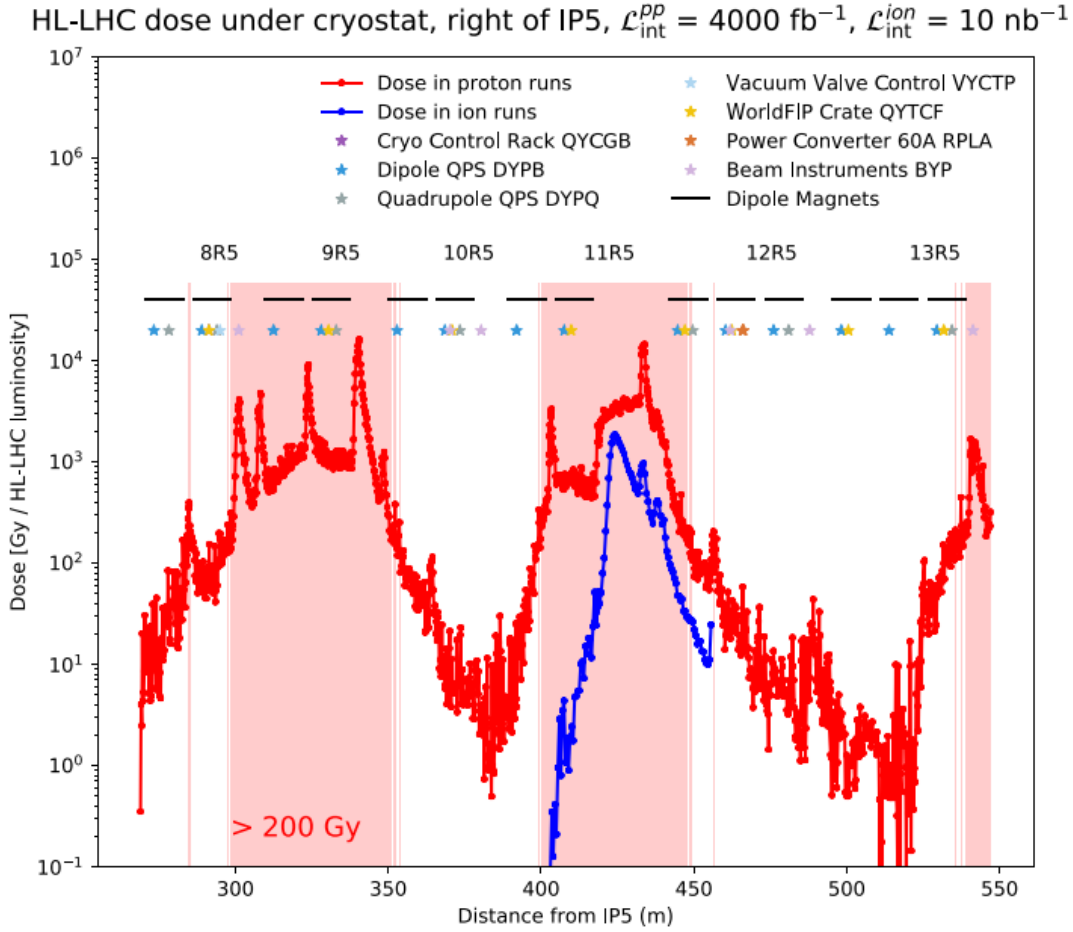

IR1 and IR5 Dispersion Suppressor (DS): fluences

HL-LHC FLUKA **fluence of HEH, thermal neutrons and 1MeV equivalent neutrons** below the beamline for proton operation (4000 fb^{-1}):

- the pattern is similar to the one observed for TID, with peaks in cells 9-11.
- **HEH fluence** in the **10^{9}-10^{13} cm^{-2}** range → SEE risk for sensitive equipment.
- Ion operation not considered in the plot (remember: no active electronics in proximity of the BFPP peak).

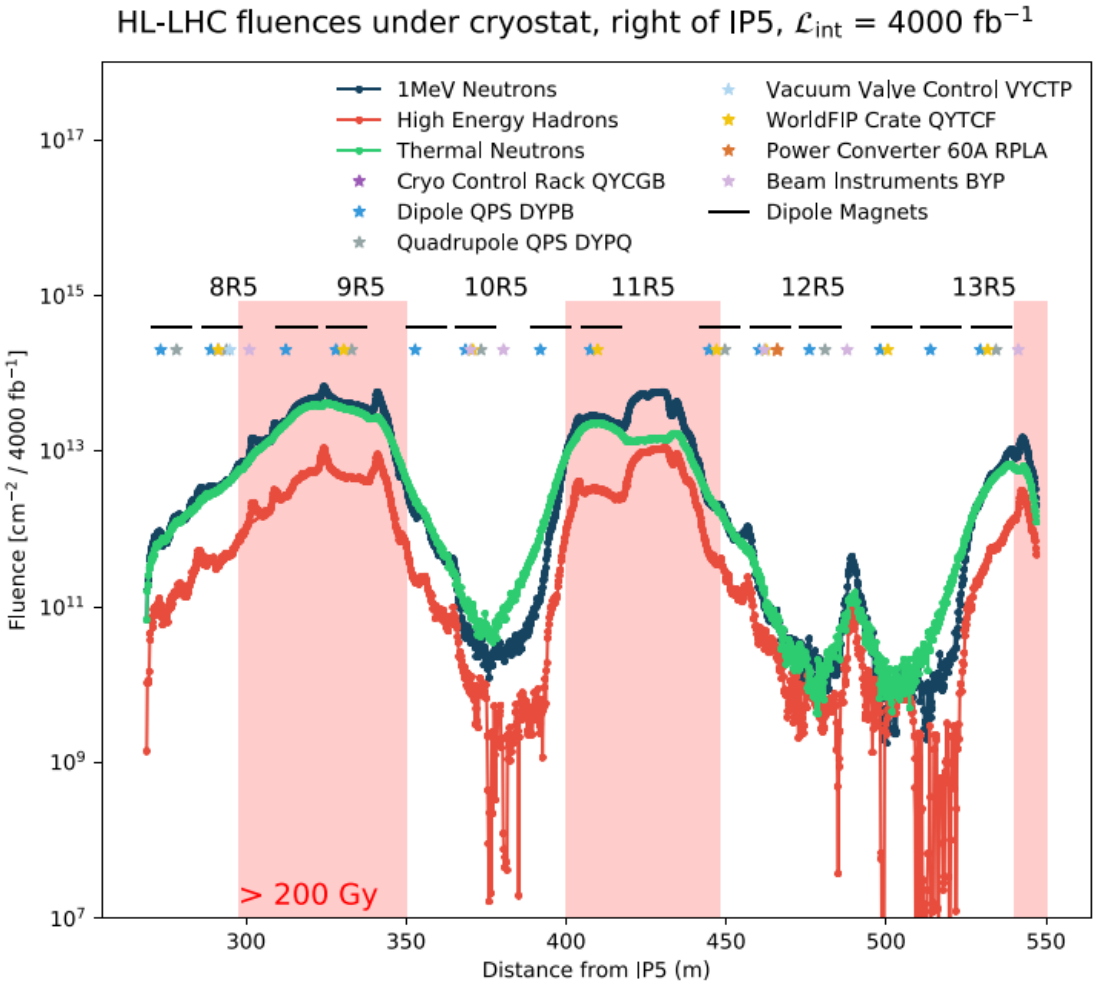

Integrated luminosity scaling and machine parameters

Profile of **TID per unit integrated luminosity** vs distance from IP1 (from cell 4 to 10) in 2016, 2017 and 2018 as measured by the BLM system.

TID is proportional to integrated luminosity up to cell 5, then **discrepancies emerge** due to changes in machine parameters (e.g. collimator settings).

The impact of such changes can be critical for R2E → important to monitor the radiation levels during operation.

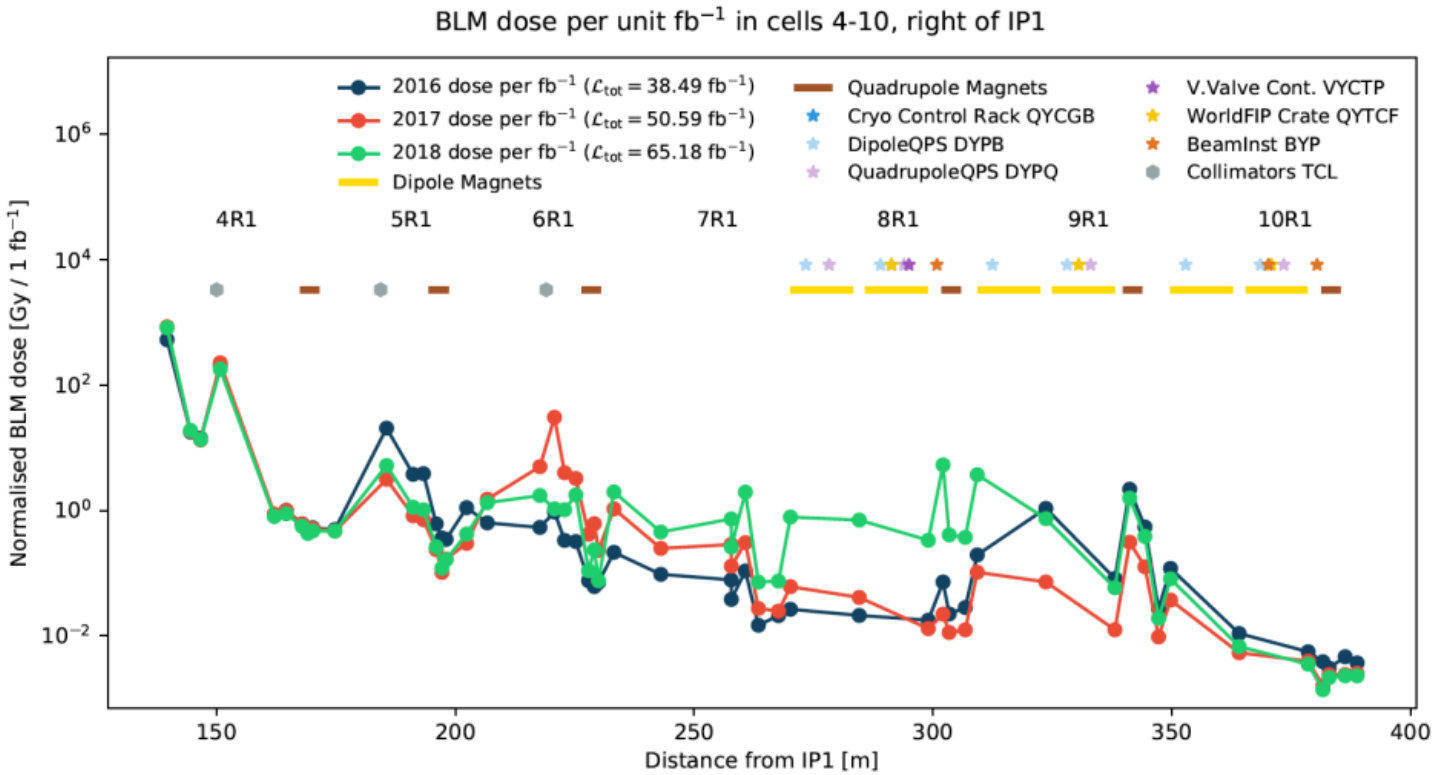

Benchmark against simulation

13th Int. Particle Acc. Conf. IPAC2022, Bangkok, Thailand JACoW Publishing
ISBN: 978-3-95450-227-1 ISSN: 2673-5490 doi:10.18429/JACoW-IPAC2022-MOPOMS042

COMPARISON BETWEEN RUN 2 TID MEASUREMENTS AND FLUKA SIMULATIONS IN THE CERN LHC TUNNEL OF THE ATLAS INSERTION REGION

D. Prelipcean, G. Lerner, R. García Alía, K. Bilko, M. Sabaté Gilarte, F. Cerutti,
D. Di Francesca, D. Ricci, A. Ciccotelli, B. Humann
CERN, Geneva, Switzerland

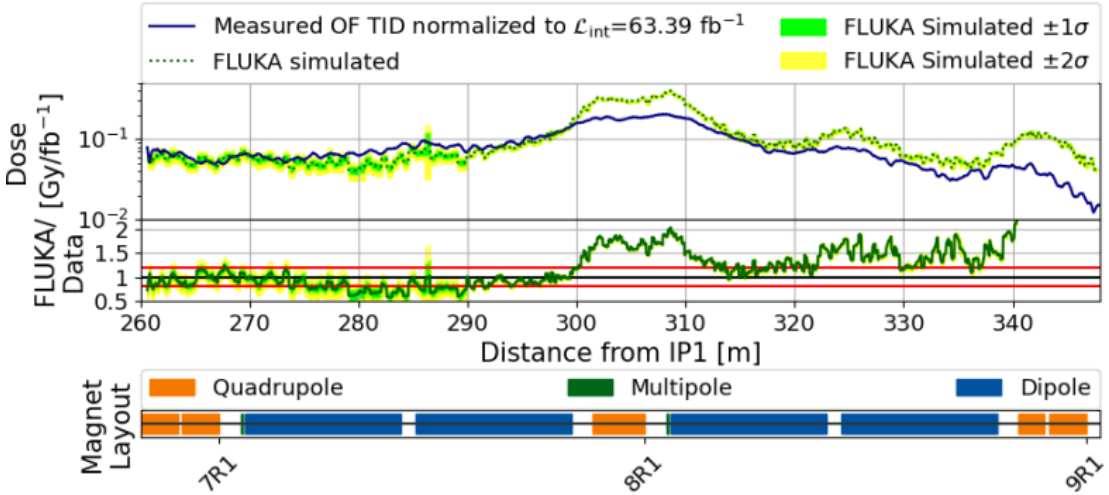

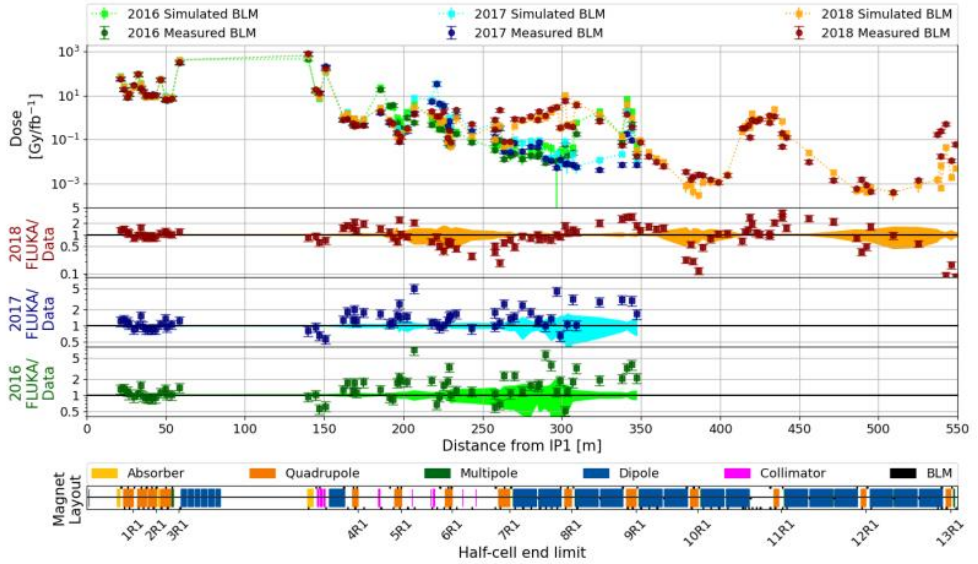

Figure 1: Top pannel: Comparison between BLM data and FLUKA predictions for the tunnel in the right side of IP1 (ATLAS detector) for 3 years of Run 2 operation with different configurations: 2018 with LSS+DS+ARC TCL456: 15s-35s-park RP: IN (red), 2017 with LSS+DS TCL456: 15s-35s-20s RP: IN (blue), and 2016 with LSS+DS TCL456: 15s-15s-open RP: OUT (green). Center pannels: The ratio of FLUKA simulated values to the BLM measurements. Lower pad: Machine beamline layout, with markers at the cell limits right of IP1.

Radiation levels in the arcs

Radiation levels in the **eight LHC arc sectors** are dominated by **beam-gas interactions**.

During the last year of operation (2018):

- **TID < 100 mGy** (from BLM measurements).
- **HEH fluence ≈5·10^{7} cm^{-2}** (from RadMons).

These levels are much lower compared to the areas of the machine examined so far, but they can still be **critical for SEEs** because the arc hosts **distributed systems with hundreds of units**
→ *even if the SEE risk for each unit is low, the system-level SEE risk (i.e. summed over all units) can be large.*

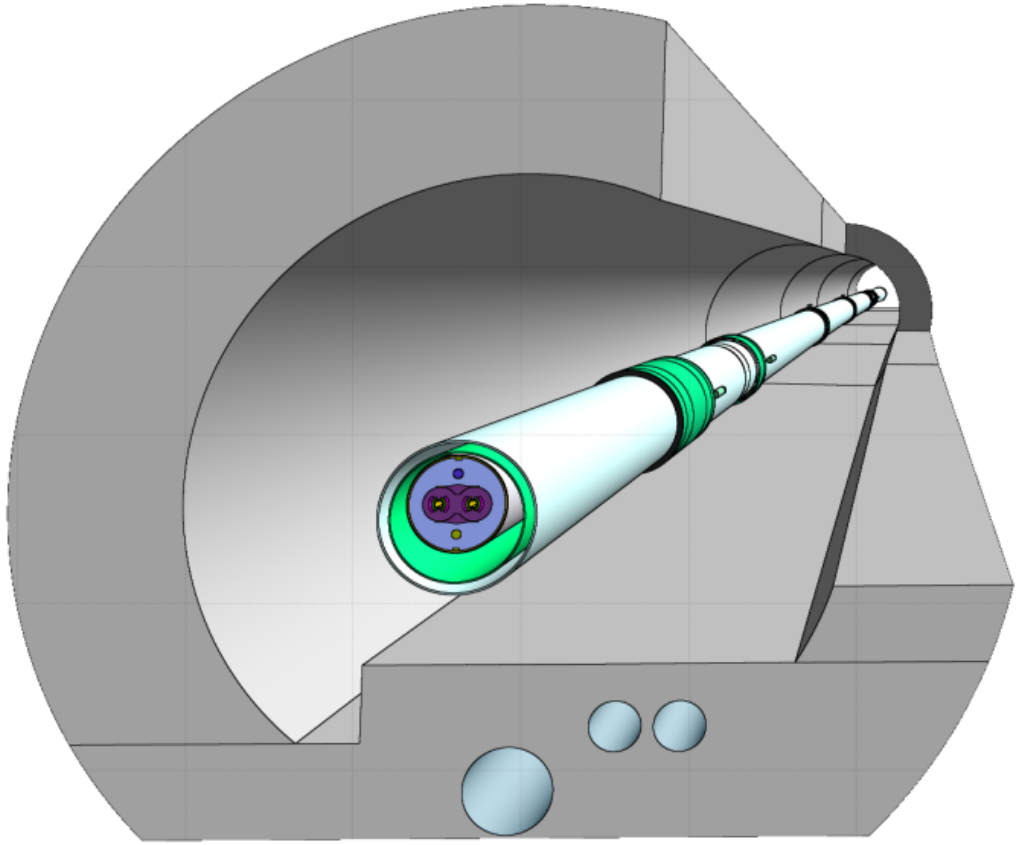

LHC arc section in FLUKA model

Radiation levels in the arcs

Radiation Environment in the LHC Arc Sections During Run 2 and Future HL-LHC Operations

Kacper Biłko, Cristina Bahamonde Castro, Markus Brugger, Rubén García Alía, Yacine Kadi, Anton Lechner, Giuseppe Lerner, and Oliver Stein

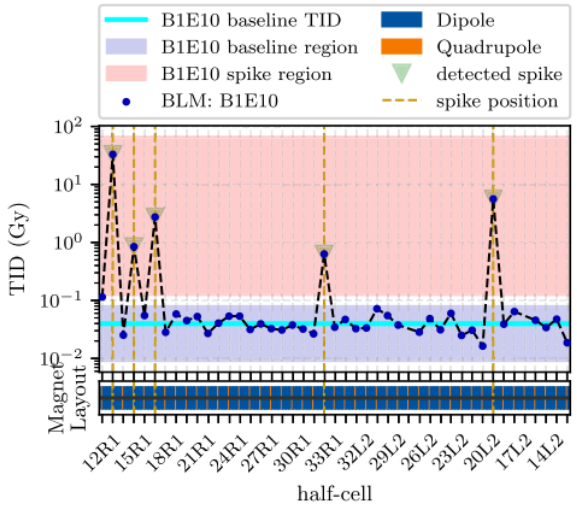

Fig. 3. TID (dose in N_2) measured during the 2018 p–p operation by the BLMs from B1E10 family (position illustrated in Fig. 2) in the arc sector 12. With few exceptions (spikes) majority of the BLMs measured similar dose level, i.e., baseline (estimated as an average TID measured within one BLM family excluding outliers).

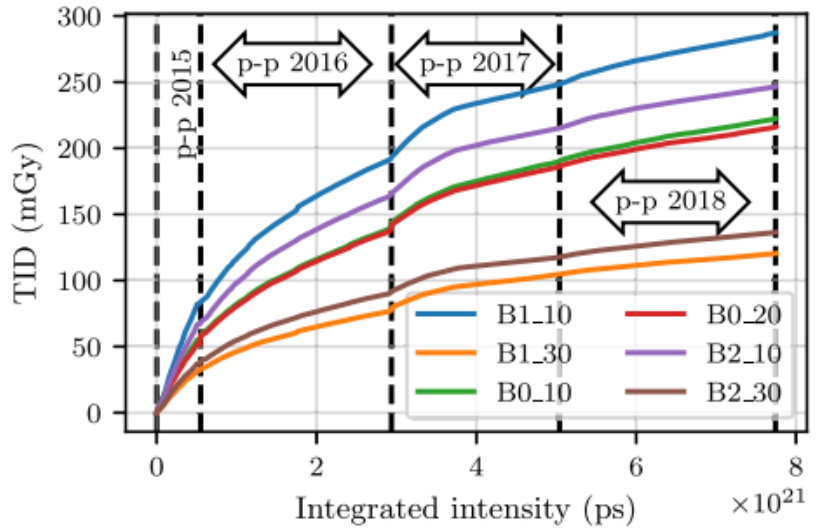

Fig. 4. Evolution of the baseline TID levels (dose in N_2) in the arc sector 12 over integrated beams intensity for top energy (protons with >5 TeV). Including integrated intensities for injection modes (protons with 450 GeV) has no impact on both the evolution and dose levels due to the low contribution of injection modes to total integrated intensity (less than 10% of total integrated beams intensity). Similar evolution trend was observed for all BLM families and all arc sectors—nonlinear evolution until mid-2017 and linearity afterward.

Summary of radiation levels at the LHC

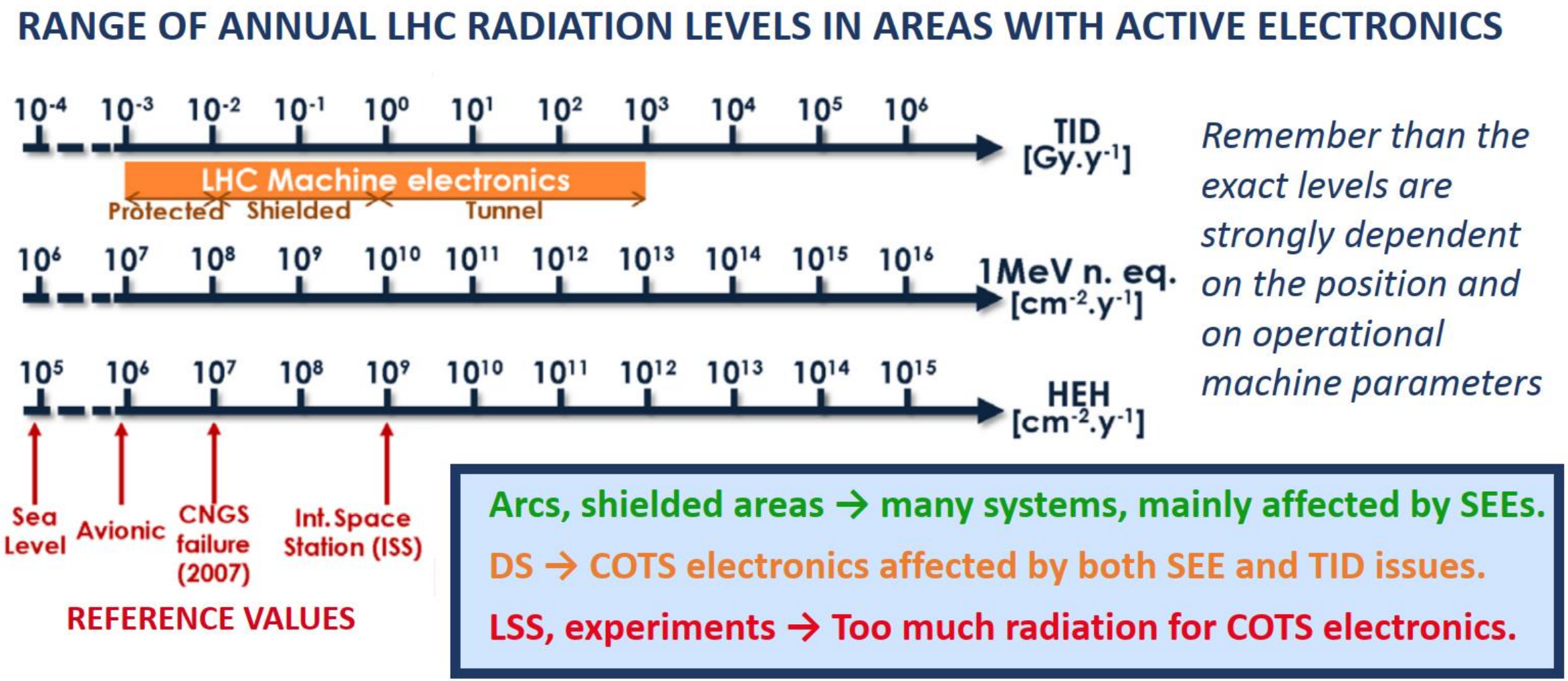

Remember than the exact levels are strongly dependent on the position and on operational machine parameters

Arcs, shielded areas → many systems, mainly affected by SEEs.

DS → COTS electronics affected by both SEE and TID issues.

LSS, experiments → Too much radiation for COTS electronics.

R2E order of magnitude levels and effects (very approximative!)

High-energy hadron fluence (cm^{-2} $year^{-1}$)		Total Ionizing Dose for 10 years (Gy)	Effects on Electronics
10^5	***Sea level***	<<1	Possible SEE impact for commercial systems with MANY units and VERY demanding availability and reliability requirements
10^7	***LHC tunnel: arc***	<1	SEE impact for systems with multiple units and demanding availability and reliability requirements
10^9	***LHC shielded areas***	10	SEE mitigation (e.g. redundancy) at system level; cumulative effects can start to play a role
10^{11}	***LHC tunnel: DS***	1000	SEE mitigation (e.g. redundancy) at system level, very challenging TID level for COTS
10^{15}	***HL-LHC experiments***	10 MGy	Rad-hard by design ASICs

Approximation (mainly for high-energy accelerator environment): 10^9 HEH/cm^2 ~ 1 Gy

Outline

- Introduction to this course and the Radiation Hardness Assurance discipline
- Basics of radiation-matter interactions and FLUKA Monte Carlo code
- Radiation environment in the LHC
  - Setting the scene
  - Radiation sources and environment description
  - Tools for radiation monitoring and calculation
  - Radiation levels in the LHC areas relevant to electronics operation
- **SPS radiation levels**
- FCC-ee radiation levels
- Extra slides

Quick look at the SPS: levels up to 100s of kGy

OVERVIEW OF THE RADIATION LEVELS IN THE CERN ACCELERATOR COMPLEX AFTER LS2

A. Canesse*, S. Danzeca, D. Di Francesca, R. Garcia Alia, G. Lerner,
D. Prelipcean†, D. Ricci, A. Zimmaro, CERN, Geneva, Switzerland

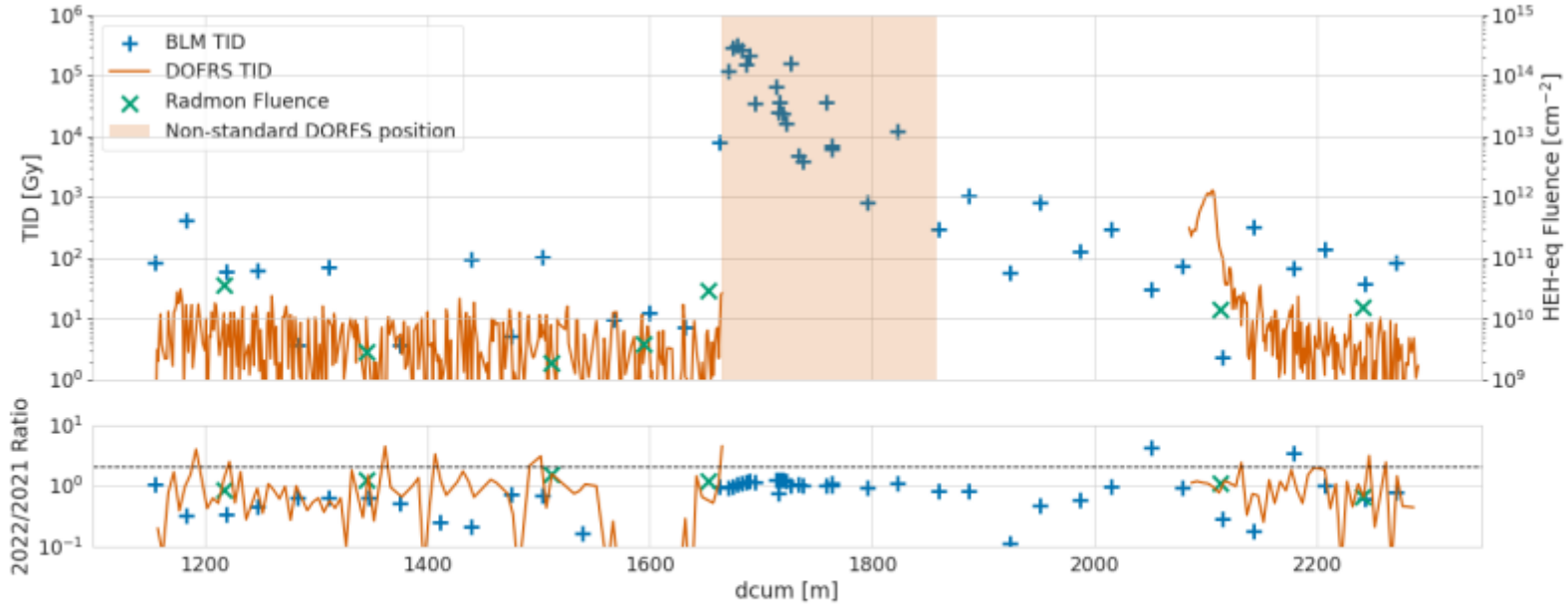

Figure 3: Radiations levels in the sector 2 of the SPS tunnel as a function of position in 2022 (top). Ratio of radiation levels between 2022 and 2021 for comparison (bottom). Due to its higher radiation hardness (compared to PSB and PS), the DOFRS used for the SPS cannot resolve to doses below ~10 Gy.

Quick look at the SPS: focus on electronics

CERN Super Proton Synchrotron radiation environment and related Radiation Hardness Assurance implications

Kacper Biłko, Rubén García Alía, *Member, IEEE*, Diego Di Francesca, Ygor Aguiar, *Member, IEEE*, Salvatore Danzeca, Simone Gilardoni, Sylvain Girard, *Senior Member, IEEE*, Luigi Salvatore Esposito, Matthew Alexander Fraser, Giuseppe Mazzola, Daniel Ricci, Marc Sebban, Francesco Maria Velotti

Fig. 4. Standard positions of the radiation sensors in the SPS arc sections, with the electronic rack of the ALPS system (with nMOS dosimeter on top, ~0.9 m distance from the beamline), directly exposed to the mixed-field radiation. Behind the magnets, at the cable tray (~1.3 m distance), as of 2021 the DOFRS monitor is installed. Before 2021, the Total Ionizing Dose was assessed by the RPL dosimeters (~1 m distance), in each arc half-period one installed at the cable tray, and one at the magnet coil. Each arc half-period contains one Beam Loss Monitor, installed either at the side of the beamline (~30 cm distance) or under the first dipole magnet, as in the presented location. Additionally, in some half-periods RadMons are deployed under the magnets.

Quick look at the SPS: losses within the cycle

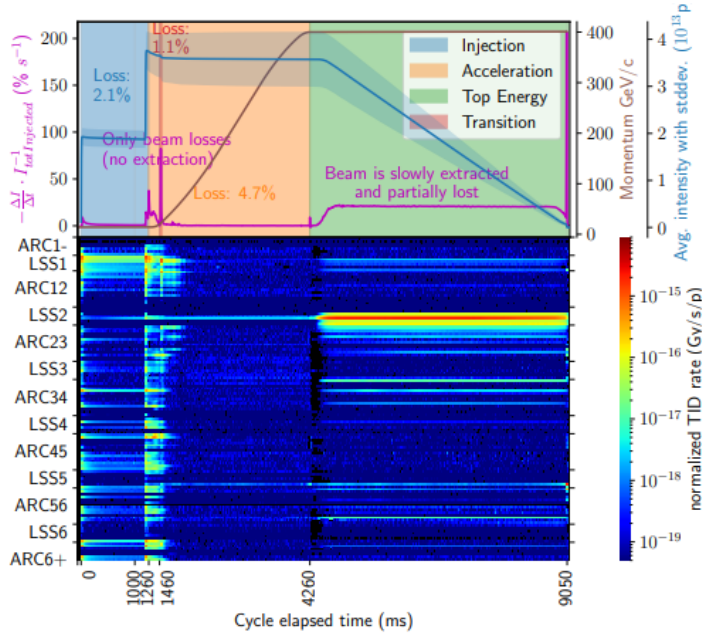

Fig. 5. The intensity loss rate normalized to the total injected intensity, as measured in 2022 during SFTPRO cycles. The loss rate includes lost, extracted and dumped protons. For comparison purposes, the beam momentum, together with an averaged beam intensity and its standard deviation is depicted. Only cycles with at least 10^{13} protons injected were considered. In these cycles, 2.1% of the total injected intensity was lost in the machine during the *Injection* period and 4.7% during the *Acceleration* phase (including 1.1% lost at *Transition* crossing). The bottom plot illustrates the injected-intensity normalized dose rate values along the accelerator as measured by the side BLMs in 2022 (until 13.09) during SFTPRO cycles.

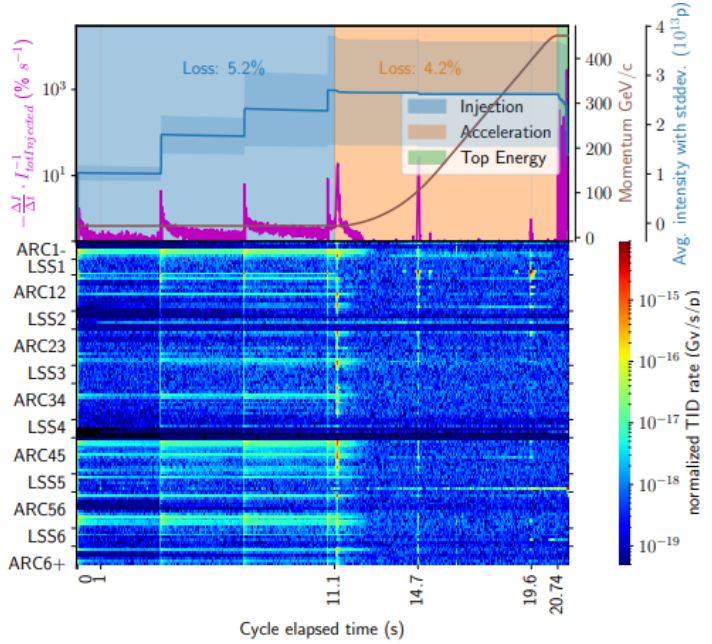

Fig. 6. The intensity loss rate normalized to the total injected intensity, as measured in 2022 during LHC cycles. The loss rate includes lost, extracted and dumped protons. For comparison purposes, the beam momentum, together with an averaged beam intensity and its standard deviation is depicted. Only cycles without dump occurring before the *Top Energy* period were considered. In these cycles, 5.1% of the total injected intensity was lost in the machine during the *Injection* period and 4.2% during the *Acceleration* phase (at the very beginning of acceleration due to uncaptured beam, and during the beam scrapping at 14.7/19.6 s.). The bottom plot illustrates the injected-intensity normalized dose rate values along the accelerator as measured by the side BLMs in 2022 (until 13.09) during the LHC cycles.

Quick look at the SPS: levels in the arc, hosting electronics

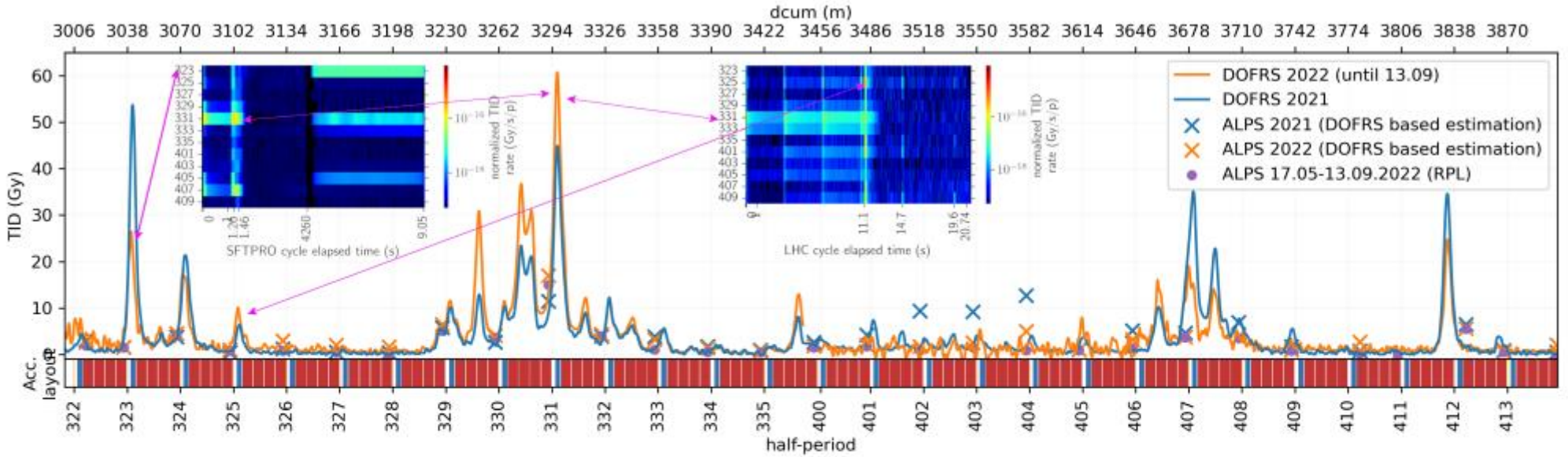

Fig. 7. TID (Gy in SiO_2, 2 m spatial resolution) in the arc sector 34 as measured by DOFRS in the years 2021 and 2022 (until September), with the schematic magnet layout. Additionally, the TID levels at the ALPS equipment are depicted, by means of RPL measurements from 2022; together with DOFRS-based estimates for 2021 and 2022. By focusing Fig. 5 and Fig. 6 on the arc sector 34, the detailed radiation peak analysis can be performed. For example, in 2022 the peak in half-period 323 was due to North Area cycles, with the majority of the TID registered during the Top Energy. The peak in half-period 325, was driven by the LHC cycles and happened at the beginning of acceleration, likely due to the loss of the uncaptured beam. The peak in 331 is due to the SPS vertical aperture restriction [27], and the losses can be observed for both SFTPRO and LHC cycles.

Quick look at the SPS: levels in the side galleries

13th Int. Particle Acc. Conf. IPAC2022, Bangkok, Thailand JACoW Publish
ISBN: 978-3-95450-227-1 ISSN: 2673-5490 doi:10.18429/JACoW-IPAC2022-MOPOMS(

IMPLICATIONS AND MITIGATION OF RADIATION EFFECTS ON THE CERN SPS OPERATION DURING 2021

Y. Q. Aguiar, G. Lerner, M. Cecchetto, R. García Alía, K. Bilko, A. Zimmaro,
M. Brucoli, S. Danzeca, T. Ladzinski, A. Apollonio, J. B. Potoine
CERN, CH-1211, Geneva, Switzerland

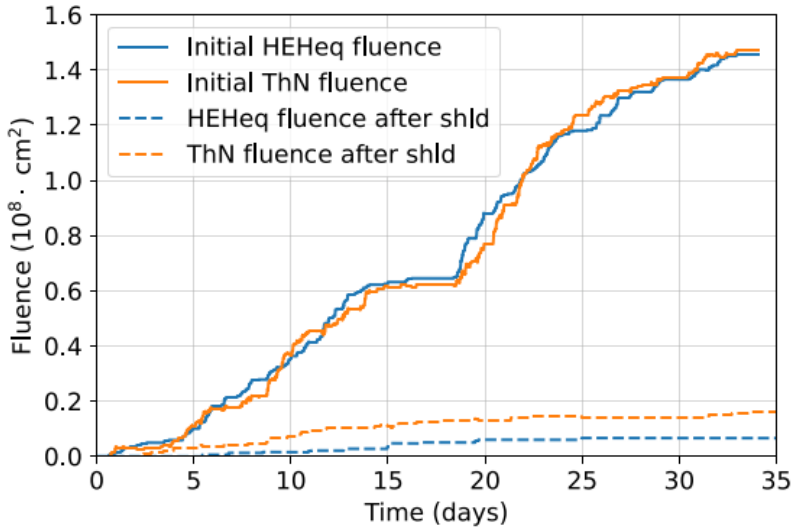

Figure 4: Particle fluences in BA1 measured by BatMons [8] before and after the installation of the iron shielding.

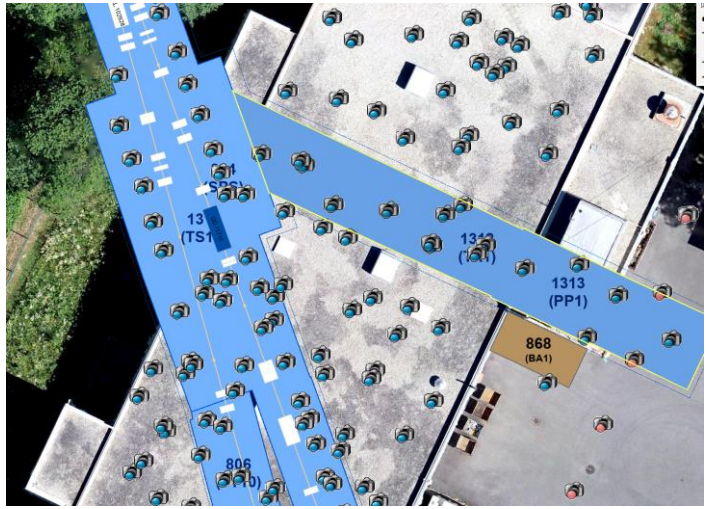

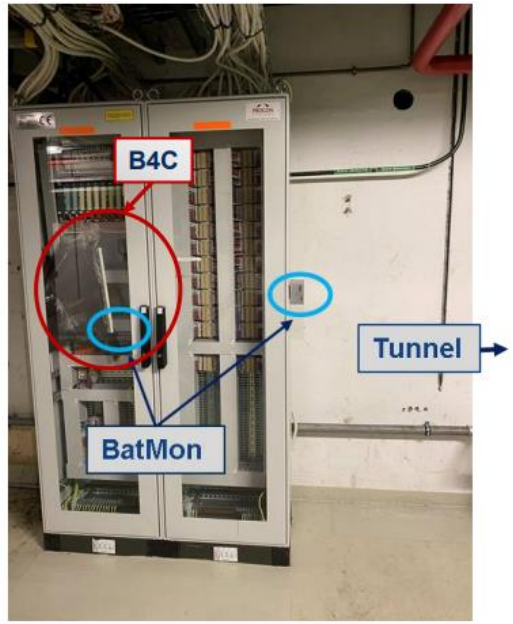

Outline

- Introduction to this course and the Radiation Hardness Assurance discipline
- Basics of radiation-matter interactions and FLUKA Monte Carlo code
- Radiation environment in the LHC
  - Setting the scene
  - Radiation sources and environment description
  - Tools for radiation monitoring and calculation
  - Radiation levels in the LHC areas relevant to electronics operation
- SPS radiation levels
- **FCC-ee radiation levels**
- Extra slides

Synchrotron radiation in lepton machines: FCC-ee

- Future circular collider lepton machine
- Inspired by LEP machine
- First stage of the FCC program (FCC-hh is supposed to follow)
- Circumference: ~91km
- 4 operation modes:

  45.6GeV-**182.5GeV**

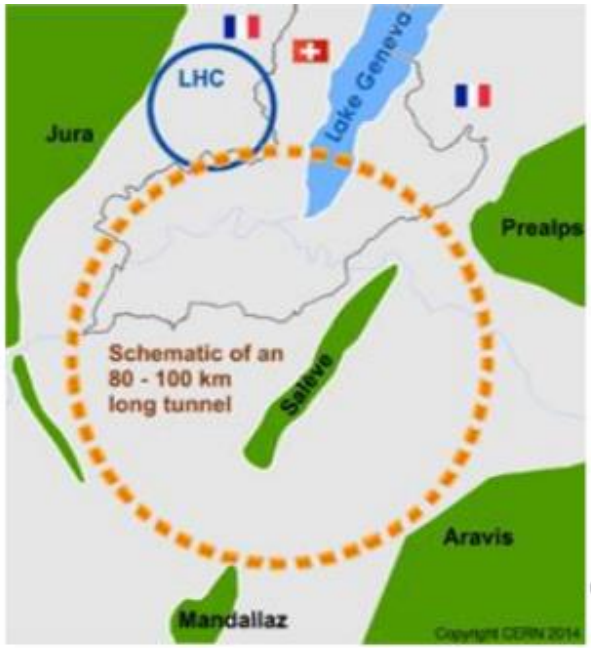

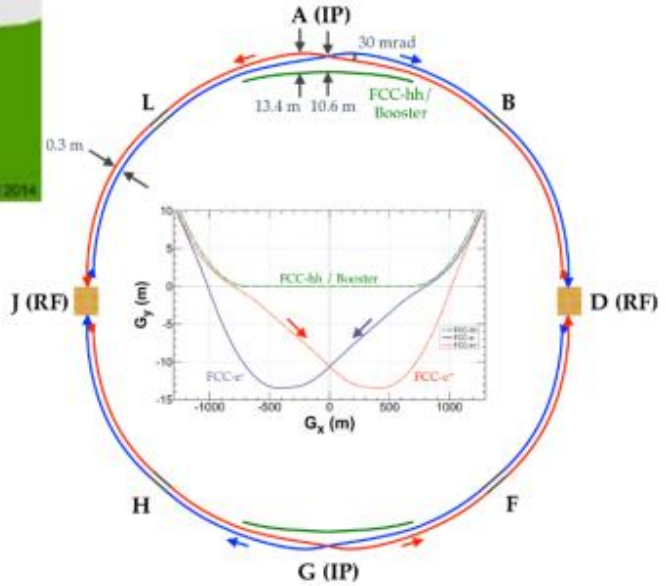

Synchrotron radiation

- **Electromagnetic radiation** emitted tangentially with an angular spread by charged particles moving along a curved trajectory
- The **lighter** the particle and the higher the **energy**, the stronger the effect:

$$\Delta E = \frac{e^2}{3\varepsilon_0 (m_0 c^2)^4} \frac{E^4}{\rho}$$

e …Electric charge
ε_0 …Vacuum permittivity
m_0 …Mass at rest
E …Momentum
ρ …Bending radius

→ SR is a major source of radiation in lepton machines

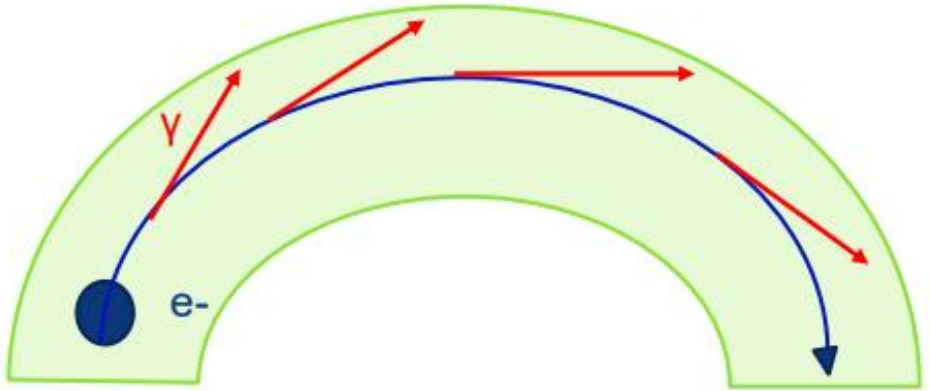

Synchrotron radiation

- **Critical energy (E_C):** divides the spectrum into two equal parts of deposited power

$$E_C[\mathrm{MeV}] = 2.21 \cdot 10^{-6} \frac{E^3[\mathrm{GeV}]}{\rho[\mathrm{km}]}$$

- **Power** on the arcs is constant:
  - $P = \Delta E[\mathrm{GeV}] \cdot I[\mathrm{mA}] = 50\mathrm{MW}$ (whole ring)
  - Same power for all operation modes
- SR related numbers in FCC-ee ($\rho = 10.76\mathrm{km}$):

Energy loss (ΔE)	9.2GeV/turn
Critical energy (E_C)	1.25MeV
Power whole ring	50MW
Power 140m	168kW

SR Spectrum of primary electrons:

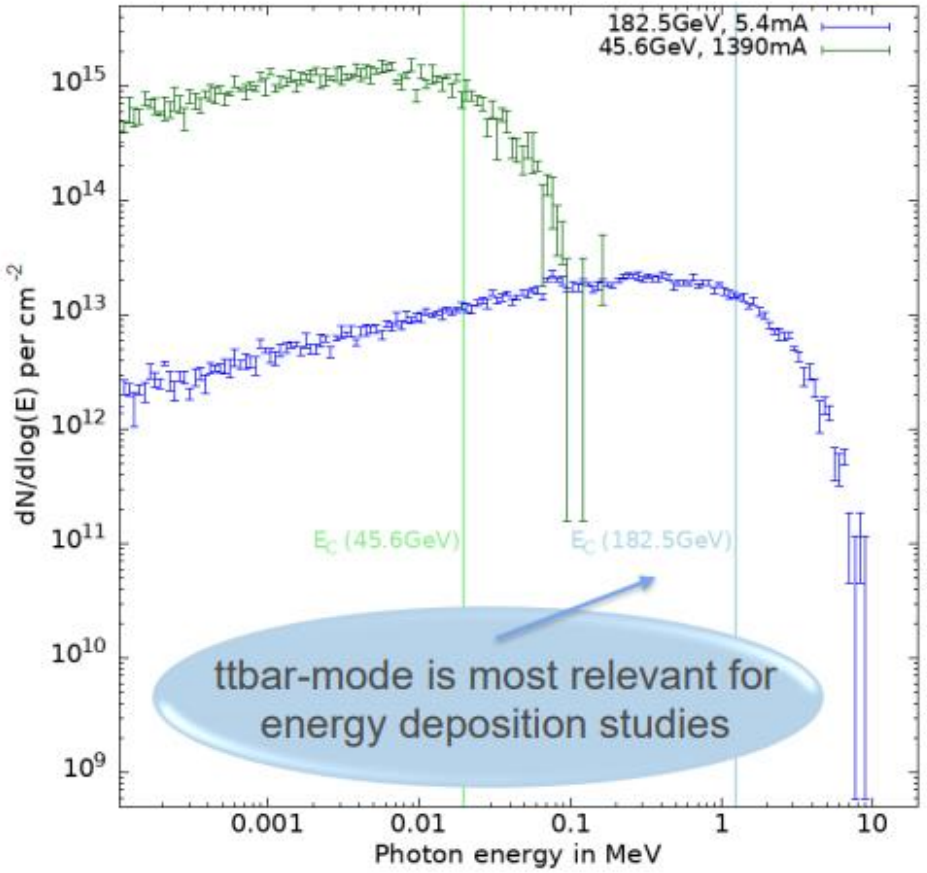

TID levels in the tunnel environment

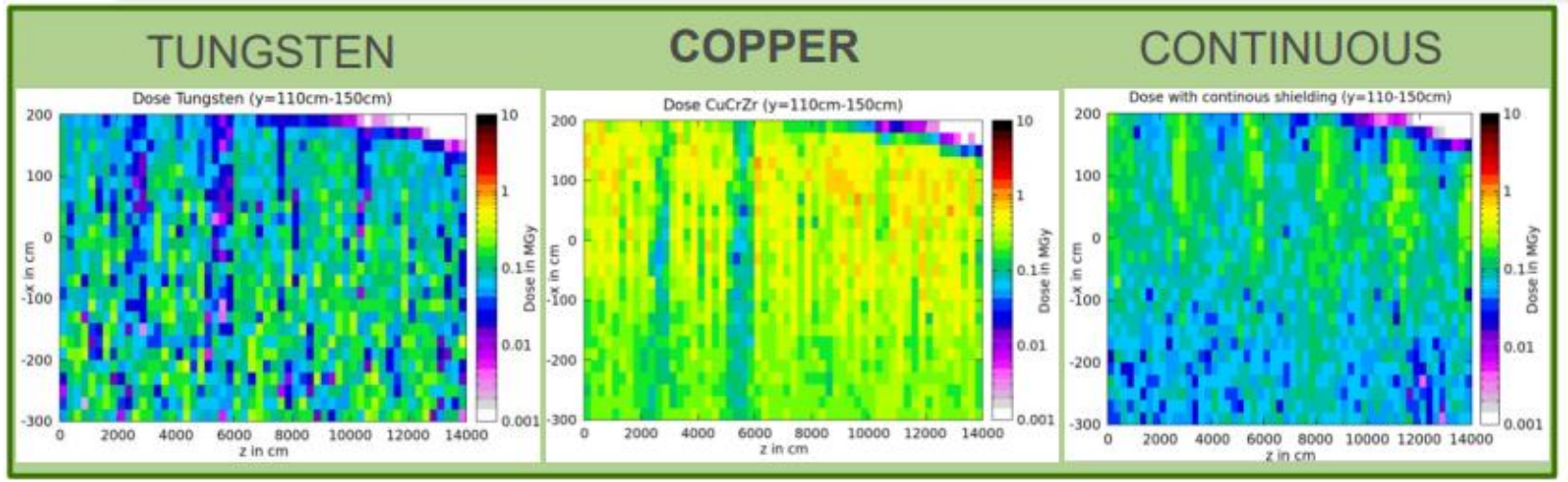

	Tungsten	Copper	Cont.
Top, Cent.	100kGy	300kGy	120kGy

Annual radiation levels → very challenging, not only for electronics, but also related to material damage

Effect of local shielding

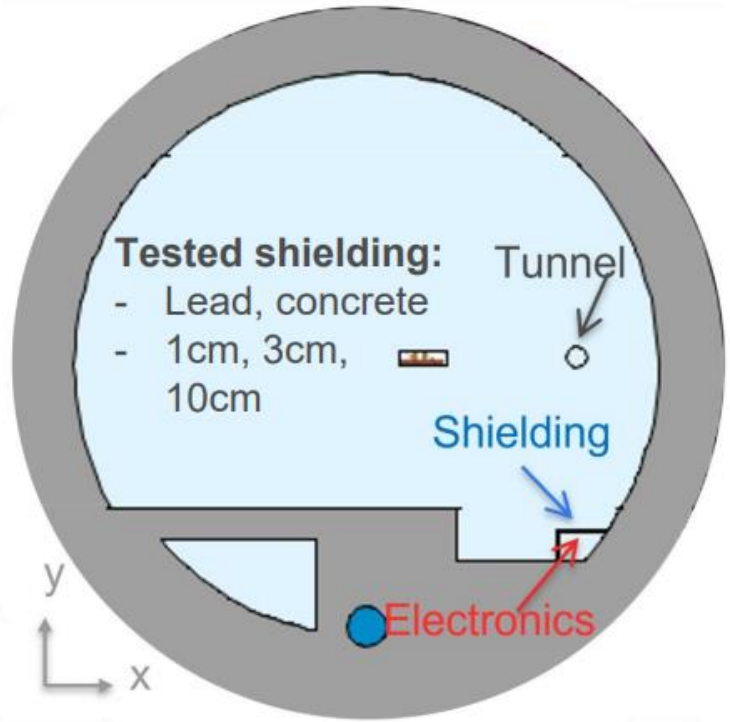

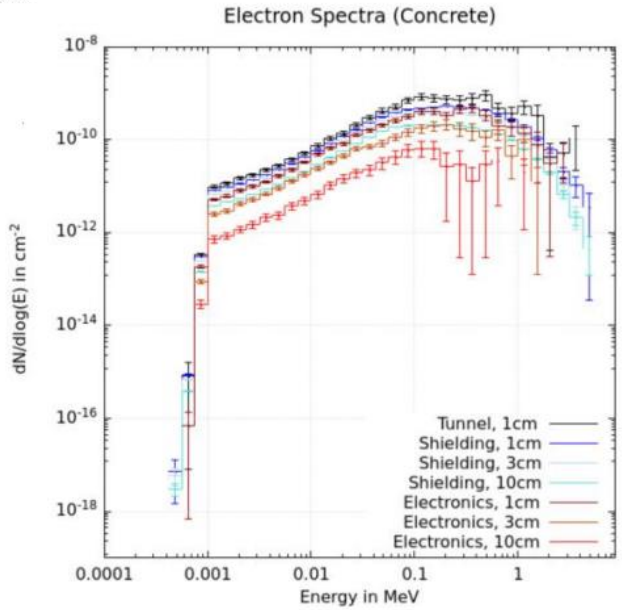

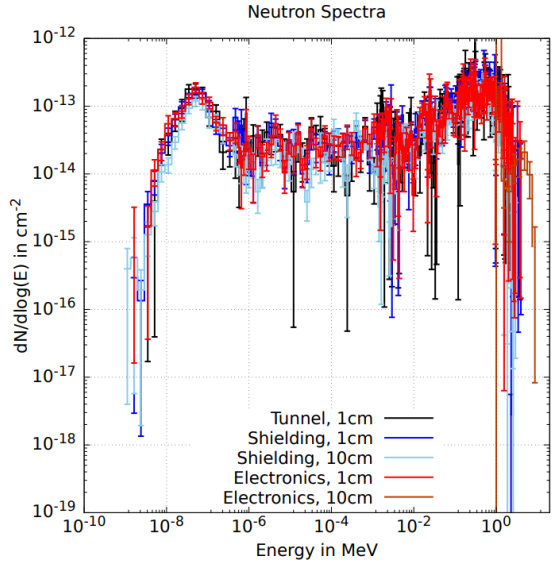

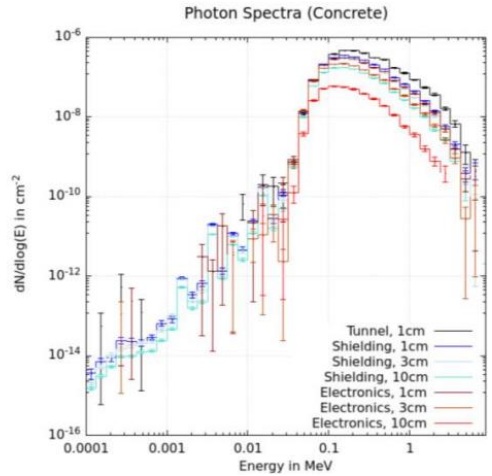

Main material sources (available publicly or through request to authors)

FLUKA and radiation-matter interaction intro:

- “An introduction to radiation-matter interaction”, Francesc Salvat-Pujol, 5th Barcelona TechnoWeek (2021)
- “An introduction to the FLUKA particle transport code for the SHIELDOSE-2 study team”, Francesc Salvat-Pujol (2022)

LHC radiation environment:

- “The Accelerator Radiation Environment”, Giuseppe Lerner, ISAE-SUPAERO Course 2020

FCC-ee radiation environment:

- “Energy deposition studies for synchrotron radiation (SR) in the FCC-ee arcs in FLUKA”, Barbara Humann, R2E Annual Meeting 2022

Space radiation environment:

- “From radiation environments to radiation-matter interactions”, Giovanni Santin, NSREC 2022 Short Course
- “ Single Event Effects in Aerospace”, Edward Petersen, John Wiley & Sons, 2011.

Atmospheric radiation environment:

- “Radiation environments: space, avionics, ground and below”, Giovanni Santin, Pete Truscott, Rémi Gaillard, Rubén García Alía, RADECS 2017 Short Course

Thanks for your attention! Any questions?

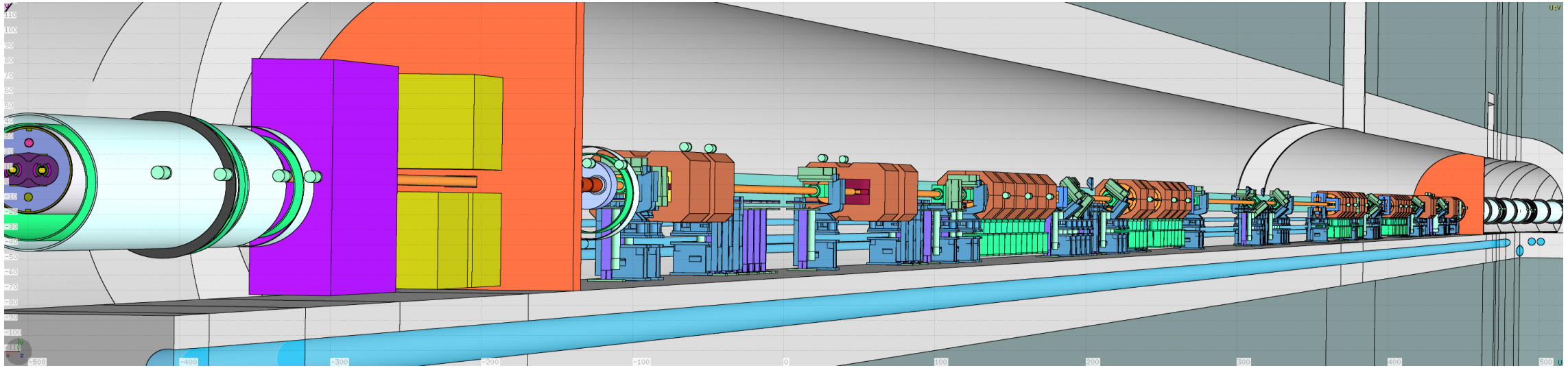

https://twiki.cern.ch/twiki/bin/view/FlukaTeam/FlukaLineBuilder

Extra slides

- Content:
  - Mimicking the accelerator radiation environment in CHARM
  - Neutrons in medical linacs
  - Heavy ion fragmentation
  - Space environment: trapped radiation belts, Solar Energetic Particles, Cosmic Rays
  - Atmospheric radiation environment

Mimicking the hadron accelerator environment in CHARM

Simulated 2-D TID distribution at beam height is shown for two configurations: CuOOOO (top) and CuCSSC (bottom).

Particle spectrum scored at the standard test locations for the CuCSSSC configuration: R1, fully shielded (top), and R13, within the residual beam direction (bottom), in a lethargy format.

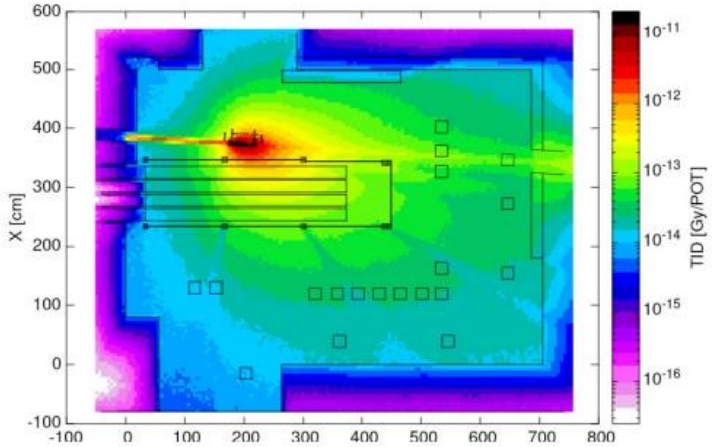

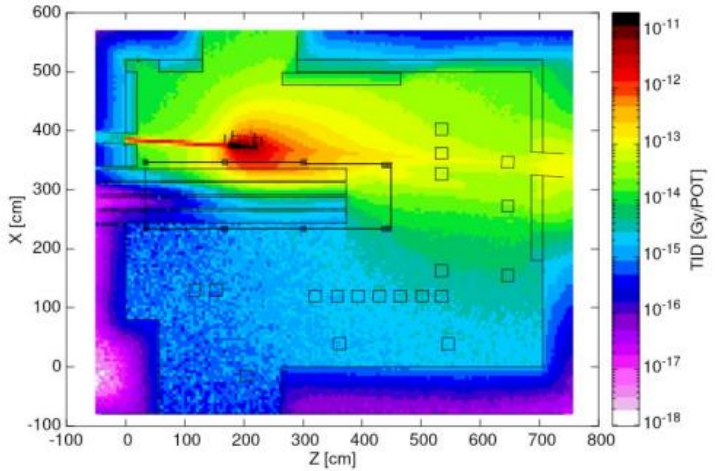

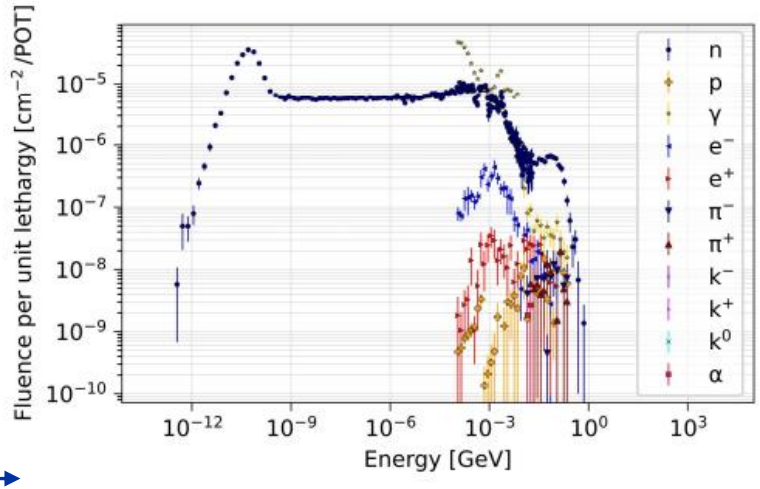

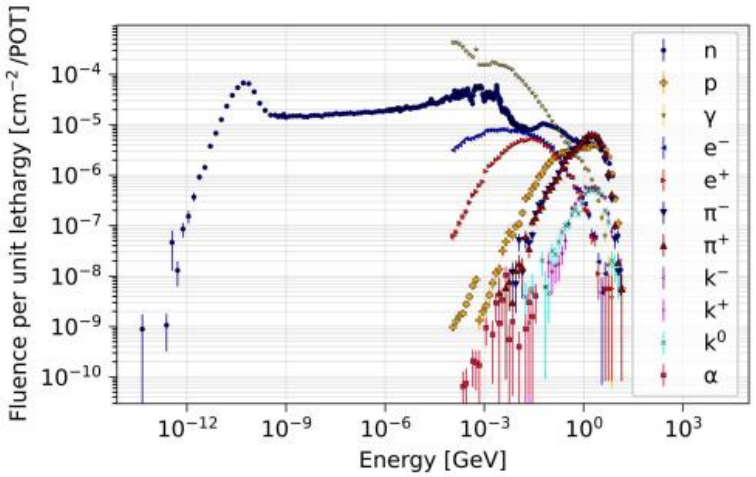

Quantity	Maximum Rate	Integrated Rate (per week)
Total Ionizing Dose	2.70 Gy/h	360 Gy
Thermal neutron fluence	3×10^6 cm^{-2}s^{-1}	1.5×10^{12} cm^{-2}
High-energy hadron fluence	1.5×10^6 cm^{-2}s^{-1}	8×10^{11} cm^{-2}

Prelipcean, Daniel, et al. "Benchmark between measured and simulated radiation level data at the Mixed-Field CHARM facility at CERN." IEEE Transactions on Nuclear Science (2022).

Mimicking the hadron accelerator environment in CHARM

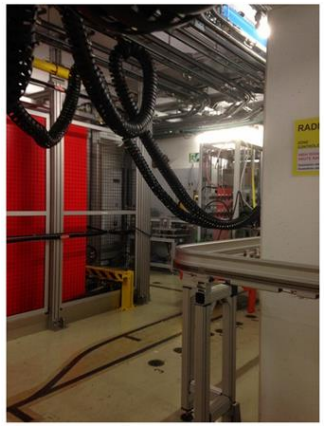

Mimicking the hadron accelerator environment in CHARM

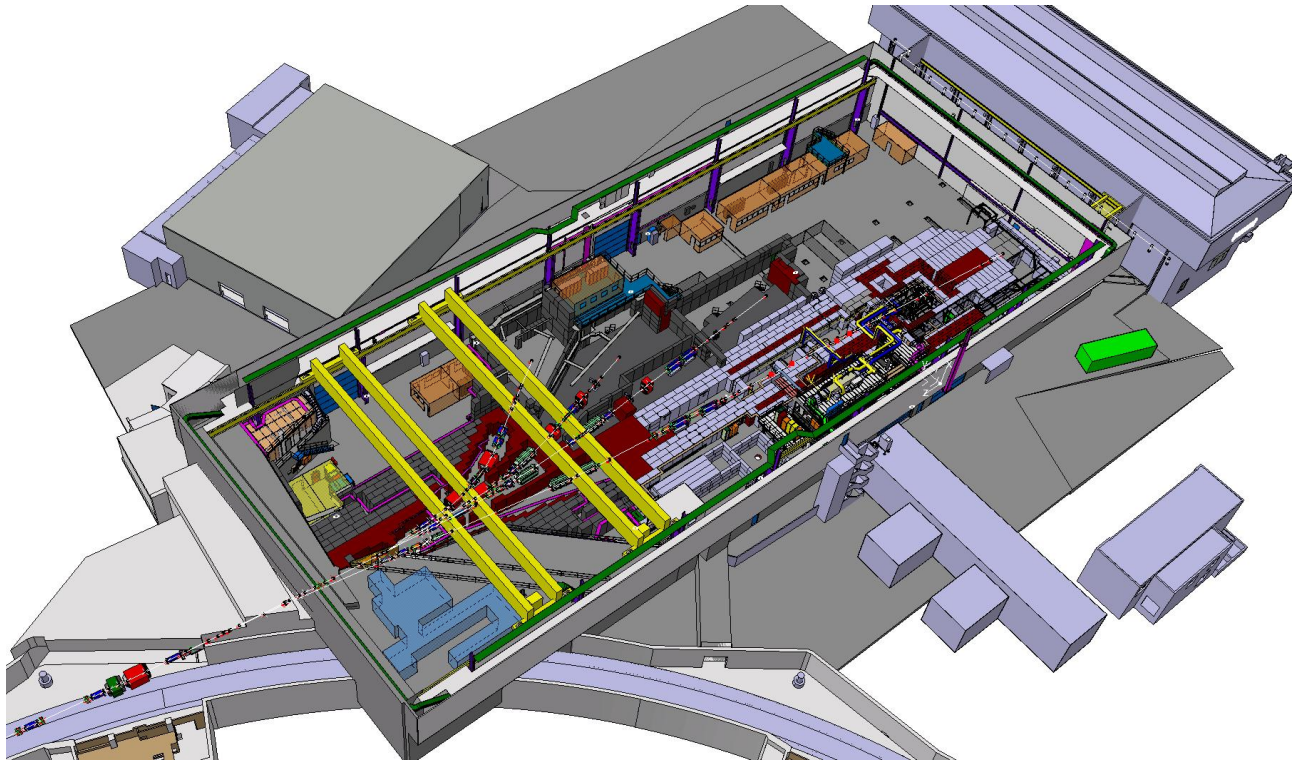

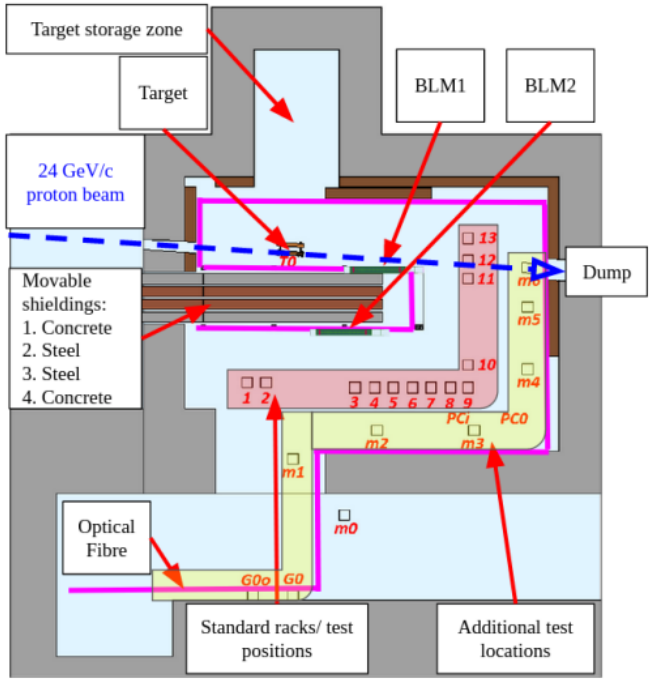

25 MeV medical linac at PTB

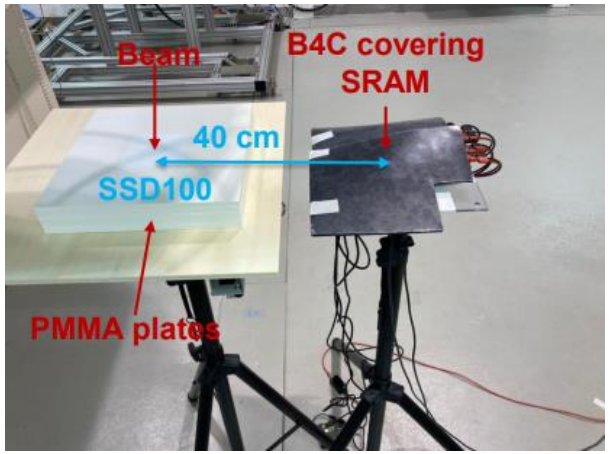

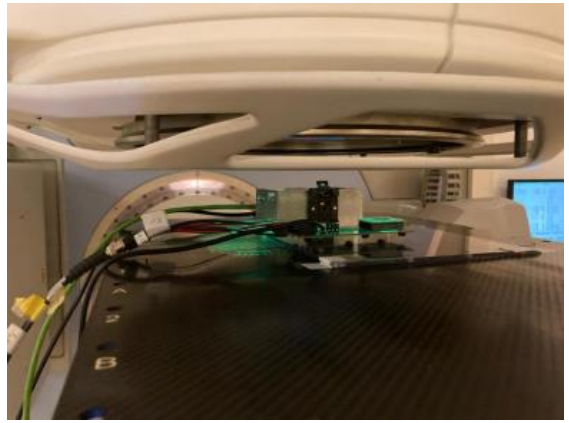

Cecchetto, Matteo, et al. "Neutron measurements in medical LINACs through SRAMs." R2E Annual Meeting (2022)

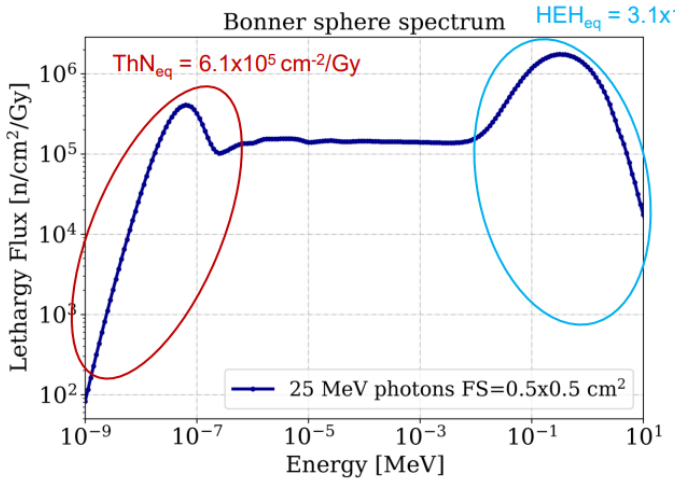

Run	E [MeV]	Field size [cm²]	HEHeq [cm⁻²/Gy]	ThNeq [cm⁻²/Gy]
SRAMs	25	0.5x0.5	4.1x10^5 ±20%	6.7x10^5 ±24%
Bonner S.	25	0.5x0.5	3.1x10^5	6.1x10^5

- **HEHeq** fluence agreement ~ **30%**
- **ThNeq** fluence agreement ~ **10%!**

High-energy heavy ion fragmentation

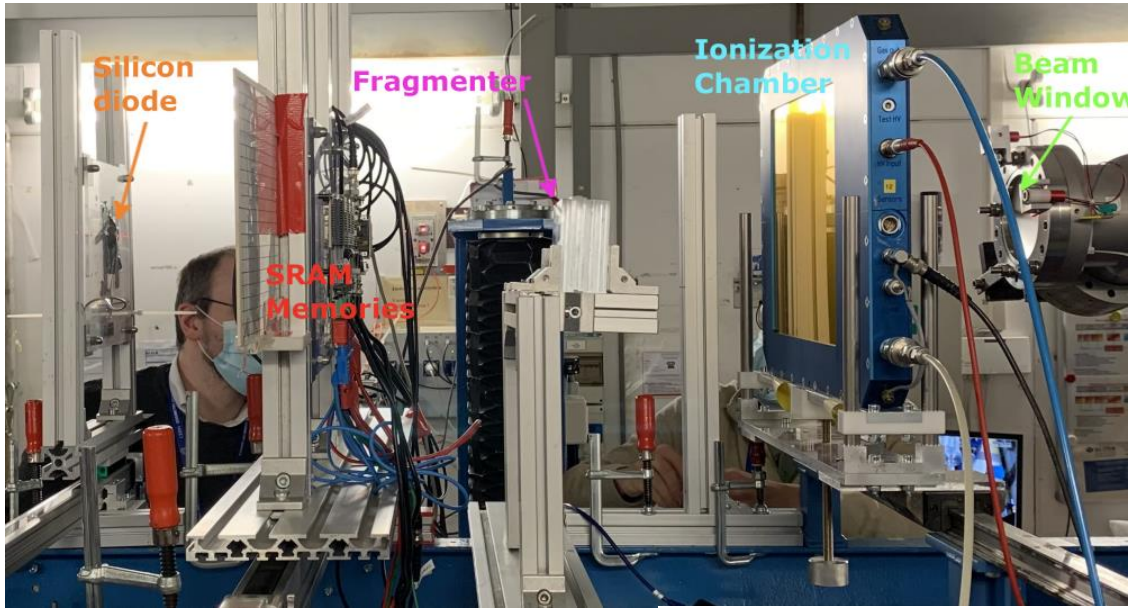

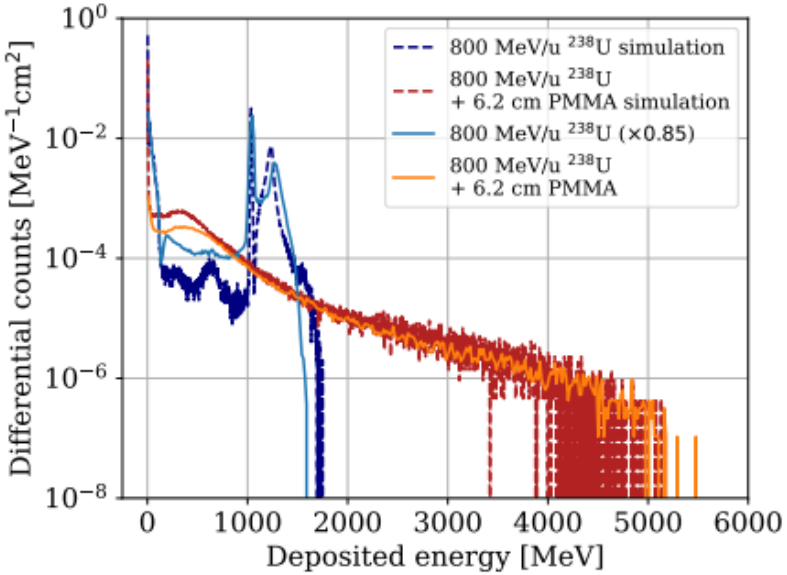

Garcia Alia, Ruben et al. "Fragmented high-energy heavy ion beams for electronics testing" NSREC 2022 conference; accepted for IEEE TNS publication

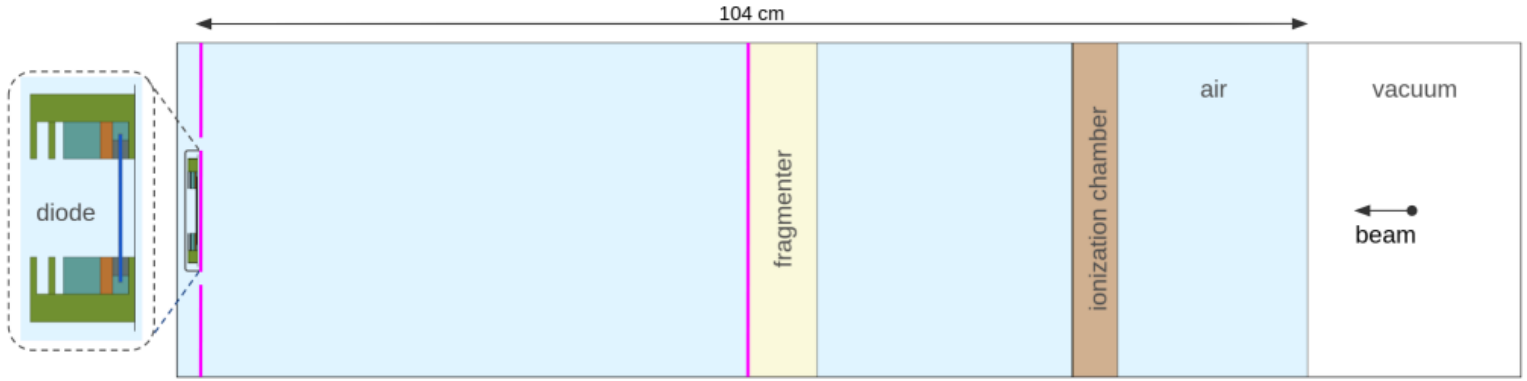

The trapped radiation belts

In the near-Earth region the global planet magnetic field keeps an electron and a protons populations trapped in a gyration, bounce and drift movement

the experimental confirmation of the trapped charged particle population only arrived with the first satellite launched by the United States, the Explorer 1, in 1958, with the measurement of its cosmic ray detector payload, based on a Geiger–Müller tube

The inner belt includes both electrons and protons. The proton population in this inner belt is dominant, and the outer belt is instead dominated by electrons.

The best known and most widely used models for the trapped particle populations are AP-8 for protons, and AE-8 for electrons, released in 1976 and 1983 respectively

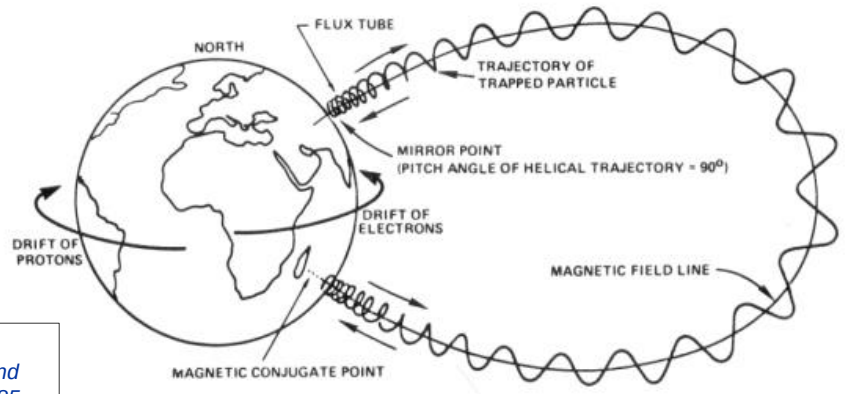

Spjeldvik and Rothwell, Handbook Of Geophysics And The Space Environment, 1985

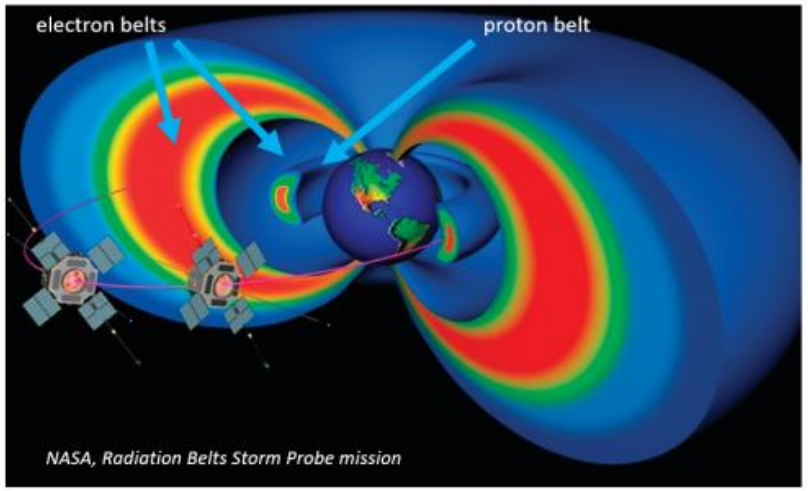

Image credit: NASA- adapted from “Van Allen” Radiation Belt Storm Probe mission graphics.

Trapped electrons

Electrons are present in the inner belt with energy up to hundreds of keV. The outer belt is dominated by a dynamic population of more energetic electrons, with (kinetic) energy E < 10 MeV.

Compared to the inner belt, the electron population of the outer belt shows a much higher variability, influenced by the solar activity, as a result of complex of complex injection and loss mechanisms associated with geomagnetic storms and solar material interacting with magnetosphere.

Trapped electrons dominate the geostationary orbit (GEO) and the medium Earth orbit (MEO) environment, but affect also missions at lower altitudes at high latitudes. Electron effects traditionally include total dose and electro-static discharges (ESD) from surface and internal charging

W. Robert Johnston et al, AE9/AP9/SPM: New Models for Radiation Belt and Space Plasma Specification, Proc. of SPIE Vol. 9085, 908508, 2014

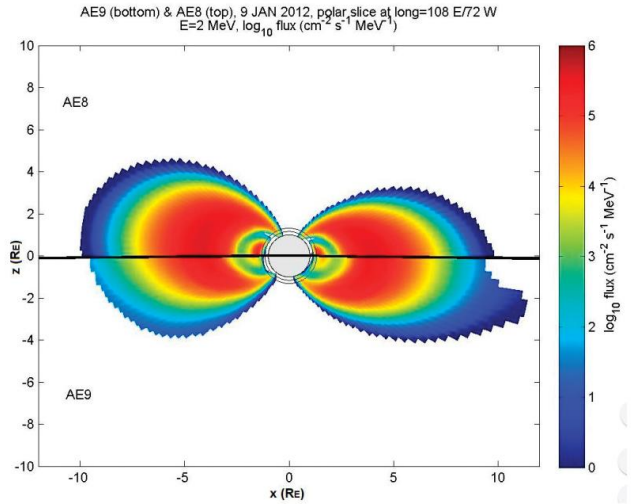

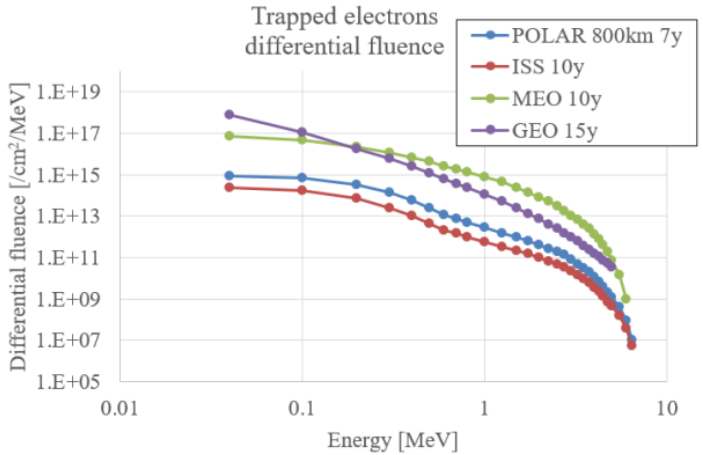

Trapped protons

The proton component of the trapped radiation belts is relatively stable in intensity. It is believed to be mainly a product of Cosmic-Ray Albedo Neutron Decay (CRAND) mechanism, although a population of trapped solar protons has been observed.

The maximum energy of trapped protons is around 500 MeV, but such high energies are only found at the core of the belt, while protons with energy above 10 MeV are limited to altitudes below ~20,000 km, and at GEO only protons energies of a few MeV can be observed.

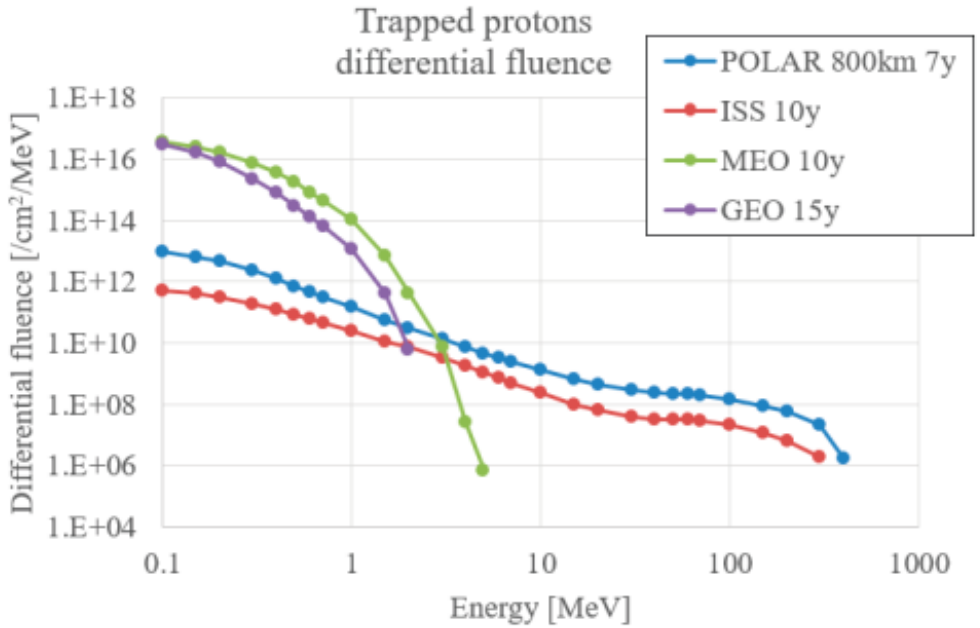

Trapped protons

The inner edge of the proton belt is encountered as the so-called South Atlantic Anomaly (SAA), which is a manifestation of the lower altitude of the inner belt protons. The SAA is due to the Earth magnetic field being tilted by 11 degrees with respect to the Earth rotation axis and offset by 500km towards the north Pacific, resulting in trapped protons getting closer to the Earth surface in the South Atlantic region.

Trapped protons (and electrons) dominate both TID and TNID effects for low Earth orbit (LEO) scenarios.

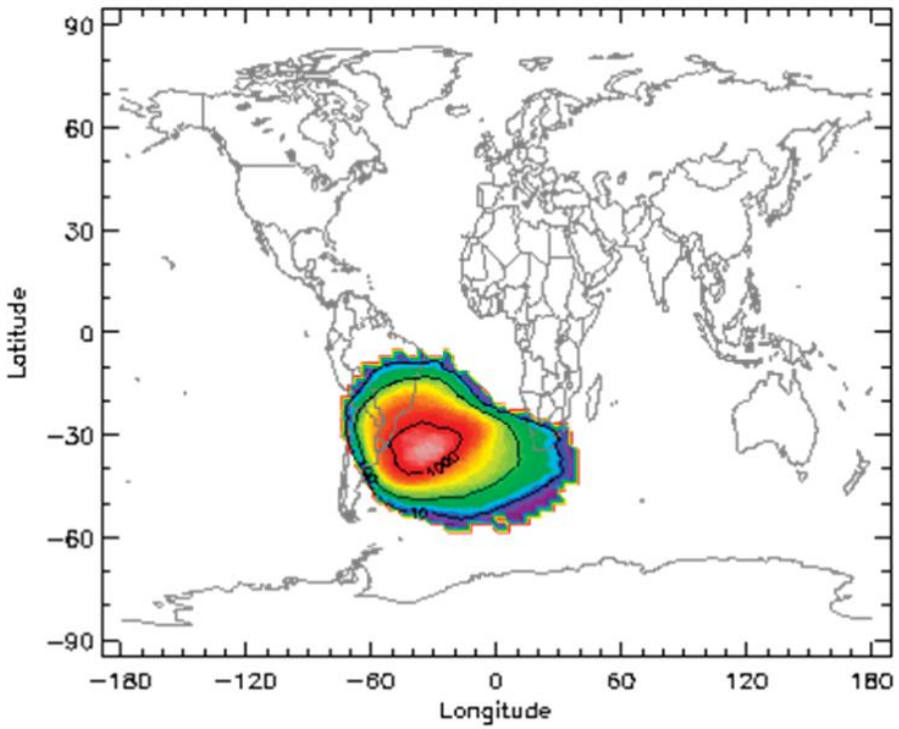

World map of the modelled trapped particle populations: AP-8 MAX integral proton flux >10 MeV at 500 km altitude

Solar Energetic Particles (SEP)

include protons, heavier ions, electrons, neutrons, gamma rays, X-rays, that are emitted from the Sun, and in some cases are accelerated either in the vicinity of the Sun, or by shocks in interplanetary space

usually divided into two categories: solar flares or Coronal Mass Ejections (CMEs), with the latter being responsible for major disturbances

characterized by occasional high fluxes over short periods, with a frequency strongly correlated with the solar activity cycle, with a period of approximately 11 years.

For missions at altitudes and magnetic latitudes much beyond LEO, the trapped environment is less dominant than at LEO, and SEPs can have an important contribution to dose levels. Outside of the proton belt SEPs are the dominant source of displacement damage effects, and SEPs are the dominant source for all cumulative effects in interplanetary environment

Solar Energetic Particles (SEP)

The energy spectral shape of solar energetic protons is very different event-by-event, and even within the same event, the proton spectra are highly variable.

The solar proton spectrum is in general much softer than that of GCRs. Mission scenarios in low Earth orbit at low inclination (LEO) are therefore typically fully shielded from the charged Solar particles (including protons) by the Earth magnetic field.

Solar particle can instead penetrate to much lower altitudes at higher latitudes, closer to the magnetic polar regions.

If the energy spectrum of the solar particles is hard enough, from their interactions in the upper layers of the atmosphere secondary particles are generated that can reach aircraft altitude, or even ground level.

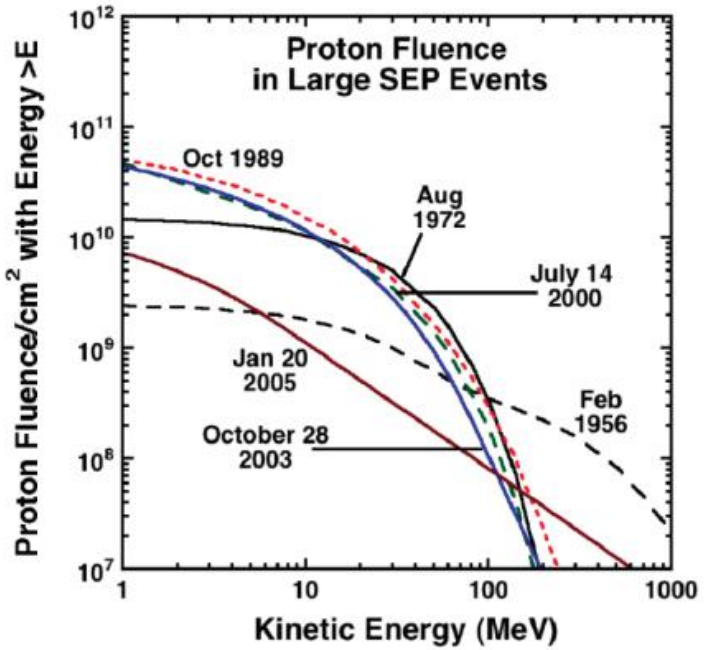

Integral energy spectra of some of the largest SEP events of the last 50 years, including three events from solar cycle 23

Mewaldt, R.A., et al.: Radiation risks from large solar energetic particle events. In: D. Shaikh, G.P. Zank (eds.) Turbulence and Nonlinear Processes in Astrophysical Plasmas, American Institute of Physics Conference Series, vol. 932, pp. 277–282 (2007).

Solar Energetic Particles (SEP)

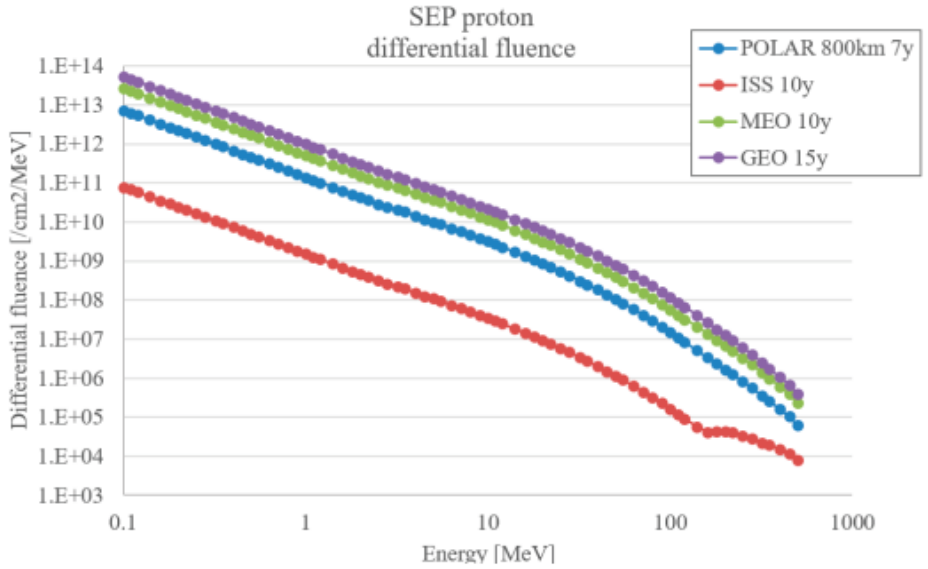

Cumulative SEP proton fluence for several reference scenarios, as predicted by the ESP model

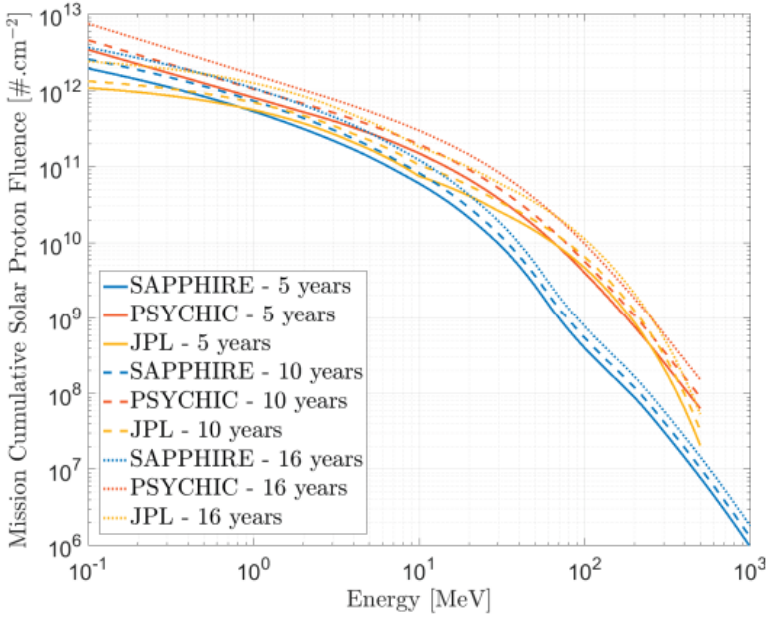

Comparison by Jiggens of SAPPHIRE, PSYCHIC and JPL cumulative integral fluence for 5-, 10- and 16-year prediction periods

P. Jiggens et al., "The Solar Accumulated and Peak Proton and Heavy Ion Radiation Environment (SAPPHIRE) Model," in IEEE Transactions on Nuclear Science, vol. 65, no. 2, pp. 698-711, Feb. 2018

Galactic Cosmic Rays

Galactic Cosmic Rays (GCR) originate from outside of the Solar System and consist of charged particles travelling near the speed of light. Their average energy is very high, around ~ 1 GeV/nuc, while the most energetic particles in the tail of the spectrum have measured energies reaching at least ~10^{21} eV.

This high energy of cosmic rays is believed to derive from acceleration by interaction with moving magnetic fields, e.g. in moving shocks originating from supernovae, via a mechanism suggested by Enrico Fermi already in 1949.

The modulation in the heliosphere of the intensity of the galactic cosmic ray fluxes causes a variability with solar cycle which becomes significant at rigidities below around 10 GV. Primary cosmic rays in outer space therefore manifest themselves as a continuous flux of about 4 particles/(cm^2 s) on average, with intensity in anti-correlation with solar activity.

The majority of the GCRs is made of atomic nuclei, and about 1% is made of electrons. Among the nuclei, protons constitute about 90%, alpha particles 9%, and the remaining ~1% of the particles consists of heavier ions.

This numerically small proportion of very penetrating particles contribute significantly both to single event effects (SEE) in microelectronics and to the predicted biological dose in astronauts in long duration interplanetary human spaceflight.

Galactic Cosmic Rays: relative abundances

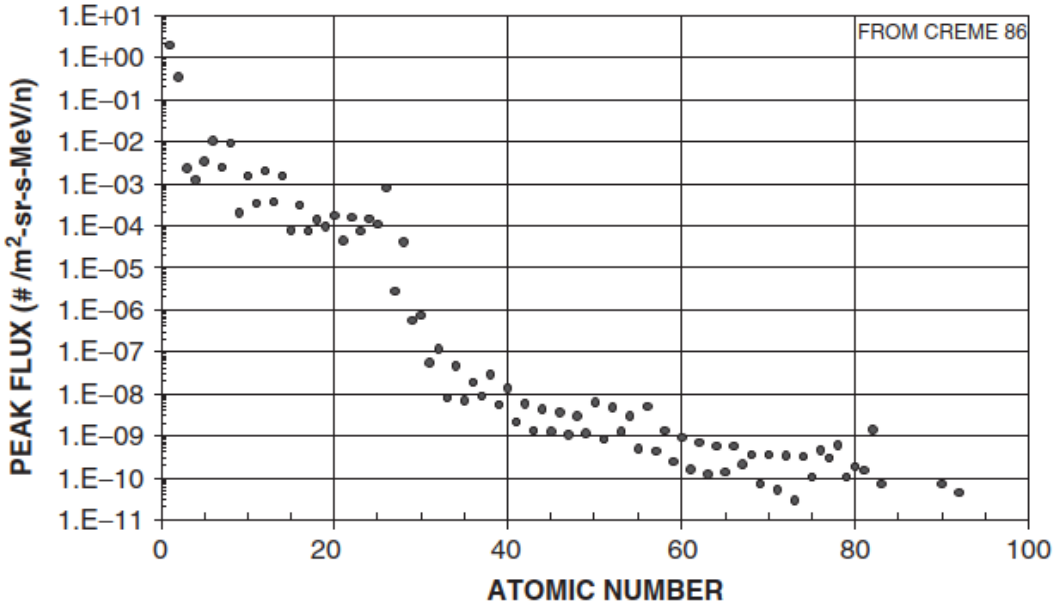

The relative abundances of all of the ions in cosmic rays. They are plotted in terms of the peak flux in their energy spectra.

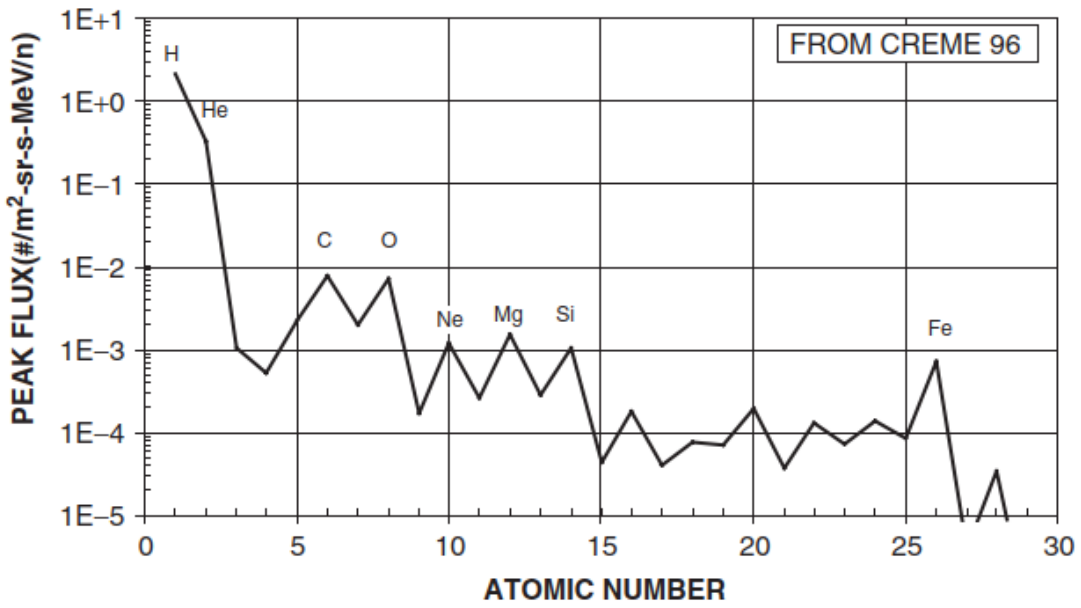

The relative abundance of the important cosmic rays through mass 30.

Galactic Cosmic Rays: solar modulation

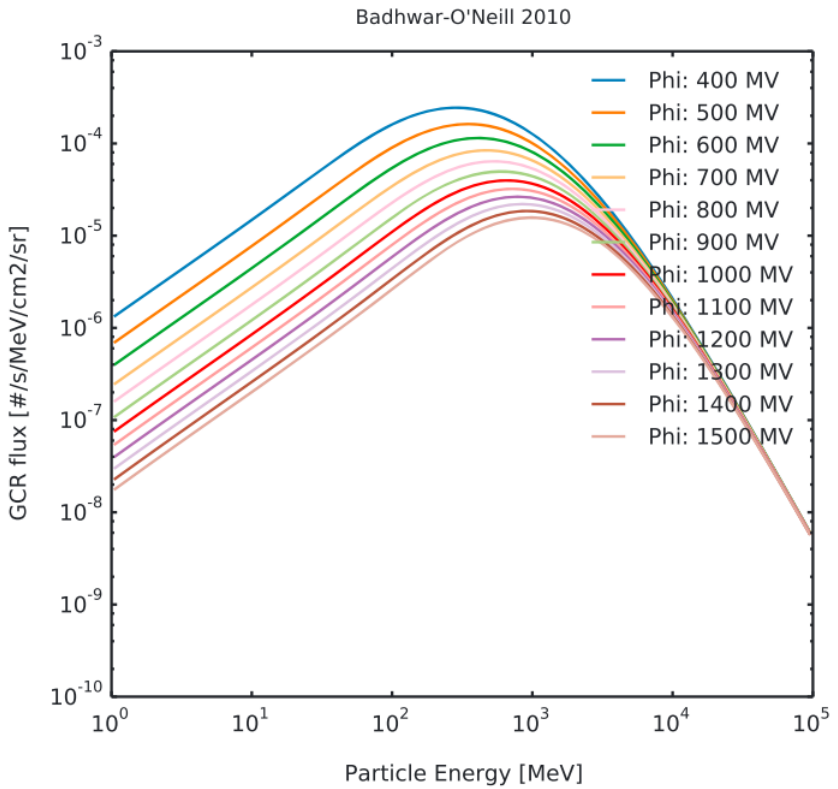

(a) GCR spectra of protons

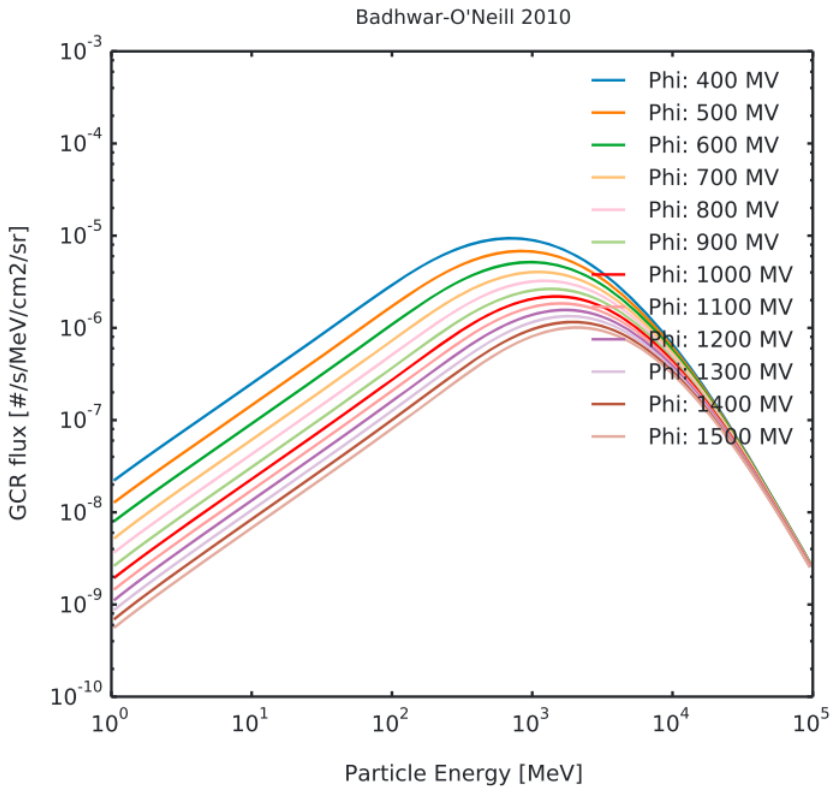

(b) GCR spectra of helium ions

Matthiä, Daniel, et al. "The radiation environment on the surface of Mars-Summary of model calculations and comparison to RAD data." Life sciences in space research 14 (2017): 18-28.

(a) GCR proton and (b) helium ion spectra in the interplanetary space generated by the BON10 model under different values of solar modulation potential Φ

Galactic Cosmic Rays: influence of geomagnetic shielding

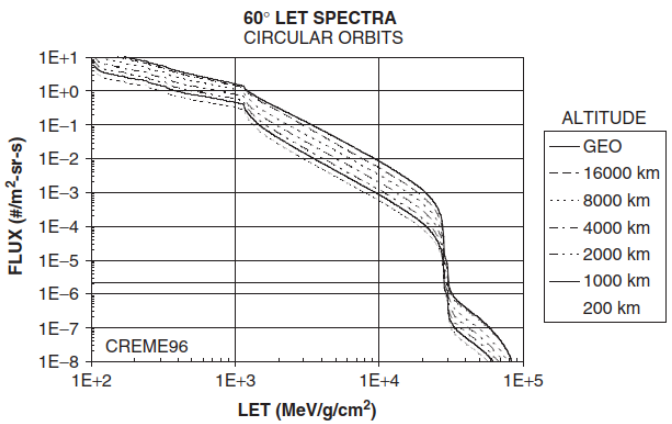

Variation of LET spectra with altitude for 60 degree inclination orbits.

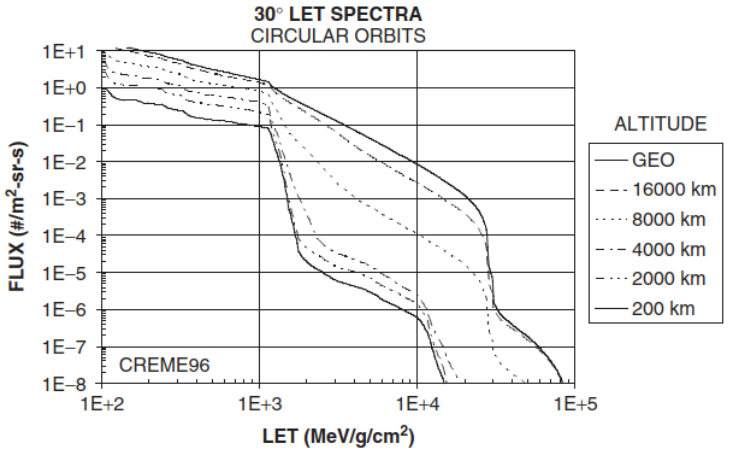

Variation of LET spectra with altitude for 30 degree inclination orbits.

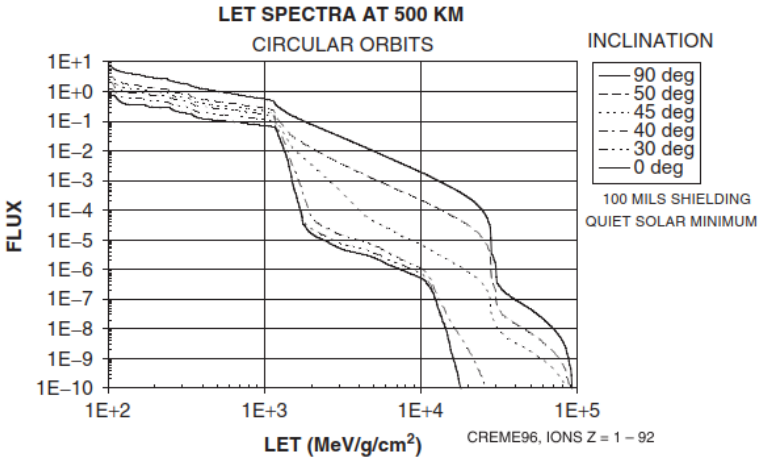

Variation of LET spectra with inclination for LEO.

Atmospheric radiation environment

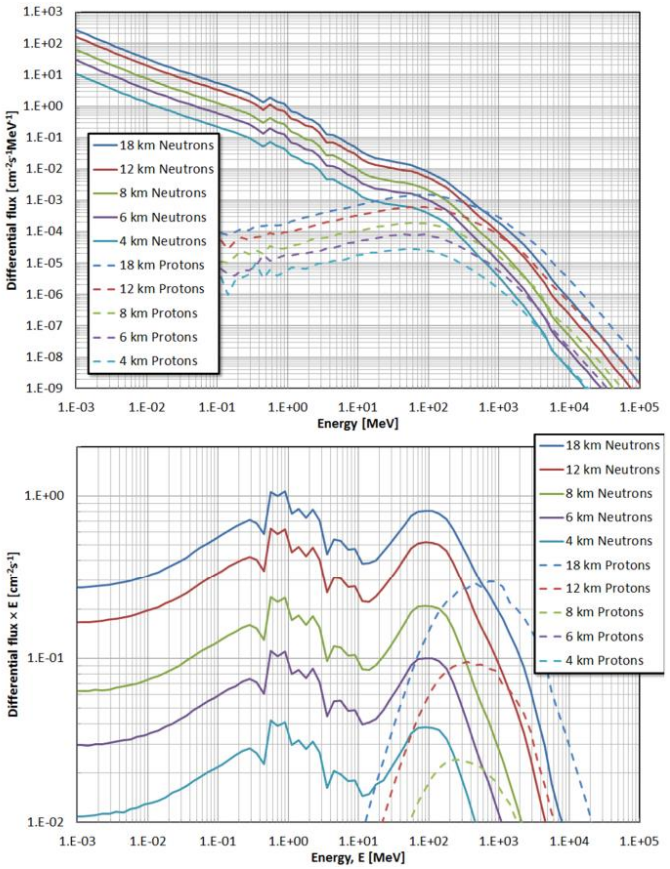

MAIRE simulation results showing the residual primary and secondary proton spectra as a function of altitude, and secondary neutron spectra at the same altitudes. Top – plotted as a conventional differential spectrum; Bottom – "lethargy plot" with the vertical axis the product of differential flux and energy, EdΦ/dE. These spectra are for location 45oN, 74oW, which has a vertical cut-off rigidity of ≅1 GV, and solar minimum conditions.

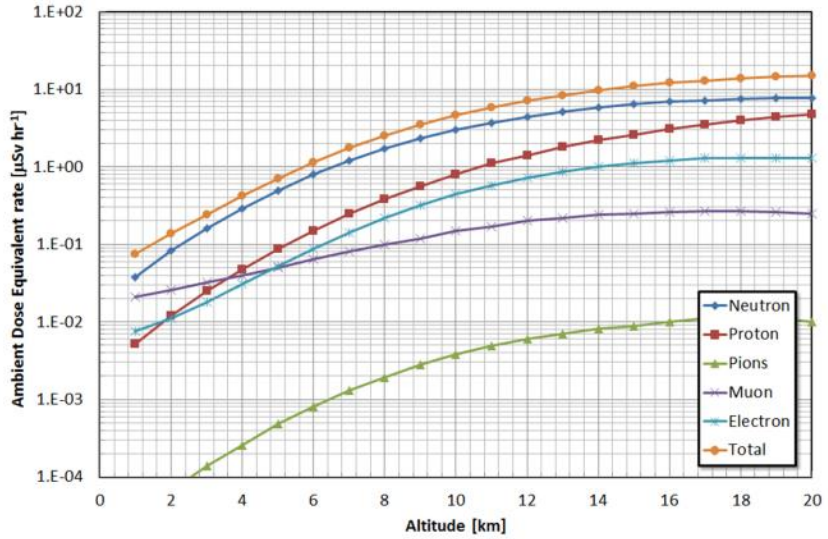

MAIRE simulation results showing the ambient dose equivalent rate as a function of altitude, and the contributions made by different particle species to the dose. The location corresponds to 45ºN, 74ºW, which has a vertical cut-off rigidity of ≅1 GV, and solar minimum conditions.

Atmospheric radiation environment

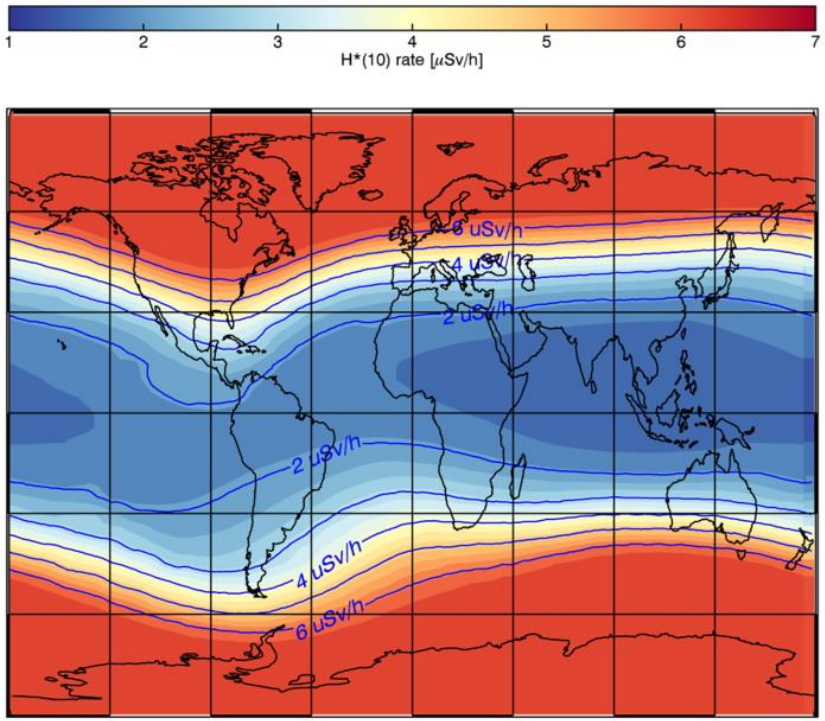

World map showing ambient dose-equivalent rate H(10) at 12 km (39,000 feet) due to galactic cosmic radiation ions.*

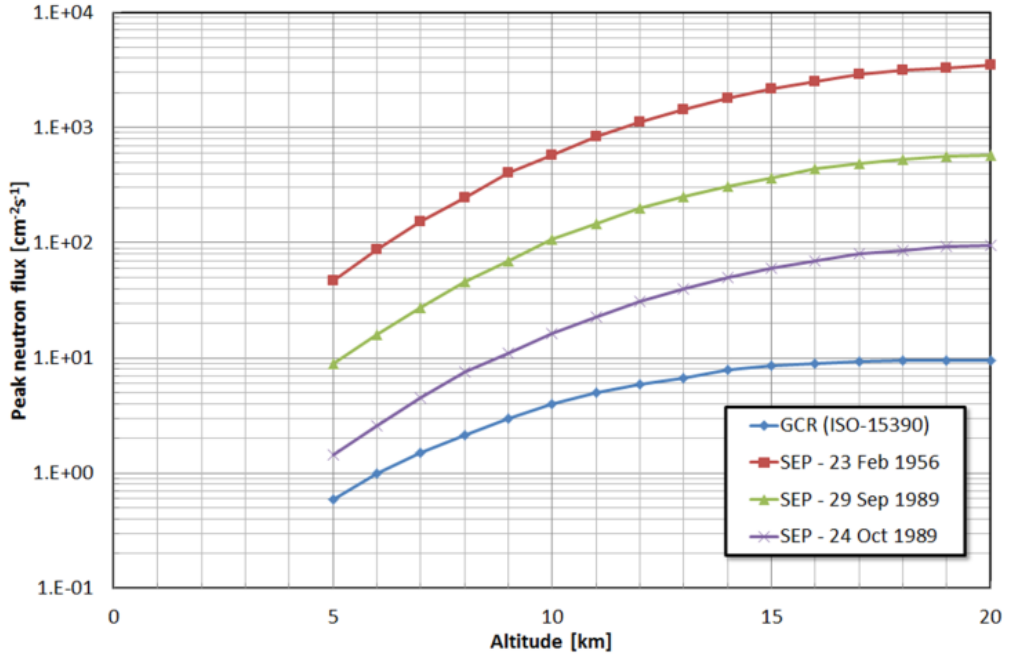

MAIRE simulation results showing the peak neutron flux as a function of altitude, for several example SEPs form February 1956 and September and October 1989, as well as the mean background level from GCR ions. Cut-off rigidity = 1 GV.

Fan Lei, Alex Hands, Simon Clucas, Clive Dyer and Pete Truscott, "Improvement to and validations of the QinetiQ Atmospheric Radiation Model (QARM)," IEEE Trans Nucl Sci, Vol 53, No 4, pp1851-1858, 2006.